Fisheries and Oceans Canada | Pêches et Océans Canada

Ecosystems and Oceans Science | Sciences des écosystèmes et des océans

Canadian Science Advisory Secretariat (CSAS)

Research Document 2015/032

Québec Region

Physical Oceanographic Conditions in the Gulf of St. Lawrence in 2014

P.S. Galbraith[1], J. Chassé[2], P. Nicot[1], C. Caverhill[3], D. Gilbert[1], B. Pettigrew[1], D. Lefaivre[1], D. Brickman[3], L. Devine[4], C. Lafleur[4]

[(1)] Fisheries and Oceans Canada, Québec Region,
Pelagic and Ecosystem Science Branch,
Maurice Lamontagne Institute,
P.O. Box 1000, Mont-Joli, Québec, G5H 3Z4

[(2)] Fisheries and Oceans Canada, Gulf Region,
P.O. Box 5030, Moncton, New Brunswick, E1C 9B6

[(3)] Fisheries and Oceans Canada, Maritimes Region,
Bedford Institute of Oceanography
P.O. Box 1006, Dartmouth, Nova Scotia, B2Y 4A2

[(4)] Fisheries and Oceans Canada, Québec Region,
Scientific Advice, Information and Support Branch,
Maurice Lamontagne Institute,
P.O. Box 1000, Mont-Joli, Québec, G5H 3Z4

June 2015

Canada

Foreword

This series documents the scientific basis for the evaluation of aquatic resources and ecosystems in Canada. As such, it addresses the issues of the day in the time frames required and the documents it contains are not intended as definitive statements on the subjects addressed but rather as progress reports on ongoing investigations.

Research documents are produced in the official language in which they are provided to the Secretariat.

Published by:

Fisheries and Oceans Canada
Canadian Science Advisory Secretariat
200 Kent Street
Ottawa ON K1A 0E6

http://www.dfo-mpo.gc.ca/csas-sccs/
csas-sccs@dfo-mpo.gc.ca

© Her Majesty the Queen in Right of Canada, 2015
ISSN 1919-5044

Correct citation for this publication:

Galbraith, P.S., Chassé, J., Nicot, P., Caverhill, C., Gilbert, D., Pettigrew, B., Lefaivre, D., Brickman, D., Devine, L., and Lafleur, C. 2015. Physical Oceanographic Conditions in the Gulf of St. Lawrence in 2014. DFO Can. Sci. Advis. Sec. Res. Doc. 2015/032. v + 82 p.

TABLE OF CONTENTS

ABSTRACT iv

RÉSUMÉ v

INTRODUCTION 1

AIR TEMPERATURE 2

PRECIPITATION AND FRESHWATER RUNOFF 2

SURFACE LAYER 3

- SST SEASONAL CYCLE CLIMATOLOGY 4
- SST IN 2014 4

SEA ICE 5

WINTER WATER MASSES 7

COLD INTERMEDIATE LAYER 8

- PREDICTION FROM THE MARCH SURVEY 8
- AUGUST CIL BASED ON THE MULTI-SPECIES SURVEY 8
- NOVEMBER CIL CONDITIONS IN THE ST. LAWRENCE ESTUARY 9
- GILBERT AND PETTIGREW (1997) CIL INDEX 9

MAGDALEN SHALLOWS JUNE SURVEY 10

BOTTOM WATER TEMPERATURES 10

SEASONAL AND REGIONAL AVERAGES OF TEMPERATURE PROFILES 11

DEEP WATERS (>150 m) 12

- TEMPERATURE AND SALINITY 12
- DISSOLVED OXYGEN AND HYPOXIA IN THE ST. LAWRENCE ESTUARY 13

CURRENTS AND TRANSPORTS 13

HIGH FREQUENCY SAMPLING AZMP STATIONS 14

OUTLOOK FOR 2015 15

SUMMARY 15

HIGHLIGHTS 16

ACKNOWLEDGEMENTS 17

REFERENCES 18

FIGURES 21

ABSTRACT

An overview of physical oceanographic conditions in the Gulf of St. Lawrence in 2014 is presented as part of the Atlantic Zone Monitoring Program (AZMP). AZMP data as well as data from regional monitoring programs are analysed and presented in relation to long-term means. The annual average freshwater runoff of the St. Lawrence River measured at Québec City and its combination with rivers flowing into the Estuary (RIVSUM II) were above-normal in 2014 (+0.7 SD and +1.1 SD respectively), as was the spring freshet (+1.9 SD and +1.8 SD). The above-normal spring freshet led to below-normal Estuarine ratio and near-normal outward transport at the Pointe-des-Monts section. The cold winter of 2014 created a thick surface mixed layer over the GSL with near-freezing temperatures, as well as a sea ice cover with the third highest seasonal maximal volume since 1969, at nearly double the climatological average. The August-September cold intermediate layer (CIL) returned to near-normal conditions after 4 years of warm conditions, as a result of the cold winter. The sea-surface temperature averaged from May to November over the Gulf was above-normal by +1.2°C, the second highest on record after 2006. A record high was reached in August with a Gulf-average anomaly of +2.5°C, breaking the +2.0°C record of August 2012. Record August highs were also set in the following regions: Estuary (+4.2°C, +4.4 SD), Northwest Gulf (+4.1°C, +4.4 SD), Anticosti Channel (+2.8°C, +3.2 SD) and Cabot Strait (+2.9°C, +3.2 SD). Deep water temperatures are increasing overall in the Gulf, with inward advection from Cabot Strait where temperature had reached a record high (since 1915) in 2012 at 200 m. Temperature averaged over the Gulf at 200 m increased overall to reach 5.3°C, the highest on record. Temperature at 300 m increased slightly in 2014 to reach 5.9°C, the highest value since 1980. Bottom area covered by waters warmer than 6°C increased in 2014 in Anticosti Channel, Esquiman Channel and Central Gulf, and reached a record value in Esquiman Channel while reducing its bottom habitat area in the temperature range of 5–6°C.

Conditions océanographiques physiques dans le golfe du Saint-Laurent en 2014

RÉSUMÉ

Le présent document donne un aperçu des conditions d'océanographie physique qui ont prévalu dans le golfe du Saint-Laurent en 2014 et est un produit du Programme de monitorage de la zone Atlantique (PMZA). Les données du PMZA ainsi que de programmes de monitorage régionaux sont analysées et présentées en relation avec des moyennes à long terme. Les débits du fleuve Saint-Laurent et de l'indice RIVSUM II étaient au-dessus de la normale en 2014 (+ 0,7 É.T. et + 1,1 É.T. respectivement), comme l'était la crue printanière (+ 1,9 É.T. et + 1,8 É.T.). L'hiver froid de 2014 a causé la formation d'une volumineuse couche de surface avec des températures près du point de congélation, ainsi qu'un important couvert de glace de mer qui a atteint un volume saisonnier maximal le troisième plus élevé depuis 1969, avec une valeur qui était près du double de la moyenne climatologique. La couche intermédiaire froide des mois d'août et septembre est retournée vers des conditions près de la normale après quatre années chaudes, causée par l'hiver froid de 2014. Les températures à la surface de l'eau moyennées de mai à novembre étaient au-dessus de la normale de +1,2 °C et représentaient les secondes plus chaudes de la série. Le mois d'août a connu un record de + 2,5 °C au-dessus de la climatologie, battant le record d'août 2012 qui était de + 2,0 °C. Des records ont aussi été battus dans les régions suivantes : estuaire (+ 4,2 °C, + 4,4 É.T.), nord-ouest du golfe (+ 4,1 °C, + 4,4 É.T.), chenal Anticosti (+ 2,8 °C, + 3,2 É.T.) et le détroit de Cabot (+ 2,9 °C, + 3,2 É.T.). Les températures des eaux profondes du golfe sont en augmentation avec le transport depuis le détroit de Cabot d'eaux qui avaient atteint une température record (depuis 1915) en 2012 à 200 m. Globalement, les eaux de 200 m ont atteint 5,3 °C, soit un record de série. Les eaux de 300 m ont aussi réchauffé pour atteindre 5,9 °C, un record depuis 1980. La superficie du fond marin recouvert par des températures plus grandes que 6 °C a augmenté dans le chenal d'Anticosti, le chenal Esquiman et dans le centre du golfe, atteignant un record de série dans le chenal Esquiman au détriment de l'habitat de fond dans la plage de température de 5 à 6 °C.

INTRODUCTION

This document examines the physical oceanographic conditions and related atmospheric forcing in the Gulf of St. Lawrence in 2014 (Fig. 1). It complements similar reviews of the environmental conditions on the Newfoundland and Labrador Shelf and the Scotian Shelf and Gulf of Maine as part of the Atlantic Zone Monitoring Program (AZMP; see Therriault et. al., 1998 for background information on the program and Colbourne et al. 2014, and Hebert et al. 2014 for examples of past reviews in other AZMP regions). The last detailed report of physical oceanographic conditions in the Gulf of St. Lawrence was produced for the year 2013 (Galbraith et al. 2014). Specifically, it discusses air temperature, freshwater runoff, sea-ice volume, surface water temperature and salinity, winter water mass conditions (e.g., the near-freezing mixed layer volume, the volume of dense water that entered the Gulf through the Strait of Belle Isle), the summertime cold intermediate layer (CIL), and the temperature, salinity, and dissolved oxygen of the deeper layers. Some of the variables are spatially averaged over distinct regions of the Gulf (Fig. 2). The report uses data obtained from the Department of Fisheries and Oceans' (DFO) Atlantic Zone Monitoring Program (AZMP), other DFO surveys, and other sources. Environmental variables are usually expressed as anomalies, i.e., deviations from their long-term mean. The long-term mean or normal conditions are calculated for the 1981–2010 reference period when possible. Furthermore, because these series have different units (°C, m^3, m^2, etc.), each anomaly time series is normalized by dividing by its standard deviation (SD), which is also calculated using data from 1981–2010 when possible. This allows a more direct comparison of the various series. Missing data are represented by grey cells, values within ±0.5 SD of the average as white cells, and conditions corresponding to warmer than normal (higher temperatures, reduced ice volumes, reduced cold-water volumes or areas) by more than 0.5 SD as red cells, with more intense reds corresponding to increasingly warmer conditions. Similarly, blue represents colder than normal conditions. Higher than normal freshwater inflow is shown as red, but does not necessarily correspond to warmer-than-normal conditions. Higher than normal stratification is shown in blue because it usually corresponds to lower salinity.

The summertime water column in the Gulf of St. Lawrence consists of three distinct layers: the surface layer, the cold intermediate layer (CIL), and the deeper water layer (Fig. 3). Surface temperatures typically reach maximum values in early to mid-August. Gradual cooling occurs thereafter, and wind forced mixing during the fall leads to a progressively deeper and cooler mixed layer, eventually encompassing the CIL. During winter, the surface layer thickens partly because of buoyancy loss (cooling and reduced runoff) and brine rejection associated with sea-ice formation, but mostly from wind-driven mixing prior to ice formation (Galbraith 2006). The surface winter layer extends to an average depth of 75 m and >150 m in places such as the Mécatina Trough (where intruding waters through the Strait of Belle Isle from the Labrador Shelf may extend from the surface to the bottom in depths >200 m) by the end of March when temperatures have decreased to near freezing (-1.8 to 0°C) (Galbraith 2006). During spring, surface warming, sea-ice melt waters, and continental runoff produce a lower-salinity and higher-temperature surface layer. Underneath this surface layer, cold waters from the previous winter are partly isolated from the atmosphere and form the summer CIL. This layer will persist until the next winter, gradually warming up and deepening during summer (Gilbert and Pettigrew 1997; Cyr et al. 2011) and more rapidly during the fall as vertical mixing intensifies.

This report considers these three layers in turn. First, air temperature is examined because it is a significant driver of the surface layer, followed by the freshwater runoff. The winter sea ice and winter oceanographic conditions are described; these force the summer CIL, which is presented next. The deeper waters, mostly isolated from exchanges with the surface, are presented last along with a summary of major oceanographic surveys.

AIR TEMPERATURE

The monthly air temperature anomalies for several stations around the Gulf are shown in Fig. 4 for 2013–2014. Data up to 2013 are the Second Generation of Homogenized Surface Air Temperature Data, part of the Adjusted and Homogenized Canadian Climate Data (AHCCD), which accounts for shifts due to the relocation of stations, changes in observing practices and automation (Vincent et al. 2012). These are updated for 2014 using climate summaries from Environment Canada's National Climate Data and Information Archive (NCDIA). Comparisons between the two data sets are available for several stations around the Gulf in Galbraith and Larouche (2013) for April-November averages and in Galbraith et al. (2013) for December-February averages. Several airport weather reporting stations have switched over to new NAV Canada sensors and reporting tool and have changed station identification numbers. Nevertheless these data have been merged with previous data if the station positions and altitudes are close to previous EC stations.

Fig. 5 shows the annual, winter (December-March), and April-November mean air temperature anomalies averaged over all stations shown in Fig. 4, since 1873. Record-high annual and winter temperatures occurred in 2010 and record-high April-November temperatures in 2012. Galbraith et al. (2012) found the average NCDIA April-November air temperature over the Gulf to be a good proxy for May-November sea-surface temperature over the Gulf (but excluding the estuary) and found within the former a warming trend of 0.9°C per century between 1873 and 2011; the same trend is found here over the selected ACCHD stations between 1873 and 2014 (Fig. 5). The NCDIA December-March air temperatures in the western Gulf are highly correlated (r^2=0.67) with sea-ice properties, as well as with winter mixed layer volumes (Galbraith et al. 2010). Galbraith et al. (2013) found slightly higher correlations (r^2=0.72) with sea-ice using December-February ACCHD averages, possibly because March temperature are of less importance during low sea-ice cover since much of the sea-ice cover decrease has occurred much earlier in February.

Air temperatures were below normal in December 2013, by 6.3°C at Chevery (-2.2 SD, coldest since 1972 and fifth coldest since 1873), and by 5.1°C on average over available Gulf stations (-2.3 SD, coldest since 1972 and tenth lowest since 1873). March 2014 air temperatures were lowest since 1939 at Mont-Joli (-4.6°C, -2.8 SD) and Bathurst (-5.7°C, -3.1 SD), and lowest averaged over all stations since 1948 (-4.4°C, -2.1 SD). Overall the winter was cold, with a December-March average air temperature anomaly of -2.5°C (-1.6 SD). July air temperatures were at series record highs at Plum Point (since 1972, +3.2°C, +2.4 SD), Baie-Comeau (since 1965, +2.2°C, +3.0 SD), Îles-de-la-Madeleine (since 1934, +2.8°C, +2.0 SD) and Daniel's Harbour (since 1947, +3.6°C, +2.5 SD), and at a high since 1921 at Stephenville (+2.8°C, +2.5 SD). Averaged over all stations, July had the warmest air temperatures on record (since 1873, +2.1°C, +2.3 SD). The warm period persisted into August in the Estuary and northwest Gulf, with an anomaly of +2.2 SD at Sept-Îles (highest since 1955; +2.3 SD) and anomalies of +1.8°C at Mont-Joli and Baie-Comeau.

April-November air temperatures were just above-normal with an anomaly of +0.3°C (+0.5 SD) and the annual averaged air temperatures were near-normal overall.

PRECIPITATION AND FRESHWATER RUNOFF

Freshwater runoff data for the St. Lawrence River are updated monthly (Fig. 6, lower curve) using the water level method from Bourgault and Koutitonsky (1999) and are available from the St. Lawrence Global Observatory. A hydrological watershed model was used to estimate the monthly runoff since 1948 for all other major rivers flowing into the Gulf of St. Lawrence, with discharge locations as shown in Fig. 7. The precipitation data (NCEP reanalysis, six hourly

intervals) used as input in the model were obtained from the NOAA-CIRES Climate Diagnostics Center (Boulder, Colorado, USA; Kalnay et al. 1996). The data were interpolated to a ¼° resolution grid and the water routed to river mouths using a simple algorithm described here. When air temperatures were below freezing, the water was accumulated as snow in the watershed and later melted as a function of warming temperatures. Water regulation is modelled for three rivers that flow into the estuary (Saguenay, Manicouagan, Outardes) for which the annual runoff is redistributed following the climatology of the true regulated runoffs for 12 months thereafter. Runoffs were summed for each region shown and the climatology established for the 1981–2010 period. The waters that flow into the Estuary (region 1, Fig 7.) were added to the St. Lawrence River runoff measured at Québec City to produce the RIVSUM II index, although no advection lags were introduced (Fig. 6, upper curve).

Monthly anomalies of the summed runoffs for 2013 and 2014 are shown in Fig. 8. Rivers other than the St. Lawrence contribute about 5 000 $m^3 s^{-1}$ runoff to the Estuary, the equivalent of 40% of the St. Lawrence River, while the other tributaries distributed along the border of the GSL provide an additional 3 500 $m^3 s^{-1}$ in freshwater runoff to the system. River regulation has a strong impact on the relative contributions of sources. For example, in May 2012 the higher-than-average river runoff into the Estuary (an effect of the heavy precipitation in 2011 and river regulation) was almost as important as the then below-normal St. Lawrence run-off (not shown). The 2014 simulation shows that rivers in regions 2, 3, 4 and 5 behaved similarly, with below normal runoff in winter and above normal in June. The long-term time series are shown, summed by large basins, in Fig. 9. Broad long-term patterns of runoff over the large basins were similar to that of the St. Lawrence River but interannual variability is low in the Northeast basin and Magdalen Shallows basin. The annual average runoff of the St. Lawrence River measured at Québec City and RIVSUM II both show a general downward trend from the mid-1970s until 2001, an upwards trend since 2001 and were above-normal in 2014 (Fig. 9) at 12 600 $m^3 s^{-1}$ (+0.7 SD) and 18 100 $m^3 s^{-1}$ (+1.1 SD) respectively. Runoff was low in winter, consistent with the very cold air temperatures. The spring freshet was above-normal at +1.8 SD and +1.9 SD for the St. Lawrence River and RIVSUM II respectively, but its timing in May was normal for RIVSUM II (Fig. 6). The fall freshet was also above normal and earlier than normal.

SURFACE LAYER

The surface layer conditions of the Gulf are monitored by various complementary methods. The shipboard thermosalinograph network (Galbraith et al. 2002) consists of temperature-salinity sensors (SBE-21; Sea-Bird Electronics Inc., Bellevue, WA) that have been installed on various ships starting with the commercial ship Cicero of Oceanex Inc. in 1999 (retired in 2006) and on the Cabot from 2006 to fall 2013. While no data are available for 2014, its replacement, the Oceanex Connaigra, was outfitted with a thermosalinograph by early 2015.

The second data source is the thermograph network (Gilbert et al. 2004, Galbraith et al. 2007), which consists of a number of stations with moored instruments recording water temperature every 30 minutes (Fig. 10). Most instruments are installed on Coast Guard buoys that are deployed in the ice-free season, but a few stations are monitored year-round. The data are typically only available after the instruments are recovered except for oceanographic buoys that transmit data in real-time. Data from Shediac station acquired by the DFO Gulf Region are also included here. The network provides valuable near-surface temperature data at fixed sites and at short sampling intervals, but usually not in real-time nor during winter months.

The third data source are 1 km resolution monthly composite Sea Surface Temperature (SST) generated using National Oceanic and Atmospheric Administration (NOAA) and European Organisation for the Exploitation of Meteorological Satellites (EUMETSAT) Advanced Very High

Resolution Radiometer (AVHRR) satellite images available from the Maurice Lamontagne Institute sea surface temperature processing facility (details in Galbraith and Larouche, 2011, and Galbraith et al. 2012). These data are available for sea-ice free months with 1985-2010 climatologies computed for the months of May to November. Unfortunately, the MLI data processing has been on hold since September 2013 because of unresolved lack of hard disk space, and so the months since were filled-in using AVHRR composites provided by the Bedford Institute of Oceanography (BIO) Operational Remote Sensing. However a thorough comparison of the data sets has not been completed.

SST SEASONAL CYCLE CLIMATOLOGY

The May to November cycle of weekly averaged surface temperature is illustrated in Fig. 11 using a 1985–2010 climatology based on AVHRR remote sensing data for ice-free months complemented by 2001–2010 thermosalinograph data for the winter months. Galbraith et al. (2012) have shown that Gulf-averaged air temperature and SST monthly climatologies match up quite well with SST lagging air temperature by half a month. Maximum sea-surface temperatures are reached on average during the second week of August but that can vary by a few weeks from year to year. The maximum surface temperature averages 15.6°C over the Gulf during the second week of August (1985–2010), but there are spatial differences: temperatures on the Magdalen Shallows are the warmest of the Gulf, averaging 18.1°C over the area, and the coolest are at the head of the St. Lawrence Estuary and upwelling areas along the lower north shore.

SST IN 2014

The 2014 monthly mean sea-surface temperatures from AVHRR imagery are shown in Fig. 12 as colour-coded maps and the corresponding temperature anomaly maps are shown in Fig. 13 referenced to 1999–2010 monthly climatologies. Missing anomaly pixels are because of incomplete climatologies due to ice cover in winter months. The SST information is summarized in Fig. 14, showing the 2013 and 2014 monthly surface temperature anomalies spatially averaged over the Gulf and over each of the eight regions delimited by the areas shown in Fig. 2, and further into sub-regions of the Estuary as shown in Fig. 15 (Saguenay not available in data from BIO at this time). In contrast to the generally near-normal temperatures of 2013, near-surface water temperatures were generally normal or above normal in 2014. Record highs were reached in August averaged over the Gulf (T=17.8°C, above normal by +2.5°C and breaking the August 2012 record of +2.0°C) and in the following regions: Estuary (+4.2°C, +4.4 SD), Northwest Gulf (+4.1°C, +4.4 SD), Anticosti Channel (+2.8°C, +3.2 SD) and Cabot Strait (+2.9°C, +3.2 SD).

Figures 16 and 17 show the 1985–2014 time series of monthly surface temperature anomalies spatially averaged over the Gulf of St. Lawrence and over the eight regions of the Gulf. These results show that Gulf-wide averaged temperatures in 2014 were above normal from May to November by +1.2°C (+1.8 SD), similar to temperatures in 2012.

Sea-surface temperature monthly climatologies and time series were also extracted for more specific regions of the Gulf. The monthly average SST for the St. Lawrence Estuary as a whole (region 1) is repeated in Fig. 18 along with averages for the proposed Manicouagan Marine Protected Area (MPA), the proposed St. Lawrence Estuary MPA, and the Saguenay – St. Lawrence Marine Park. The overall pattern is similar across regions, but there are differences associated with episodic local events such as eddies and upwellings. The climatology averages also differ, for example the Manicouagan maximum monthly average temperature is 1.0°C warmer than for the Estuary as a whole.

The Magdalen Shallows, excluding Northumberland Strait, is divided into western and eastern areas as shown in Fig. 19. The monthly average SST for the Magdalen Shallows as a whole (region 8) is repeated in Fig. 20 along with averages for the western and eastern areas. Climatologies differ by roughly 0.5°C to 1°C between the western and eastern regions. Temperatures were above normal from June through August in both regions and below normal in November.

Thermograph network observations are compared to daily average temperatures calculated using all available data for each day of the year at each station and depth (Figs. 21-23). The seasonal cycle of near-surface temperature is measured by shallow instruments, while Cold Intermediate Layer warming from spring to fall is captured by instruments moored between 30 and 120 m depth. Monthly average temperatures are also shown, with the magnitude of their anomaly colour-coded. Salinities are shown in a similar fashion in Fig. 24. The average monthly temperatures for each station at shallow sampling depths (< 20 m) for 2013 and 2014 are also shown in Fig. 25.

Monthly anomalies were fairly consistent across all stations of each of the three regions listed in Fig. 25. As with AVHRR data sources and in spite of different climatological periods, the months of June and August show widespread warm anomalies in the Estuary, and August shows warm near-surface anomalies at almost every station. Winter temperatures were below at Île Shag. Fig. 23 shows spring warming at Île Shag and the red lines span the historical dates when spring temperature increased over 1.5°C, a temperature associated with increased lobster mobility. This occurred for a brief period in late April but only definitely on May 2, which is one of the latest dates of occurrence since measurements began there in 1994.

Fig. 26 shows information similar to Fig. 25, but for thermograph sensors moored deeper than 20 m. The deep (>300 m) waters of the Estuary had above normal temperatures in 2014 with a series record of the daily average temperature (since 2005) of 5.53°C occurring in July, also the month with a record-high monthly average of 5.45°C (Figs. 21 and 27).

Fig. 27 shows the history of monthly averaged temperature anomalies for selected stations. The Île Shag (10 m) station shows bottom temperatures close to Îles-de-la-Madeleine that are important to the lobster fishery and highlights the coldest month of May since 2002. The Shediac Valley (82 m) station shows interannual variability and the seasonality of bottom temperatures on the Magdalen Shallows which were below normal in 2014, associated with the Cold Intermediate Layer. The Rimouski station (330 m) shows the recent warming trend in bottom temperatures within the Estuary since the cold anomaly of 2010. There are large differences in springtime bottom temperature at the Strait of Belle Isle (71 m) depending on how late the cold inflow of Labrador Shelf Water persists. Figs. 22 and 27 show that deep temperatures in the Strait of Belle Isle were below -1°C well into June, which could be associated with prolonged entry of Labrador Shelf waters into the Gulf. However Fig. 24 shows that salinities dropped to values well below 32.2 after late May, a cut-off value associated with wintertime Labrador Shelf waters (Galbraith, 2006); sea-ice melt may be responsible, but the dilution still makes it difficult to discern Gulf waters from Labrador Shelf waters.

SEA ICE

Ice volume is estimated from three gridded databases of ice cover and ice categories obtained from the Canadian Ice Service (CIS). Weekly GIS charts covering the period 1969-2014 and daily charts covering the period 2009-2014 were gridded on a 0.01° latitude by 0.015° longitude grid (approximately 1 km resolution), and 5-km resolution gridded daily files were obtained directly from the CIS covering the period 1998-2008. Some of the analyses described below were done using the weekly data exclusively, for long-term consistency, while for others daily

data were used when available with results filtered using a 3-day running mean in order to make them more comparable to results calculated from weekly data.

Ice typically forms first in December in the St. Lawrence estuary and in shallow waters along New Brunswick, Prince Edward Island and the lower north shore and melts last in the northeast Gulf where the ice season duration tends to be longest apart from shallow bays elsewhere (Fig. 28). Offshore sea ice is typically produced in the northern parts of the Gulf and drifts towards Îles-de-la-Madeleine and Cabot Strait during the ice season. The maximum estimated ice volume in 2014 occurred the week of March 17 and is compared with the 1981-2010 climatology in Fig. 29 (upper panels). The 1981-2010 climatology and 2014 distribution of the thickest ice recorded during the season at any location is also shown in Fig. 29 (lower panels); the climatological thick areas in the northeast are mostly associated with ice that has entered the Gulf through the Strait of Belle Isle and are pushed by the wind either on the lower north shore or on the coast of Newfoundland.

Fig. 30 shows the daily evolution of the estimated sea-ice volume in relation to the climatology and historical extremes. It clearly shows why the high interannual variability in ice cover leads to weak normalized anomalies even in cases of near-absence of sea-ice. Fig. 31 shows the estimated seasonal maximum ice volumes within the Gulf as well as on the Scotian Shelf. The combined Gulf and Scotian Shelf ice volume shown separately as top and bottom panels of Fig. 31 is indicative of the total volume of ice produced in the Gulf, including the advection out of the Gulf, but it also includes the thicker sea ice that drifts into the Gulf from the Strait of Belle Isle. The volume shown on the bottom panel of Fig. 31 corresponds to that found seaward of Cabot Strait (defined by its narrowest crossing). It would represent the volume of ice exported from the Gulf provided that no melt had already occurred.

Fig. 32 shows the day of first and last occurrence of ice in each of the regions of the Gulf of St. Lawrence as well as duration of the ice season and maximum observed volume during each season. The regional averages were extracted exclusively from the weekly database while the three volume estimates for the Gulf and Scotian Shelf at the bottom of Fig. 32 use daily data for 1998 onwards (with 3-day filtering).

Fig. 33 shows the time series of seasonal maximum ice volume and area (excluding thin new ice), ice season duration and December-to-March air temperature anomaly (from Fig. 5). The figure shows declining trends in ice cover severity since 1990 with the rebound of 2014. The correlation between annual maximum ice volume (including the Scotian Shelf) and the December-February air temperature averaged over five Western Gulf stations (Sept-Îles, Mont-Joli, Gaspé, Charlottetown and Îles-de-la-Madeleine) accounted for 72% of the variance using the 1969–2012 time series (Galbraith et al. 2013). Fig. 33 shows a similar comparison using ice volume and the ACCHD December-to-March air temperature anomaly from Fig. 5 yielding R^2 = 0.74. The correlation between air temperature and the ice parameters season duration and area are also very high (R^2 = 0.78-0.79). Correlation coefficients are slightly higher when using January to February air temperatures, perhaps because March air temperatures have no effect on ice cover that has almost disappeared by then during very mild winters.

In 2014, the seasonal maximum ice volume was 126 km^3 (Fig. 32), third highest of the 1969–2014 time series and nearly double the climatological average. This is in stark contrast to the four of the six lowest maximum ice volumes of the time series that have occurred in the previous four years. Ice was exported from the Gulf of St. Lawrence onto the Scotian Shelf for the first time after a four-year hiatus. The sea-ice cover throughout the season was typically above the 1981-2010 climatology except from mid-January to mid-February, and the seasonal maximum was reached at a near-normal time of year in mid-March (Fig. 30). The duration of the ice season was longer than normal in all regions except Cabot Strait, due to early ice formation in

all these regions and late melt in the northeast (Figs. 28 and 32). Sea-ice conditions are consistent with the December-March Gulf air temperature anomaly of -2.5°C (-1.6 SD, Fig. 5 and Fig. 33).

WINTER WATER MASSES

A wintertime survey of the Gulf of St. Lawrence waters (0–200 m) has been undertaken in early March since 1996 using a Canadian Coast Guard helicopter. This has added a considerable amount of data to the previously very sparse winter data for the region. The survey, sampling methods, and results of the cold-water volume analysis in the Gulf and the estimate of the water volume advected into the Gulf via the Strait of Belle Isle over the winter are described in Galbraith (2006) and in Galbraith et al. (2006). Fig. 34 and Fig. 35 show gridded interpolations of near-surface temperature, temperature above freezing, salinity, cold layer thickness and bottom contacts, and thickness of the Labrador Shelf water intrusion for 2014 as well as climatological means. Stations were only sampled from the ice in March 2014 such that ice-free areas are not represented in the analysis; the ice cover was however very widespread at that time of year (Fig. 29).

During winters prior to 2010, the surface mixed layer was usually very close (within 0.1°C) to the freezing point in most regions of the Gulf but thickness of the surface layer varied, leaving only variability in the cold-water volume between mild and severe winters. This was not the case in 2010 for the first time since the inception of the winter survey, when the mixed layer was on average 1°C above freezing. Similar conditions to those of 2010 were observed in March 2011, although not quite as warm. The winter surface mixed layer returned to near-normal conditions in 2012, as observed prior to 2010, whereby waters were near freezing at the end of winter over a large portion of the Gulf. Conditions in March 2014 were similarly cold (Fig. 34), consistent with the almost total ice cover. Areas missed by our sampling in the northern Gulf because of thin ice were areas where ice was actively being produced and transported away by winds, and are assumed to have been similarly cold.

During typical winters, surface waters in the temperature range of ~ 0°C to -1°C are only found on the northeast side of Cabot Strait. Some of these warm waters have presumably entered the Gulf during winter and flowed northward along the west coast of Newfoundland, however it is also possible that local waters could have simply not cooled close to freezing. There was no such area in 2014. Near-freezing waters with salinities of around 32 are responsible for the (local) formation of the CIL since that is roughly the salinity at the temperature minimum during summer. These are coded in blue in the salinity panel of Fig. 34 and are typically found to the north and east of Anticosti Island. Surface salinities were generally higher than usual in this part of the Gulf during the winter of 2014.

Near-freezing waters with salinity >32.35 (colour-coded in violet) are considered to be too saline to have been formed from waters originating within the Gulf (Galbraith 2006) and are presumed to have been advected from the Labrador Shelf through the Strait of Belle Isle. These waters were present at the surface in Mécatica Trough and in the Strait of Belle Isle (Fig. 34) in March 2014. A T-S water mass criterion from Galbraith (2006) was used to identify intruding Labrador Shelf waters that have exhibited no evidence of mixing with warm and saline deep Gulf water. These waters occupied the northern portion of Mécatina Trough in March 2014 and extended in parts from the surface to the bottom at over 200 m depth (top-right panel of Fig. 35). The recent history of Labrador Shelf water intrusions is shown in Fig. 36, where its volume is shown as well as the fraction it represents of all the cold-water volume in the Gulf. This volume was near normal in March 2014, at 1200 km^3 (-0.3 SD), but below normal as the percentage of cold water (T<-1°C) it represents, at 8% (-0.6 SD).

The cold mixed layer depth typically reaches about 75 m in the Gulf and is usually delimited by the -1°C isotherm because the mixed layer is typically near-freezing and deeper waters are much warmer (Galbraith, 2006). In March 2010 and 2011 much of the mixed layer was warmer than -1°C such that the criterion of T<0°C was also introduced (see middle panels of Fig. 35). The cold surface layer is the product of local formation as well as cold waters advected from the Labrador Shelf, and can consist either of a single water mass or of layers of increasing salinity with depth. Integrating the cold layer depth over the area of the Gulf (excluding the Estuary and the Strait of Belle Isle) yields a cold-water (<- 1°C) volume of 14 100 km³ (Fig. 35), 0.8 SD above the 1996–2014 average and similar to the volume observed in 2009. The mixed layer volume increases to 15 100 km³ when water temperatures <0°C are considered which is 0.2 SD above the 1999–2014 average. This volume of cold water corresponds to 45% of the total water volume of the Gulf (33 500 km³, excluding the Estuary). The time series of winter cold-water (<-1°C) volume observed in the Gulf is shown in Fig. 37.

COLD INTERMEDIATE LAYER

PREDICTION FROM THE MARCH SURVEY

The summer CIL minimum temperature index (Gilbert and Pettigrew 1997) has been found to be highly correlated with the Gulf (excluding the estuary) volume of cold water (<-1°C) measured the previous March when much of the mixed layer is near-freezing (Galbraith 2006, updated relation in right panel of Fig. 37). This is expected because the CIL is the remnant of the winter cold surface layer. A measurement of the volume of cold water present in March is therefore a valuable tool for forecasting the coming summer CIL conditions. The winter mixed layer in 2014 was thick and near freezing throughout the Gulf, up to Cabot Strait, after four consecutive winters with warmer conditions. The overall thickness and volume of the layer colder than -1°C was second highest in the 1996-2014 time series after the record of 2003, a year when a record volume of Labrador Shelf Water also contributed towards the high overall volume. The Cold Intermediate Layer for summer 2014 was therefore forecasted to be colder than during the previous four summers and resemble conditions of 2009 with a Gilbert and Pettigrew (1997) index of around -0.5°C (Galbraith et al. 2014).

AUGUST CIL BASED ON THE MULTI-SPECIES SURVEY

The CIL minimum temperature, thickness and volume for T<0°C and <1°C were estimated using temperature profiles from all sources for August and September. Most data are from the multi-species surveys in September for the Magdalen Shallows and August for the rest of the Gulf. Using all available temperature profiles, each 1-m depth layer of the Gulf was spatially interpolated for temperature, with the interpolated field bound between the minimum and maximum values observed within each of the different regions of the Gulf (Fig. 2) to avoid spurious extrapolations. The CIL thickness at each grid point is simply the sum of depth bins below the threshold temperature, and the CIL minimum temperature is only defined at grid points where temperature rises by at least 0.5°C at depths greater than that of the minimum, or if the grid point minimum temperature is below the CIL spatial average of the Gulf.

Fig. 38 shows the gridded interpolation of the CIL thickness <1°C and <0°C and the CIL minimum temperature for August–September 2014 as well their 1985-2010 climatology (1994-2010 for Mécatina Trough). The CIL thickness for T<0°C and T<1°C rebounded to near-normal values since the 2012 minimum, with conditions similar to 2009 (not shown). Similar maps were produced for all years back to 1971 (although some years have no data in some regions), allowing the calculation of volumes for each region for each year as well as the climatologies shown on the left side of Fig. 38. The 2014 CIL conditions are similar to the 1985-2010

climatologies, but with higher thicknesses and lower minimum temperatures in Mécatina Trough and lower thicknesses and higher minimum temperatures in the Estuary and Cabot Strait.

The time series of the regional August–September CIL volumes are shown in Fig. 39 (for <0°C and <1°C). Most regions show increased CIL volumes in 2014 compared to 2013, with a record-high <1°C volume in Mécatina Trough. Fig. 40 shows the average CIL core temperature and the total volume of CIL water (<0°C and <1°C) from the August–September interpolated grids (e.g., Fig. 38). The CIL areal minimum temperature average and volume shown in Fig. 40 exclude data from Mécatina Trough which has very different water masses from the rest of the Gulf; it is influenced by inflow through the Strait of Belle Isle and is therefore not indicative of the climate in the rest of the Gulf. The CIL volume as defined by T<1°C increased significantly (to -0.4 SD) compared to 2013 conditions (-2.1 SD) and reached a volume similar to 2009 (-0.5 SD). In the case of the volume delimited by 0°C, it increased to a near-normal value (-0.2 SD) after a two-year near absence at that time of year and last year's record low (since 1985).

The time series of the CIL regional average minimum core temperatures are shown in Fig. 41. All regions show a decrease in core temperature. The 2014 average temperature minimum (excluding Mecatina Trough, the Strait of Belle Isle and the Magdalen Shallows) was -0.2°C, a decrease of 0.6°C, and is shown in Fig. 40 (bottom panel, green line). The overall 2014 CIL water mass properties are similar to observations of 2009.

NOVEMBER CIL CONDITIONS IN THE ST. LAWRENCE ESTUARY

The AZMP November survey provides a high-resolution conductivity-temperature-depth (CTD) sampling grid in the St. Lawrence estuary since 2006 although measurements are sparser in recent years including 2014. This allows a higher resolution display of the CIL minimum temperature in the Estuary (Fig. 42). The data also show the temporal warming (Fig. 39) and thinning (Fig. 41) since the August survey, although the data show a slightly higher volume in November 2014 compared to August-September, indicating some recirculation from the Gulf (see also CIL thickness observed at Rimouski station in Fig. 65 which shows a similar pattern). The CIL was colder and much thicker in November 2014 than in 2013. Fig. 41 shows that the fairly rapid increase of the CIL minimum temperature occurring between August and November is fairly constant inter-annually in spite of the differences in August temperature.

GILBERT AND PETTIGREW (1997) CIL INDEX

The Gilbert and Pettigrew (1997) CIL index is defined as the mean of the CIL minimum core temperatures observed between 1 May and 30 September of each year, adjusted to 15 July. It was updated using all available temperature profiles measured within the Gulf between May and September inclusively since 1947 (black line of the bottom panel of Fig. 40). As expected, the CIL core temperature interpolated to 15 July is almost always colder than the estimate based on August and September data for which no temporal corrections were made. This is because the CIL is eroded over the summer and therefore its core warms over time.

This CIL index for summer 2014 was -0.49°C, 0.2 SD below normal. The 0.58°C decrease from the summer 2013 CIL index is consistent with the increase in CIL volume between August 2013 and 2014 discussed above and the decrease of 0.64°C in the areal average of the minimum temperature in August. The warm winter conditions since 2010 led to CIL indices that were still far below the record high observed in the 1960s and 1980s. The earlier CIL temperature minimums will be re-examined to confirm that they were calculated using data with sufficient vertical resolution to correctly resolve the core minimum temperature. It is also becoming increasingly clear that the winter mixed layer is not the only factor explaining summertime CIL conditions and that mechanisms having a multi-year cumulative effect are required to explain

the interannual autocorrelations observed. For example, this may be linked to temperatures below the CIL, which in warm years may create a higher temperature gradient that leads to higher heat fluxes and faster summertime CIL warming rates.

As a summary, Fig. 43 shows selected time series of winter and summertime CIL conditions (June bottom temperatures also related to the CIL are outlined below) and highlights the strong correlations between these various time series. The CIL was colder and thicker in 2014 than in 2013, a return to near-normal values after the coldest winter since 1993. Overall CIL conditions were similar to those of 2009.

MAGDALEN SHALLOWS JUNE SURVEY

A long-standing assessment survey covering the Magdalen Shallows has taken place in June for mackerel and since merged with the June AZMP survey. It provides good coverage of the temperature conditions that are greatly influenced by the cold intermediate layer that reaches the bottom at roughly half of the surface area at this time of time.

Near-surface waters warm quickly in June, mid-way between the winter minimum and the annual maximum in early August. This can introduce a bias if the survey dates are not the same each year. To account for this, the seasonal warming observed at the Shediac Valley AZMP monitoring station was evaluated. A linear regression was performed of temperature versus time for each meter of the water column for each year with monitoring data at Shediac Valley between May and July. Visual inspection showed that the depth-dependent rate was fairly constant for all years and an average was computed for every depth. Warming is maximal at the surface at 18°C per 100 days and, in spite of some uncertainties between 30 and 55 m, decreases almost proportionally with depth to reach 2°C per 100 days at 40 m, followed by a further linear decrease to reach 1°C per 100 days at 82 m (Galbraith and Grégoire, 2015).

All available temperature profiles taken in June from a given year are binned at 1m depth intervals (or interpolated if the resolution is too coarse) and then adjusted according to the sampling date to offset them to June 15th according to the depth-dependent warming rate extracted from Shediac Valley monitoring data. An interpolation scheme is used to estimate temperature at each 1 m depth layer on a 2 km resolution grid. Fig. 44 shows temperatures and anomalies at depths of 20, 30 and 50 m. Fig. 45 shows averages over the grids at 0, 10, 20, 30, 50 and 75 m for all years when interpolation was possible, as well as SST June averages since 1985, for both western and eastern regions of the Magdalen Shallows (Fig. 19). Temperatures were normal to well below normal at 20, 30 and 50 m (Fig. 44). On average, temperatures were below normal at all depths except at 75 m on the western Shelf (Fig. 45).

BOTTOM WATER TEMPERATURES

Bottom temperature is also estimated at each point of the above grids by looking up the interpolated temperature at the depth level corresponding to a bathymetry grid provided by the Canadian Hydrographic Service with some corrections applied (Dutil et al. 2012). The method is fully described in Tamdrari et al. (2012). A climatology was constructed by averaging all available temperature grids between 1981 and 2010 and anomaly grids were computed for each year. The June bottom temperature climatology as well as the 2014 reconstructed temperature and anomaly fields are shown in Fig. 46. Temperature anomalies are typically greater than +2.0°C in shallow waters, but in deeper waters the bottom area occupied by waters colder than 0°C is larger than the climatology, with some areas with waters colder than -1°C.

The same method was applied to the entire Gulf by combining all available CTD data from August and September, thus including the multispecies surveys for the northern Gulf in August

and for the Magdalen Shallows in September into a single map (Fig. 47). Most of the northeastern Gulf had above normal bottom temperatures, with large areas of Anticosti and Esquiman Channels above 6°C.

Time series of the bottom area covered by water in various temperature intervals were estimated from the gridded data for the June surveys as well as for the September multispecies survey on the Magdalen Shallows (Fig. 48). Unlike the very cold conditions observed on the bottom in 2008, very little of the bottom of the Magdalen Shallows was covered by water with temperatures <-1°C in June 2014, however a large area with temperatures <0°C covered the bottom. The area had decreased considerably by September 2014, but still represented colder conditions than in years since 2008. The time series of areas of the Magdalen Shallows covered by water colder than 0, 1, 2, and 3°C in September are also shown in Fig. 43. The area covered by water temperatures <1°C had reached a low not seen since 1983 in 2012 but rebounded to near-normal in 2014 (Fig. 43). Areas with T< 0°C, < 1°C, < 2°C and < 3°C were also near-normal in 2014. The thermograph network (Fig. 23) also showed bottom temperatures at Shediac Valley (82 m) to be below normal (using a different reference period) from June to October.

Time series of the bottom area covered by water in various temperature intervals were also estimated for the other regions of the Gulf based on August-September temperature profile data (Figs. 49 and 50). Many areas had bottom waters colder than 0°C, and Mécatina Trough had bottom waters colder than -1°C. The figures also show compression of the bottom habitat area in the temperature range of 5–6°C in 1992. In 2012, a return of >6°C temperatures to the sea floor was observed. The bottom area covered by waters warmer than 6°C increased in 2014 in Anticosti Channel, Esquiman Channel and Central Gulf, and reached a record value in Esquiman Channel while reducing its bottom habitat area in the temperature range of 5–6°C.

SEASONAL AND REGIONAL AVERAGES OF TEMPERATURE PROFILES

In order to show the seasonal progression of the vertical temperature structure, regional averages are shown in Figs. 51 to 54 based on the profiles collected during the March helicopter survey, the June AZMP and mackerel surveys, the August multi-species survey (September survey for the Magdalen Shallows), and the October-November AZMP survey and including all additional archived CTD data for those months. The temperature scale was adjusted to highlight the CIL and deep-water features; the display of surface temperature variability is best suited to other tools such as remote sensing and thermographs. During the surveys, a total of 79 CTD casts in March, 126 casts in June, 290 casts in August, 256 in September, 128 in October and 78 in November were obtained within the regions shown in Fig. 2. Average discrete depth layer conditions are summarized for the months of the 2013 and 2014 AZMP surveys in Fig. 55 for temperature and in Fig. 56 for salinity and 0-50 m stratification. For each survey the anomalies were computed relative to monthly temperature and salinity climatologies calculated for each region.

Monthly temperature and salinity climatologies for 1981–2010 were constructed for various depths using a method similar to that used by Petrie et al. (1996) but using the geographical regions shown in Fig. 2. All available data obtained during the same month within a region and close to each depth bin are first averaged together for each year. Monthly averages from all available years and their standard deviations are then computed. This two-fold averaging avoids the bias that occurs when the numbers of profiles in any given year are different. The temperature climatologies are shown in grey as the mean value ± 0.5 SD (Figs. 51 to 54).

The March water temperature conditions were discussed at length in earlier sections and are included here for completeness (Fig. 51), but caution is needed in interpreting the mean profiles.

Indeed, regional averaging of winter profiles does not work very well in the northeast Gulf (regions 3 and 4) because very different water masses are present in the area such as the cold Labrador Shelf intrusion with saltier and warmer deeper waters of Anticosti Channel or Esquiman Channel. For example, the sudden temperature decrease near the bottom of Mécatina Trough in 2013 resulted from the deepest cast used in each of the averages, which contained colder Labrador Shelf intrusion water. Large changes near 200 m are due to our usual sampling cutoff near 200 m for the March airborne survey, with some casts being slightly deeper than others. The highlights of March water temperatures shown in Fig. 51 include the previously discussed winter mixed layer, with below-normal temperatures and above-normal thickness. The thermocline was much shallower than usual in most regions, associated with temperatures well above normal at 200 m. Temperatures of 7.5°C recorded in a few casts around 200 m on the Newfoundland side of Cabot Strait were some of the highest for deep waters on record for the Gulf.

Temperatures in June 2014 (Fig. 52 and summary in Fig. 55) were characterized by CIL conditions that were above normal in thickness and below-normal in minimum temperature. Deep-water temperatures were above normal in all regions along the Laurentian Channel, with most regions showing increases compared with 2013 conditions. Temperatures at the depth of the temperature maximum (200 to >250 m) were above normal in Esquiman Channel and central Gulf, exceeding 6°C at depth, presumably advected in from the Cabot Strait 2012 record-high conditions. In November (Fig. 54), waters found in the first 100 m in Mécatina Channel were much warmer than normal. Their temperature and salinity range (Figs. 54 and 55) identifies them as waters typically found in Esquiman Channel, indication that an unusual circulation pattern had occurred.

DEEP WATERS (>150 M)

The deeper water layer (>150 m) below the CIL originates at the entrance of the Laurentian Channel at the continental shelf and circulates towards the heads of the Laurentian, Anticosti, and Esquiman channels without much exchange with the upper layers. The layer from 150 to 540 m is characterized by temperatures between 1 and >7°C and salinities between 32.5 and 35 (except for Mécatina Trough where near-freezing waters may fill the basin to 235 m in winter and usually persist throughout the summer). Interdecadal changes in temperature, salinity, and dissolved oxygen of the deep waters entering the Gulf at the continental shelf are related to the varying proportion of the source cold–fresh and high dissolved oxygen Labrador Current water and warm–salty and low dissolved oxygen slope water (McLellan 1957, Lauzier and Trites 1958, Gilbert et al. 2005). These waters travel from the mouth of the Laurentian Channel to the Estuary in roughly three to four years (Gilbert 2004), decreasing in dissolved oxygen from in situ respiration and oxidation of organic material as they progress to the channel heads. The lowest levels of dissolved oxygen (around 20 percent saturation in recent years) are therefore found in the deep waters at the head of the Laurentian Channel in the Estuary.

TEMPERATURE AND SALINITY

The calculation of monthly temperature and salinity climatologies mentioned earlier using a method similar to that of Petrie et al. (1996) also provides time series of monthly averaged values. These monthly averages were further averaged into regional yearly time series that are presented in Fig. 57 for 200 and 300 m. The 300 m observations in particular suggest that temperature anomalies are advected up-channel from Cabot Strait to the northwestern Gulf in two to three years, consistent with the findings of Gilbert (2004). The regional averages are weighted into a Gulf-wide average in accordance to the surface area of each region at the specified depth. These Gulf-wide averages are shown for 200 and 300 m in Fig. 57 as well as

for 150, 200, and 300 m in Fig. 58. Linear trends in temperature and salinity at 300 m of 2.2°C and 0.3 per century, respectively are shown on Fig. 58 (See also Galbraith et al. 2013 for other long term trends). Some older values have changed since last year's report from the removal of some anomalously suspect historical temperature-salinity profiles.

In 2014, the gulf-wide average temperatures and salinities were above normal at all depths shown in Fig. 57. Temperature at 300 m increased overall to reach 5.9°C (+2.4 SD); the highest since 1980. It increased in central Gulf and Cabot Strait to reach 6.0°C (+2.1 SD) and 6.2°C (+2.2 SD), highest since 1980 and 1977 respectively. Temperature at 200 m increased overall to reach 5.3°C (+2.0 SD); the highest on record. It increased in central Gulf and Cabot Strait to reach 5.8°C (+2.4 SD) and 6.3°C (+2.3 SD), highest since 1979 and 2012 respectively. The warm anomaly present since 2010 at Cabot Strait should continue to progress up the channel towards the Estuary for a few more years; the 300-m temperature in the Northwest Gulf was well above normal (+1.9 SD) but may still increase in upcoming years.

Salinity increased overall by 0.7 SD at 200 m but decreased by 0.3 SD at 300 m where it became near normal. Salinity at 300 m was near normal in all regions, but was above normal in the southern portion of the Laurentian Channel from Esquiman Channel to Cabot Strait. This warm-salty anomaly should continue to progress up the channel towards the Estuary in the next 3 years.

DISSOLVED OXYGEN AND HYPOXIA IN THE ST. LAWRENCE ESTUARY

Fig. 58 shows an update of the Gilbert et al. (2005) oxygen time series of the mean dissolved oxygen value at depths ≥295 m in the St. Lawrence Estuary expressed as a percentage of saturation at surface pressure. Since some of the variability is associated with changing water masses, the temperature at 300 m in the Estuary is also shown. The deep waters of the Estuary were briefly hypoxic in the early 1960s and have consistently been hypoxic since 1984. Dissolved oxygen decreased to its second lowest annual average in 2014, at 56.7 μmol l^{-1} (-1.2 SD).

Based on interdecadal variability, the inflow of warmer (colder) waters to the Estuary is expected to deteriorate (ameliorate) the hypoxic conditions since these waters are typically poorer (richer) in dissolved oxygen (McLellan 1957, Lauzier and Trites 1958, Gilbert et al. 2005). The decrease in dissolved oxygen since 2013 is greater than that anticipated from source water mass changes; a change of dissolved oxygen of 147.4 μmol l^{-1} is accounted for by a 10.09°C temperature difference in source water masses in Gilbert et al 2005, implying that a decrease of 1.3 μmol l^{-1} would be expected with the 0.09°C temperature increase between 2013 and 2014, while a decrease of 9.4 μmol l^{-1} was observed. Recent interannual variability in the Gilbert et al. 2005 updated time series and CTD-based regional time series shown in Fig. 57 (bottom block) do not show changes in dissolved oxygen that would have been expected to be associated with changes in temperature. Differences between the Gilbert et al. 2005 updated time series and the CTD-based time series from the Estuary should be investigated (bottom panel of Fig. 57).

CURRENTS AND TRANSPORTS

Currents and transports are derived from a numerical model of the Gulf of St. Lawrence, Scotian Shelf, and Gulf of Maine. The model is prognostic, i.e., it allows for evolving temperature and salinity fields. It has a spatial resolution of 1/12° with 46 depth-levels in the vertical. The atmospheric forcing is taken from the Global Environmental Multiscale (GEM) model run at the Canadian Meteorological Center (CMC). Freshwater runoff is obtained from observed data and the hydrological model, as discussed in the freshwater runoff section. A simulation was run for

2006–2014 from which transports were calculated. The reader is cautioned that the results outlined below are not measurements but simulations and improvements in the model may lead to changes in the transport values.

Figs. 59–61 show seasonal depth-averaged currents for 0–20 m, 20–100 m, and 100 m to the bottom for 2014. Currents are strongest in the surface mixed layer, generally 0–20 m, except in winter months when the 20–100 m and the 100m to bottom averages are almost as high (note the different scale for this depth). Currents are also strongest along the slopes of the deep channels. The Anticosti Gyre is always evident but strongest during winter months, when it even extends strongly into the bottom-average currents.

Monthly averaged transports across seven sections of the Gulf of St. Lawrence are shown in Fig. 62 for sections with estuarine circulation, and in Fig. 63 for sections where only net transports are relevant. In Fig. 62, the net transport integrates both up and downstream circulation and, for example, corresponds to freshwater runoff at the Pointe-des-Monts section. The outflow transport integrates all currents heading toward the ocean, while the estuarine ratio corresponds to the outflow divided by the net transports.

Transports through sections under the direct estuarian influence of the St. Lawrence River (e.g., Pointe-des-Monts) have a more direct response to change in freshwater runoff while others (e.g., Cabot Strait, Bradelle Bank) have a different response, presumably due to redistribution of circulation in the GSL under varying runoff. The estuarine circulation ratio is determined by the mixing intensities within the estuary and is greatly influenced by stratification. It is on average greatest during winter months and weakest during the spring freshet. In fact, it is sufficiently reduced in spring that the overall outward transport at Pointe-des-Monts reaches its minimum value in June even though this month corresponds to the third highest net transport of the year, i.e. the estuary becomes sufficiently stratified that fresh water runoff tends to slip on top of the denser salty waters underneath. In 2014, the estuarine ratio at Pointe-des-Monts was above-normal in winter, August and fall. The above-normal spring freshet led to below-normal Estuarine ratio and near-normal outward transport at the Pointe-des-Monts section, however the above-normal fall freshet (of lower overall flow rate than in spring) led to above-normal Estuarine ratio and outward transport.

HIGH FREQUENCY SAMPLING AZMP STATIONS

Sampling by the Maurice Lamontagne Institute began in 1991 at a station offshore of Rimouski (48° 40' N 68° 35' W; Plourde et al. 2009), typically once a week during summer and less often during spring and fall and almost never in winter (Fig. 64). In 2013, following several analyses that identified good correlations and correspondences between the prior AZMP Anticosti Gyre and Gaspé Current stations with the Rimouski station, it was decided to drop sampling efforts at other logistically difficult stations and integrate the Rimouski station officially in the AZMP program. The AZMP station in the Shediac Valley (47° 46.8' N, 64° 01.8' W) is sampled on a regular basis by the Bedford Institute of Oceanography as well as occasionally by DFO Gulf Region and by the Maurice Lamontagne Institute during their Gulf-wide surveys (Fig. 64). This station has been sampled irregularly since 1947, nearly every year since 1957, and more regularly during the summer months since 1999 when the AZMP program began. However, observations were mostly limited to temperature and salinity prior to 1999.

Isotherms and isohalines as well as monthly averages of layer temperature and salinity, stratification, and CIL core temperature and thickness at <1°C are shown for 2010-2014 for the Rimouski station in Fig. 65 and for the Shediac Valley station in Fig. 66. The scorecard climatologies are calculated from 1991-2010 data for Rimouski station, and for 1981-2014 for Shediac Valley (given the sparseness of data prior to 1999).

At the Rimouski station, the CIL typically had below-normal thickness and above-normal minimum temperature in spite of the near-normal conditions prevailing in the Gulf. At 200-300 m, the gradual shift of cold-fresh waters present in 2010 to warmer-saltier waters advected from Cabot Strait lead to a shift to warm anomalies by May 2013 and series records in temperature and salinity observed during the summer of 2014 (See also the Rimouski Station record observed in the thermograph network data; Fig. 27). At the Shediac Valley station, deep waters started off the spring with below-normal temperatures consistent with the cold winter conditions, but were near normal by August. Stratification was above normal in July (+2.3 SD) in agreement with the above-normal (+1.9 SD) spring freshet runoff.

Fig. 67 shows the interannual variability of some bulk layer averages from May to October for the two stations. Bulk surface layer temperature and salinity were normal at Rimouski station while stratification and CIL minimum temperature were above normal, and CIL thickness below normal. Near-bottom temperature (290 m) was at a record high. Bulk surface layer (0-50 m) temperature had been above normal at Shediac Valley station for three consecutive years but was near normal in 2014.

OUTLOOK FOR 2015

Air temperatures were respectively 1°C, 4.5°C and 2.8°C below normal over the Gulf in January, February and March. This was the setting for the March 2015 survey, which provides an outlook for CIL conditions expected for the remainder of 2015. Fig. 68 shows the surface mixed layer temperature, salinity, and thickness (at T<-1°C and T<0°C), as well as the thickness and extent of the cold and saline layer that has intruded into the Gulf from the Labrador shelf. The winter mixed layer was thick and near freezing throughout the Gulf, up to Cabot Strait, similar to conditions of March 2014. The overall thickness and volume of the layer colder than -1°C was near normal and the Cold Intermediate Layer for summer 2015 is therefore forecasted to be a bit warmer than in 2014, with a Gilbert and Pettigrew (1997) index of around -0.4°C compared to -0.5°C in 2014.

Conditions are quite different at depth. Recall that record high temperatures were recorded in Cabot Strait in 2012 and again in 2014. There were 7 stations sampled in March 2015 with some deep-water temperatures greater than 6°C, located from Cabot Strait up to Centre Gulf. This signifies the continuation of warmer than normal conditions at depth.

SUMMARY

Fig. 69 summarizes SST, CIL and deep-water average temperatures. For May-November SST, a proxy is used prior to 1985 using the April-November air temperature anomaly averaged over all stations of Fig. 4 except the two from the Estuary, similar to the index developed in Galbraith et al. (2012). Fig. 69 shows increases from 2013 values for May-November average SST, average temperature at 200 m and 300m, but a decrease in the CIL temperature minimum. The SST was similar to that of 2012 and was the 3rd highest on record, temperature at 200 m was the highest on record and was second highest after 1980 at 300 m. The CIL temperature minimum returned to near-normal following the coldest winter since 1993.

To further summarize the temperature state of the Gulf of St. Lawrence, nine time series are chosen to represent surface and deep conditions (Fig. 70). Here, the CIL is grouped as a shallow feature since the winter surface mixed layer generates it. Fig. 71 shows three annual composite index time series (Petrie et al. 2007) constructed as the sum of these anomalies, representing the state of different parts of the system, with each time series contribution shown as stacked bars. The first anomaly sum represents the entire water column, whereas the

second and third sums represent the state of the shallow and deep parts of the water column, which are decoupled. These composite indices measure the overall state of the climate system with positive values representing warm conditions and negative representing cold conditions. The plot also indicates the degree of correlation between the various measures of the environment. The record combined high occurred in 1980 from the record deep anomalies and the near-record shallow anomalies, whereas the record high shallow anomaly occurred in 2012. The record low occurred in 1992, combining records in both shallow and deep anomalies. In 2014, the shallow index decreased to near normal, driven by cold CIL conditions. The deep index increased to its 2nd highest value on record. This leads to an overall composite temperature index of +1.3 SD, the 7th highest of the series.

HIGHLIGHTS

- Air temperatures in July were the warmest on record (since 1873, +2.1°C, +2.3 SD) when averaged over all stations. Annual mean air temperatures in 2014 were near normal over the Gulf (+0.0°C, +0.0 SD).
- Winter (December-March) air temperatures were below normal by -2.5°C (-1.6 SD), including the coldest March since 1948 (-4.4°C, -2.1 SD), leading to a heavy sea-ice cover.
- April-November air temperatures were just above normal with an anomaly of +0.3°C (+0.5 SD).
- The annual average runoff of the St. Lawrence River measured at Québec City and RIVSUM II were above normal in 2014 (+0.7 SD and +1.1 SD respectively), as was the spring freshet (+1.9 SD and +1.8 SD).
- The estuarine ratio at Pointe-des-Monts was above normal in winter, August and fall. The above-normal spring freshet led to below-normal Estuarine ratio and near-normal outward transport at the Pointe-des-Monts section, however the above-normal fall freshet led to above-normal Estuarine ratio and outward transport.
- Sea ice maximum volume was 3rd highest since 1969 at 126 km^3, nearly double the climatological average.
- The August-September cold intermediate layer (CIL) returned to near-normal conditions after 4 years of warm conditions, as a result of the cold winter.
- May-November sea-surface temperature averaged over the Gulf was above normal by +1.2°C (+3.2 SD) and second highest on record after 2006. Record highs were reached in August averaged over the Gulf (T=17.8°C, above normal by +2.5°C and breaking the August 2012 record of +2.0°C) and in the following regions: Estuary (+4.2°C, +4.4 SD), Northwest Gulf (+4.1°C, +4.4 SD), Anticosti Channel (+2.8°C, +3.2 SD) and Cabot Strait (+2.9°C, +3.2 SD).
- Deep water temperatures are increasing overall in the Gulf, with inward advection from Cabot Strait where temperature had reached a record high (since 1915) in 2012 at 200 m. Temperature averaged over the Gulf at 300 m increased slightly to reach 5.9°C (+2.4 SD); the highest since 1980. Temperature at 200 m increased overall to reach 5.3°C (+2.0 SD); the highest on record.
- Bottom area covered by waters warmer than 6°C increased in 2014 in Anticosti Channel, Esquiman Channel and Central Gulf, and reached a record value in Esquiman Channel while reducing its bottom habitat area in the temperature range of 5–6°C.

ACKNOWLEDGEMENTS

We are grateful to the people responsible for CTD data acquisition during the surveys used in this report:

- Rimouski station monitoring: Roger Pigeon, Félix St-Pierre, Michel Rousseau, Sylvain Chartrand, Pierre Joly, Lily St-Amand, Line McLaughlin, Marie-Lyne Dubé, Michel Starr, Yves Gagnon, Rémi Desmarais, François Villeneuve, Caroline Lafleur, Jean-François St-Pierre, Michael Scarratt, Peter Galbraith, Bernard Pelchat, Isabelle St-Pierre, Laure Devine.
- March 2014 helicopter survey: Chief scientist Peter Galbraith; scientific personnel Rémi Desmarais; helicopter pilot Robert Delisle; aircraft technician David Gauvin.
- June AZMP transects: Yves Gagnon, Michel Rousseau, Sylvain Chartrand, Marie-Lyne Dubé, François Villeneuve, Kim Émond, Johanne Guérin, Benoît Légaré, Isabelle St-Pierre, Roger Pigeon, Linda Girard; the officers and crew of the CCGS Teleost.
- August Multi-species survey: Sylvain Chartrand, Michel Rousseau, Bernard Pettigrew, Caroline Lafleur; the officers and crew of the CCGS Teleost.
- October-November AZMP survey: Pierre Joly, Yves Gagnon, Félix St-Pierre, Jean-François St-Pierre, François Villeneuve, Sonia Michaud, Caroline Lafleur, Jean-Pierre Allard, Michel Starr, Marie-Lyne Dubé, Laure Devine, Lily St-Amand, Roger Pigeon, Joana Roma, Jory Cabrol, Angélique Ollier, Roxanne Sage; the officers and crew of the CCGS Hudson.
- September Multi-species survey: Luc Savoie for providing the CTD data.
- Northumberland Strait survey: Chief scientists Mark Hanson and Joël Chassé.
- Data management: Laure Devine, Caroline Lafleur, Isabelle St-Pierre.
- CTD maintenance: Roger Pigeon, Félix St-Pierre, Michel Rousseau, Sylvain Chartrand.

Data from the following sources are also gratefully acknowledged:

- Air temperature: Environment Canada.
- Sea-ice: Canadian Ice Service, Environment Canada. Processing of GIS files by Paul Nicot.
- Runoff at Québec City: Denis Lefaivre.
- Runoff from hydrological modelling: Joël Chassé and Diane Lavoie.
- Thermograph network: Bernard Pettigrew, Rémi Desmarais, Félix St-Pierre.
- Historical AVHRR SST remote sensing (IML): Pierre Larouche, Bernard Pettigrew.
- AVHRR SST remote sensing (BIO): Carla Caverhill.

All figures were made using the free software Gri (Kelley and Galbraith 2000).

We are grateful to David Hebert and Eugene Colbourne for reviewing the manuscript and providing insightful comments.

REFERENCES

Benoît, H.P., C. Savenkoff, P. Ouellet, P.S. Galbraith, J. Chassé and A. Fréchet, 2012. Impacts of fishing and climate-driven changes in exploited marine populations and communities with implications for management, in State-of-the-Ocean Report for the Gulf of St. Lawrence Integrated Management (GOSLIM) Area, H. P. Benoît, J. A. Gagné, C. Savenkoff, P. Ouellet and M.-N. Bourassa, Eds. Canadian Manuscript Report of Fisheries and Aquatic Sciences 2986: viii + 73 pp.

Bourgault, D. and V.G. Koutitonsky. 1999. Real-time monitoring of the freshwater discharge at the head of the St. Lawrence Estuary. Atmos. Ocean, 37 (2): 203–220.

Colbourne, E., Holden, J., Craig, J., Senciall, D., Bailey, W., Stead, P., and Fitzpatrick, C. 2014. An assessment of the physical oceanographic environment on the Newfoundland and Labrador Shelf during 2013. DFO Can. Sci. Advis. Sec. Res. Doc. 2014/094. v + 38 p.

Cyr, F., D. Bourgault and P. S. Galbraith, 2011. Interior versus boundary mixing of a cold intermediate layer. J. Gephys. Res. (Oceans), 116, C12029, doi:10.1029/2011JC007359.

Dutil, J.-D., S. Proulx, P.S. Galbraith, J. Chassé, N. Lambert and C. Laurian, 2012. Coastal and epipelagic habitats of the estuary and Gulf of St. Lawrence. Can. Tech. Rep. Fish. Aquat. Sci. 3009: ix + 87 p.

Galbraith, P.S. 2006. Winter water masses in the Gulf of St. Lawrence. J. Geophys. Res., 111, C06022, doi:10.1029/2005JC003159.

Galbraith, P. S. et Grégoire, F. 2015. Habitat thermique du maquereau bleu: profondeur de l'isotherme de 8 °C dans le sud du golfe du Saint-Laurent entre 1960 et 2014. Secr. can. de consult. sci. du MPO. Doc. de rech. 2014/116. v + 13 p.

Galbraith, P.S. and P. Larouche, 2011. Sea-surface temperature in Hudson Bay and Hudson Strait in relation to air temperature and ice cover breakup, 1985-2009. J. Mar. Systems, 87, 66-78.

Galbraith, P.S. and P. Larouche. 2013. Trends and variability in eastern Canada sea-surface temperatures. Ch. 1 (p. 1-18) In: Aspects of climate change in the Northwest Atlantic off Canada [Loder, J.W., G. Han, P.S. Galbraith, J. Chassé and A. van der Baaren (Eds.)]. Can. Tech. Rep. Fish. Aquat. Sci. 3045: x + 190 p.

Galbraith, P.S., F.J. Saucier, N. Michaud, D. Lefaivre, R. Corriveau, F. Roy, R. Pigeon and S. Cantin. 2002. Shipborne monitoring of near-surface temperature and salinity in the Estuary and Gulf of St. Lawrence. Atlantic Zone Monitoring Program Bulletin, Dept. of Fisheries and Oceans Canada. No. 2: 26–30.

Galbraith, P.S., R. Desmarais, R. Pigeon and S. Cantin. 2006. Ten years of monitoring winter water masses in the Gulf of St . Lawrence by helicopter. Atlantic Zone Monitoring Program Bulletin, Dept. of Fisheries and Oceans Canada. No. 5: 32–35.

Galbraith, P.S., D. Gilbert, C. Lafleur, P. Larouche, B. Pettigrew. 2007. Physical oceanographic conditions in the Gulf of St. Lawrence in 2006. DFO Can. Sci. Advis. Sec. Res. Doc. 2007/024, iv + 51 pp.

Galbraith, P. S., P. Larouche, D. Gilbert, J. Chassé, and B. Petrie. 2010. Trends in sea-surface and CIL temperatures in the Gulf of St. Lawrence in relation to air temperature. Atlantic Zone Monitoring Program Bulletin, 9: 20-23.

Galbraith P.S., P. Larouche, J. Chassé, B. Petrie, 2012. Sea-surface temperature in relation to air temperature in the Gulf of St. Lawrence: interdecadal variability and long term trends. Deep Sea Res. II, V77–80, 10–20.

Galbraith. P.S., D. Hebert, E. Colbourne and R. Pettipas. 2013. Trends and variability in eastern Canada sub-surface ocean temperatures and implications for sea ice. Ch.5 In: Aspects of climate change in the Northwest Atlantic off Canada [Loder, J.W., G. Han, P.S. Galbraith, J. Chassé and A. van der Baaren (Eds.)]. Can. Tech. Rep. Fish. Aquat. Sci. 3045: x + 192 p.

Galbraith, P.S., Chassé, J., Gilbert, D., Larouche, P., Caverhill, C., Lefaivre, D., Brickman, D., Pettigrew, B., Devine, L., and Lafleur, C. 2014. Physical Oceanographic Conditions in the Gulf of St. Lawrence in 2013. DFO Can. Sci. Advis. Sec. Res. Doc. 2014/062. vi + 84 p.

Gilbert, D. 2004. Propagation of temperature signals from the northwest Atlantic continental shelf edge into the Laurentian Channel. ICES CM, 2004/N:7, 12 pp.

Gilbert, D. and B. Pettigrew. 1997. Interannual variability (1948-1994) of the CIL core temperature in the Gulf of St. Lawrence. Can. J. Fish. Aquat. Sci., 54 (Suppl. 1): 57–67.

Gilbert, D., P.S. Galbraith, C. Lafleur and B. Pettigrew. 2004. Physical oceanographic conditions in the Gulf of St. Lawrence in 2003. DFO Can. Sci. Advis. Sec. Res. Doc. 2004/061, 63 pp.

Gilbert, D., B. Sundby, C. Gobeil, A. Mucci and G.-H. Tremblay. 2005. A seventy-two-year record of diminishing deep-water oxygen in the St. Lawrence estuary: The northwest Atlantic connection. Limnol. Oceanogr., 50(5): 1654–1666.

Hammill, M.O. and P.S. Galbraith, 2012. Changes in seasonal sea-ice cover and its effect on marine mammals, in State-of-the-Ocean Report for the Gulf of St. Lawrence Integrated Management (GOSLIM) Area, H. P. Benoît, J. A. Gagné, C. Savenkoff, P. Ouellet and M.-N. Bourassa, Eds. Canadian Manuscript Report of Fisheries and Aquatic Sciences 2986: viii + 73 pp.

Hebert, D., Pettipas, R., Brickman, D., and Dever M. 2014. Meteorological, Sea Ice and Physical Oceanographic Conditions on the Scotian Shelf and in the Gulf of Maine during 2013. DFO Can. Sci. Advis. Sec. Res. Doc. 2013/070. v + 40 p.

Kalnay, E., M. Kanamitsu, R. Kistler, W. Collins, D. Deaven, L. Gandin, M. Iredell, S. Saha, G. White, J. Woollen, Y. Zhu, M. Chelliah, W. Ebisuzaki, W. Higgins, J. Janowiak, K. Mo, C. Ropelewski, J. Wang, A. Leetmaa, R. Reynolds, R. Jenne and D. Josephé. 1996. The NCEP/NCAR 40-year reanalysis project. Bull. Am. Meteorol. Soc. 77, 437–470.

Kelley, D.E. and P.S. Galbraith. 2000. Gri: A language for scientific illustration, Linux J., 75, 92 101.

Lauzier, L.M. and R.W. Trites. 1958. The deep waters of the Laurentian Channel. J. Fish. Res. Board Can. 15: 1247–1257.

McLellan, H.J. 1957. On the distinctness and origin of the slope water off the Scotian Shelf and its easterly flow south of the Grand Banks. J. Fish. Res. Board. Can. 14: 213–239.

Petrie, B., K. Drinkwater, A. Sandström, R. Pettipas, D. Gregory, D. Gilbert and P. Sekhon. 1996. Temperature, salinity and sigma-t atlas for the Gulf of St. Lawrence. Can. Tech. Rep. Hydrogr. Ocean Sci., 178: v + 256 pp.

Petrie, B., R. G. Pettipas and W. M. Petrie. 2007. An overview of meteorological, sea ice and sea surface temperature conditions off eastern Canada during 2006. DFO Can. Sci. Advis. Sec. Res. Doc. 2007/022.

Plourde, S., P. Joly, L. St-Amand and M. Starr. 2009. La station de monitorage de Rimouski : plus de 400 visites et 18 ans de monitorage et de recherche. Atlantic Zone Monitoring Program Bulletin, Dept. of Fisheries and Oceans Canada. No. 8: 51-55.

Tamdrari, H., M. Castonguay, J.-C. Brêthes, P. S. Galbraith and D. E. Duplisea, 2012. The dispersal pattern and behaviour of cod in the northern Gulf of St. Lawrence: results from tagging experiments, Can. J. of Fisheries and Aquatic Sciences, 69: 112-121.

Therriault, J.-C., B. Petrie, P. Pépin, J. Gagnon, D. Gregory, J. Helbig, A. Herman, D. Lefaivre, M. Mitchell, B. Pelchat, J. Runge and D. Sameoto. 1998. Proposal for a Northwest Atlantic zonal monitoring program. Can. Tech. Rep. Hydrogr. Ocean Sci., 194: vii + 57 pp.

Vincent, L. A., X. L. Wang, E. J. Milewska, H. Wan, F. Yang, and V. Swail. 2012. A second generation of homogenized Canadian monthly surface air temperature for climate trend analysis. *J. Geophys. Res.* 117, D18110, doi:10.1029/2012JD017859.

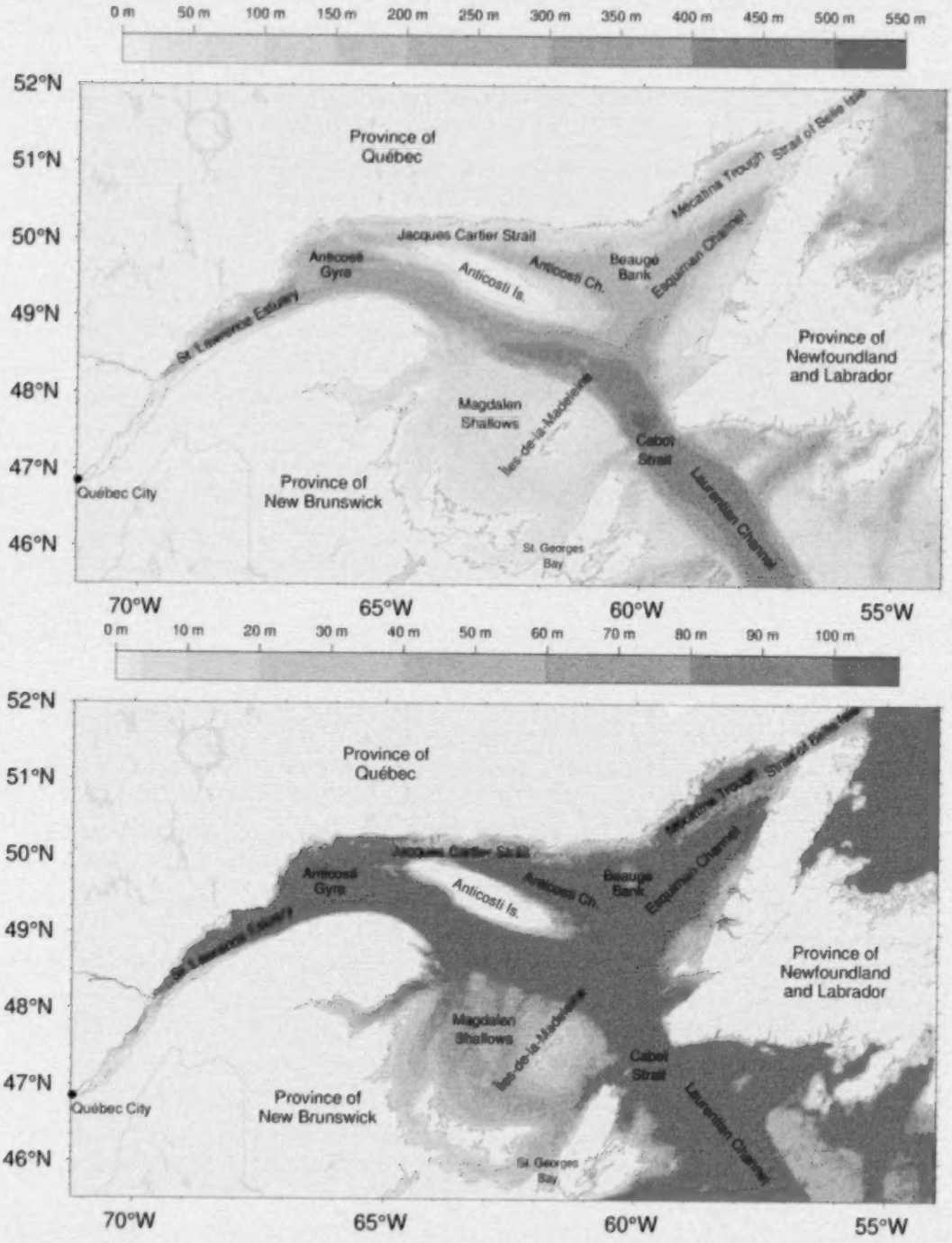

Fig. 1. The Gulf of St. Lawrence. Locations discussed in the text are indicated. Bathymetry datasets used are from the Canadian Hydrographic Service to the west of 56°47' W (with some corrections applied to the baie des Chaleurs and Magdalen Shallows) and TOPEX data to the east. Bottom panel shows detail for 0-100 m bathymetry.

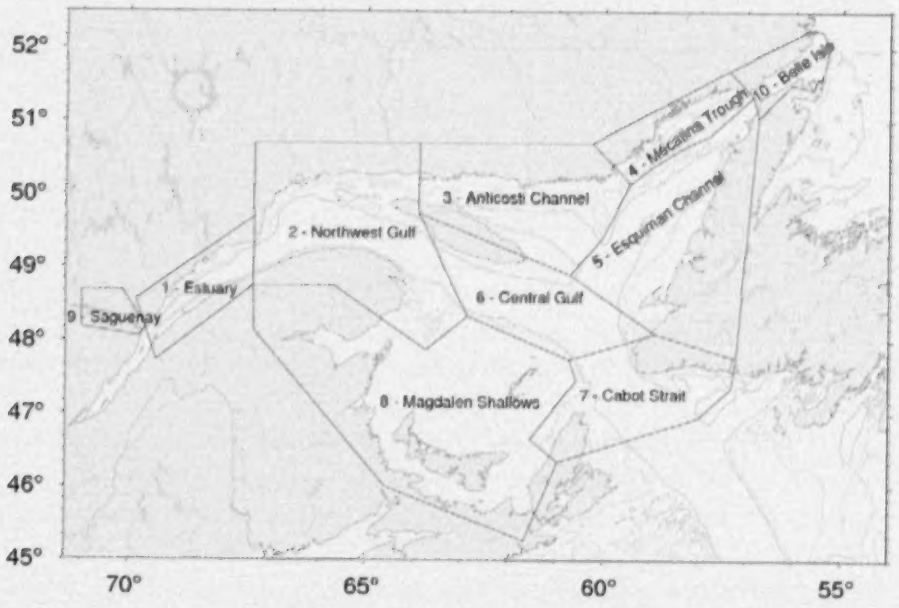

Fig. 2. Gulf of St. Lawrence divided into oceanographic regions. The first eight are typically used in this report.

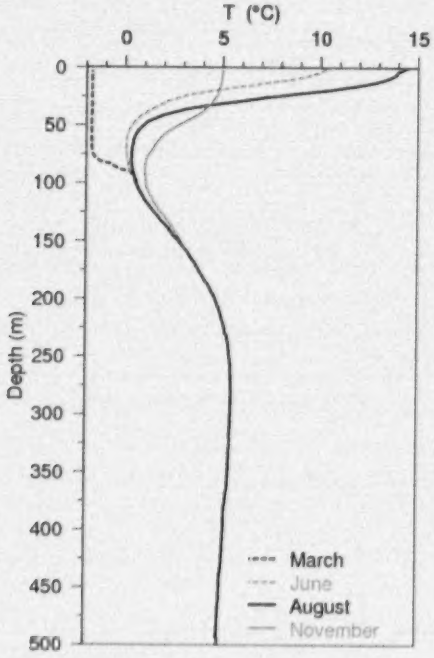

Fig. 3. Typical seasonal progression of the depth profile of temperature observed in the Gulf of St. Lawrence. Profiles are averages of observations in August, June and November 2007 in the northern Gulf. The dashed line at left shows a single winter temperature profile (March 2008), with near freezing temperatures in the top 75 m. The cold intermediate layer (CIL) is defined as the part of the water column that is colder than 1°C, although some authors use a different temperature threshold. Figure from Galbraith et al. (2012).

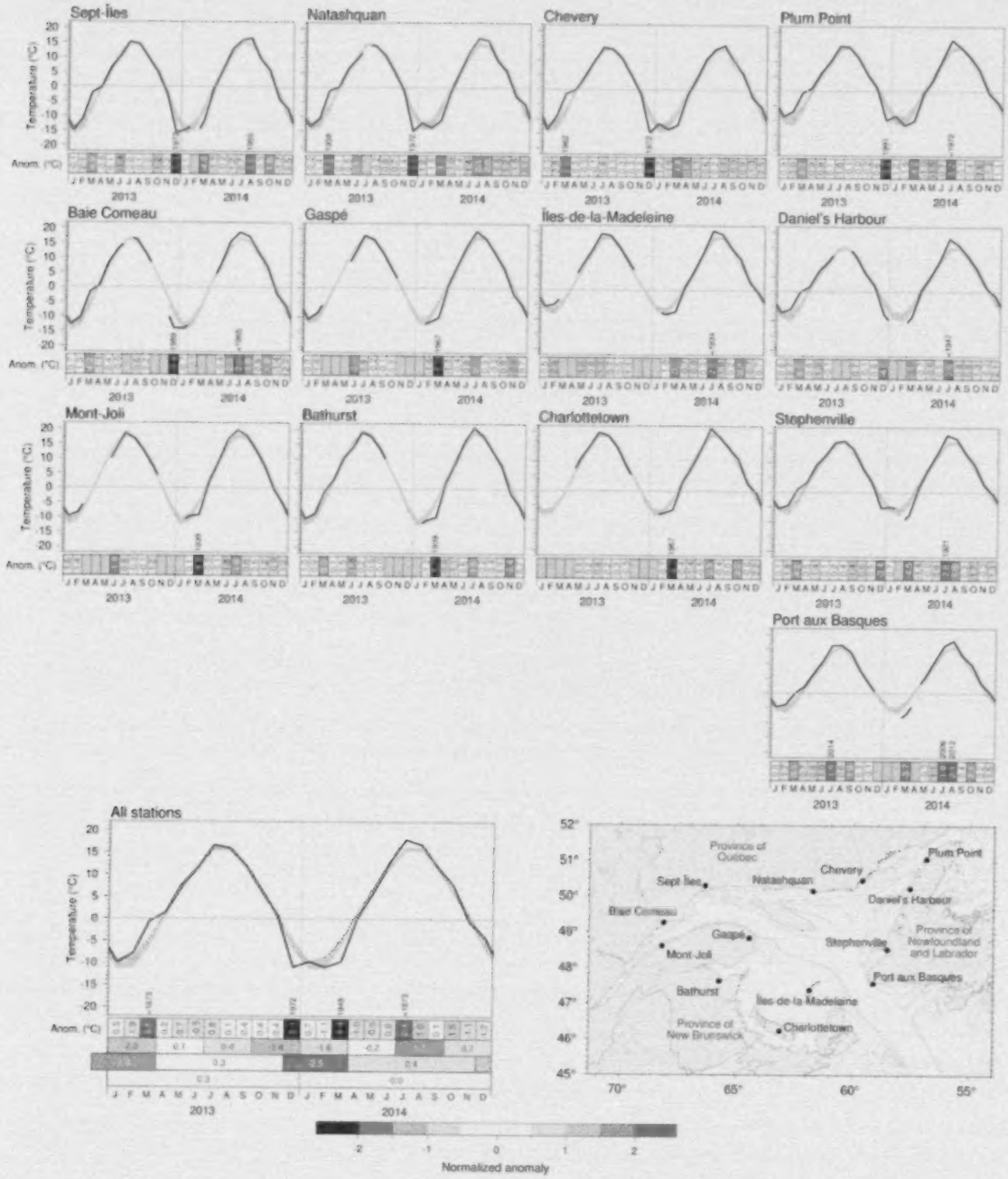

Fig. 4. Monthly air temperatures and anomalies for 2013 and 2014 at selected stations around the Gulf as well as the average for all stations. The blue area represents the 1981–2010 climatological monthly mean ± 0.5 SD. Months with 4 or more days of missing data are omitted. The bottom scorecards are colour-coded according to the monthly normalized anomalies based on the 1981–2010 climatologies for each month, but the numbers are the monthly anomalies in °C. For anomalies greater than 2 SD from normal, the prior year with a greater anomaly is indicated. Seasonal, December-March, April-November and annual anomalies are included for the all-station average.

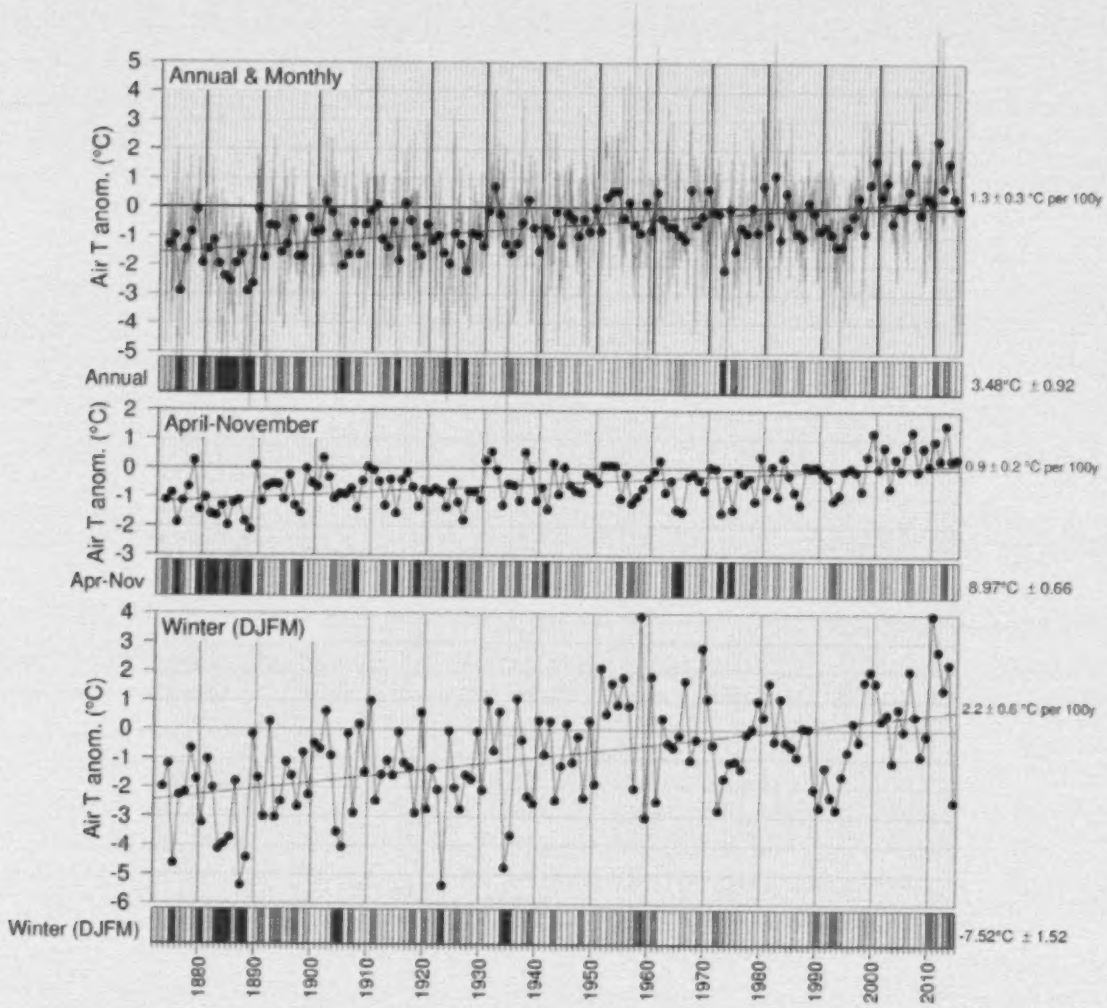

Fig. 5. Annual, April-November December-March mean air temperature anomalies averaged for the selected stations around the Gulf from Fig. 4. The bottom scorecards are colour-coded according to the normalized anomalies based on the 1981–2010 climatology. Trends plus and minus their 95% confidence intervals are shown. April-November air temperature anomalies tend to be highly-correlated with May-November sea-surface temperature anomalies (Galbraith et al. 2012; Galbraith and Larouche 2013) whereas winter air temperature anomalies correlate highly with sea-ice cover parameters and winter mixed-layer volumes (Galbraith et al. 2010; Galbraith et al. 2013).

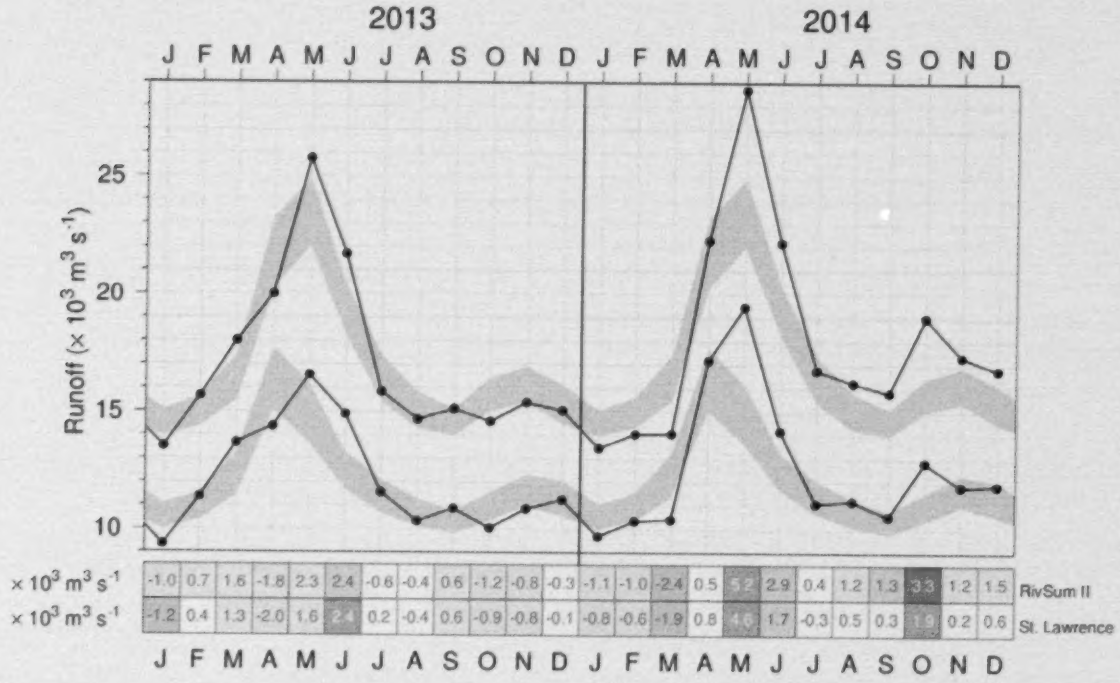

Fig. 6. Monthly mean freshwater flow of the St. Lawrence River at Québec City (lower curve) and its sum with rivers flowing into the St. Lawrence Estuary (RIVSUM II, upper curve). The 1981–2010 climatological mean (± 0.5 SD) is shown (blue shading). The scorecards are colour-coded according to the monthly anomalies normalized for each month of the year, but the numbers are the actual monthly anomalies in 10^3 m^3s^{-1}.

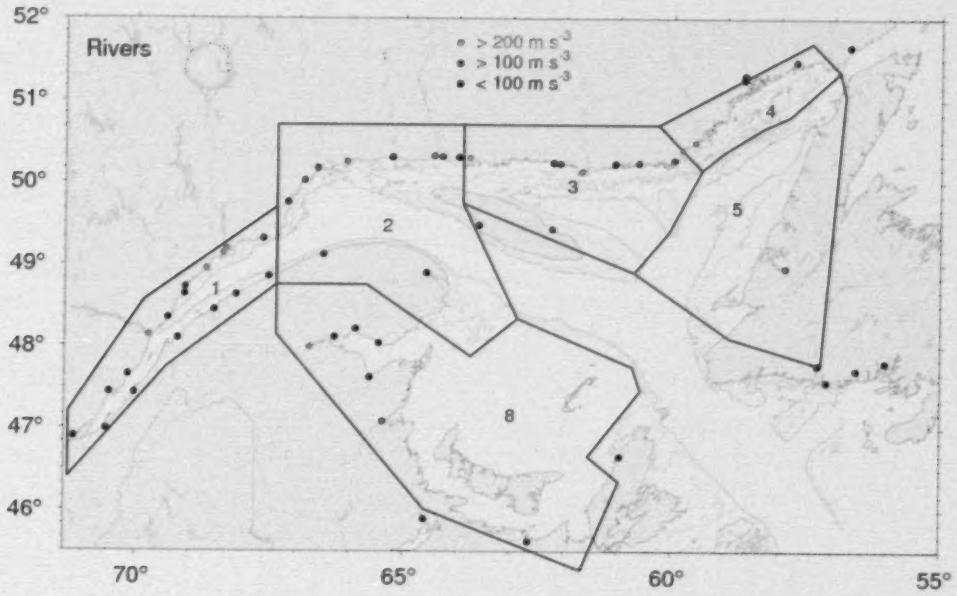

Fig. 7. River discharge locations for the regional sums of runoffs listed in Table 2. Red and blue dots indicate rivers that have climatological mean runoff greater than 200 m^3s^{-1} and between 100 and 200 m^3s^{-1}, respectively.

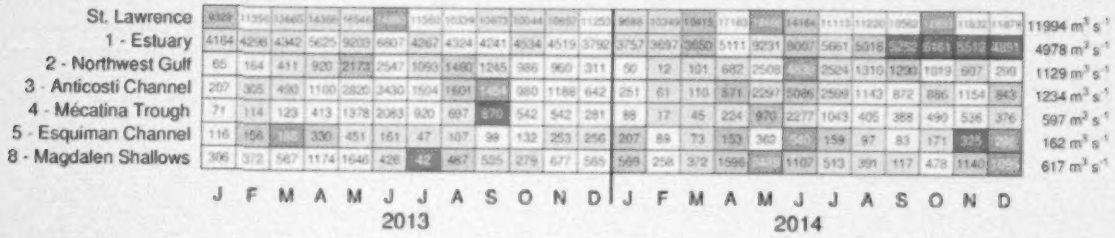
St. Lawrence
1 - Estuary
2 - Northwest Gulf
3 - Anticosti Channel
4 - Mécatina Trough
5 - Esquiman Channel
8 - Magdalen Shallows
11994 m³ s⁻¹
4978 m³ s⁻¹
1129 m³ s⁻¹
1234 m³ s⁻¹
597 m³ s⁻¹
162 m³ s⁻¹
617 m³ s⁻¹
J F M A M J J A S O N D J F M A M J J A S O N D
2013
2014

Fig. 8. Monthly anomalies of the St. Lawrence River runoff and sums of all other major rivers draining into separate Gulf regions for 2013 and 2014. The scorecards are colour-coded according to the monthly normalized anomalies based on the 1981–2010 climatologies for each month, but the numbers are the monthly average runoffs in $m^3 s^{-1}$. Numbers on the right side are annual climatological means. Runoff regulation is simulated for three rivers that flow into the Estuary (Saguenay, Manicouagan, Outardes).

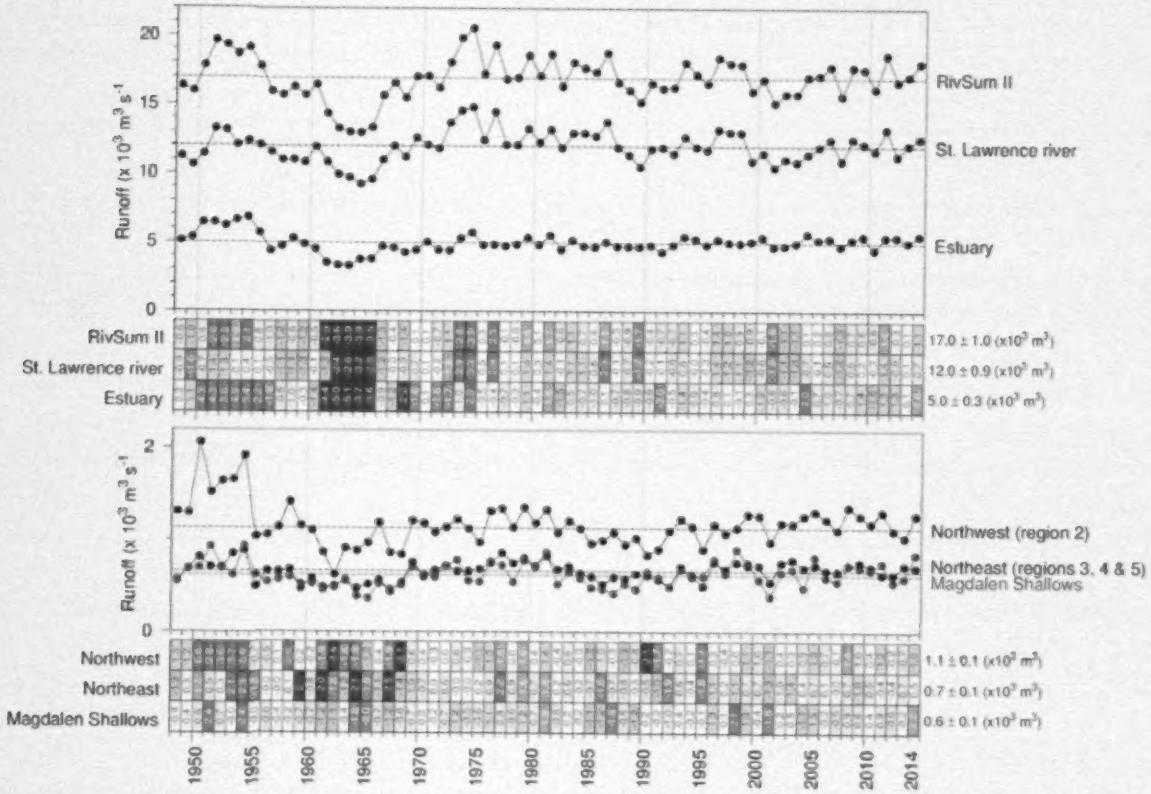
Runoff (x 10³ m³ s⁻¹)
RivSum II
St. Lawrence river
Estuary
17.0 ± 1.0 (x10³ m³)
12.0 ± 0.9 (x10³ m³)
5.0 ± 0.3 (x10³ m³)
Northwest (region 2)
Northeast (regions 3, 4 & 5)
Magdalen Shallows
Northwest
Northeast
Magdalen Shallows
1.1 ± 0.1 (x10³ m³)
0.7 ± 0.1 (x10³ m³)
0.6 ± 0.1 (x10³ m³)
1950 1955 1960 1965 1970 1975 1980 1985 1990 1995 2000 2005 2010 2014

Fig. 9. Annual mean freshwater flow of the St. Lawrence River at Québec City and of the sum of all rivers flowing into regions of the Estuary and Gulf. The 1981–2010 climatological mean is shown as horizontal lines and indicated on the right side of the scorecards. Numbers in scorecards are normalized anomalies.

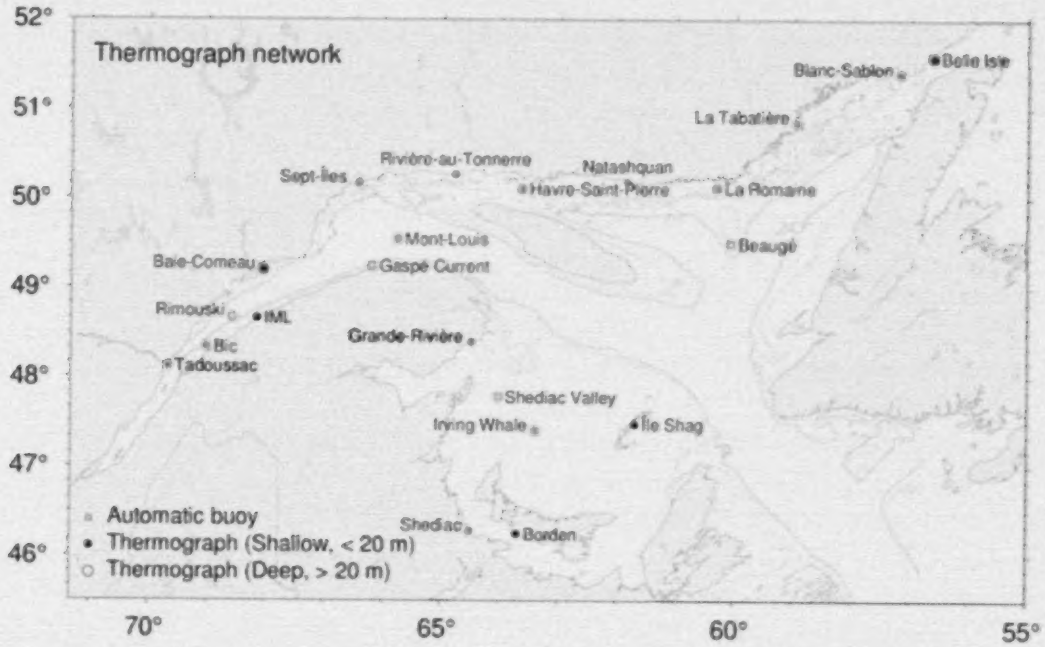

Fig. 10. Locations of the Maurice Lamontagne Institute thermograph network stations in 2014, including oceanographic buoys that transmit data in real time (squares). Deep and shallow instruments are denoted by open circles and dots, while seasonal and year-round deployments are denoted by gray and black symbols. Shediac station from DFO Gulf Region is also shown.

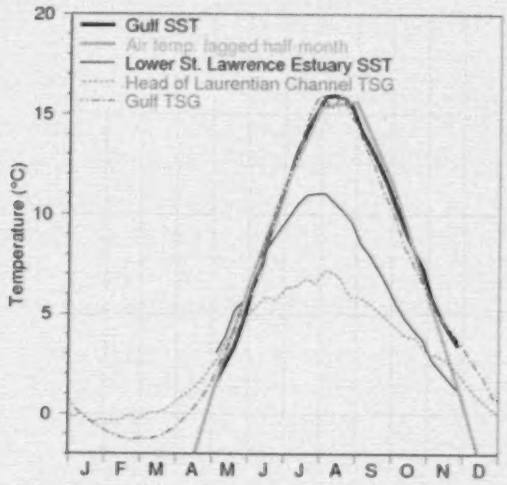

Fig. 11. Sea-surface temperature climatological seasonal cycle in the Gulf of St. Lawrence. AVHRR temperature weekly averages for 1985 to 2010 are shown from May to November (ice-free months) for the entire Gulf (thick black line) and the cooler Lower St. Lawrence Estuary (thin black line), defined as the area west of the Pointe-des-Monts section and east of approx 69°30'W. Thermosalinograph data averages for 2000 to 2010 are shown for the head of the Laurentian Channel (at 69°30'W, grey dashed line) and for the average over the Gulf waters along the main shipping route between the Pointe-des-Monts and Cabot Strait sections (gray dash-dotted line). Monthly air temperature averaged over eight stations in the Gulf of St. Lawrence are shown offset by 2 weeks into the future (thick grey line; winter months not shown). Figure from Galbraith et al. (2012).

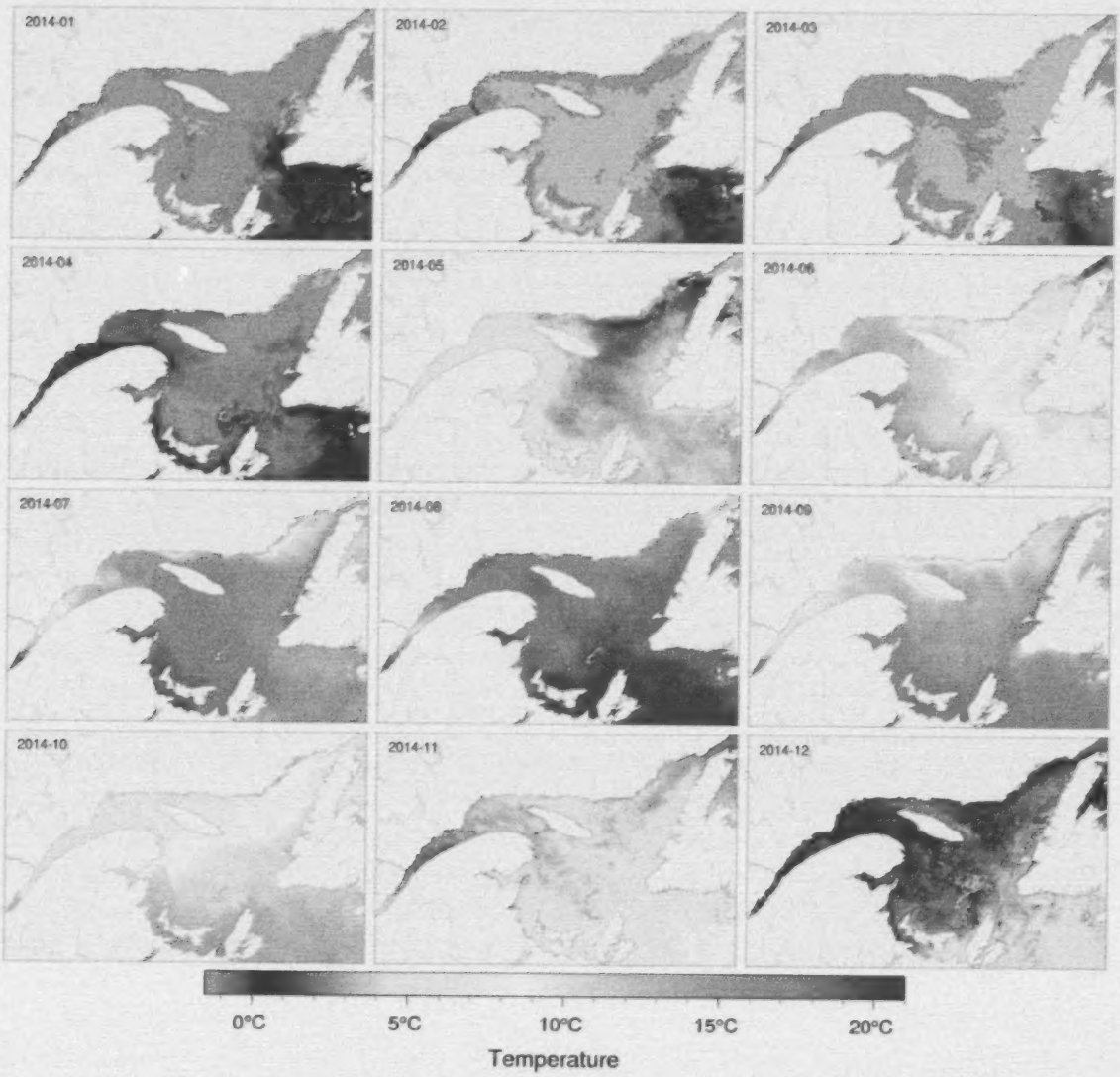

Fig. 12. Sea-surface temperature monthly averages for 2014 as observed with AVHRR remote sensing. White areas have no data for the period due to ice cover or clouds. Data are from BIO Operational Remote Sensing (C. Caverhill).

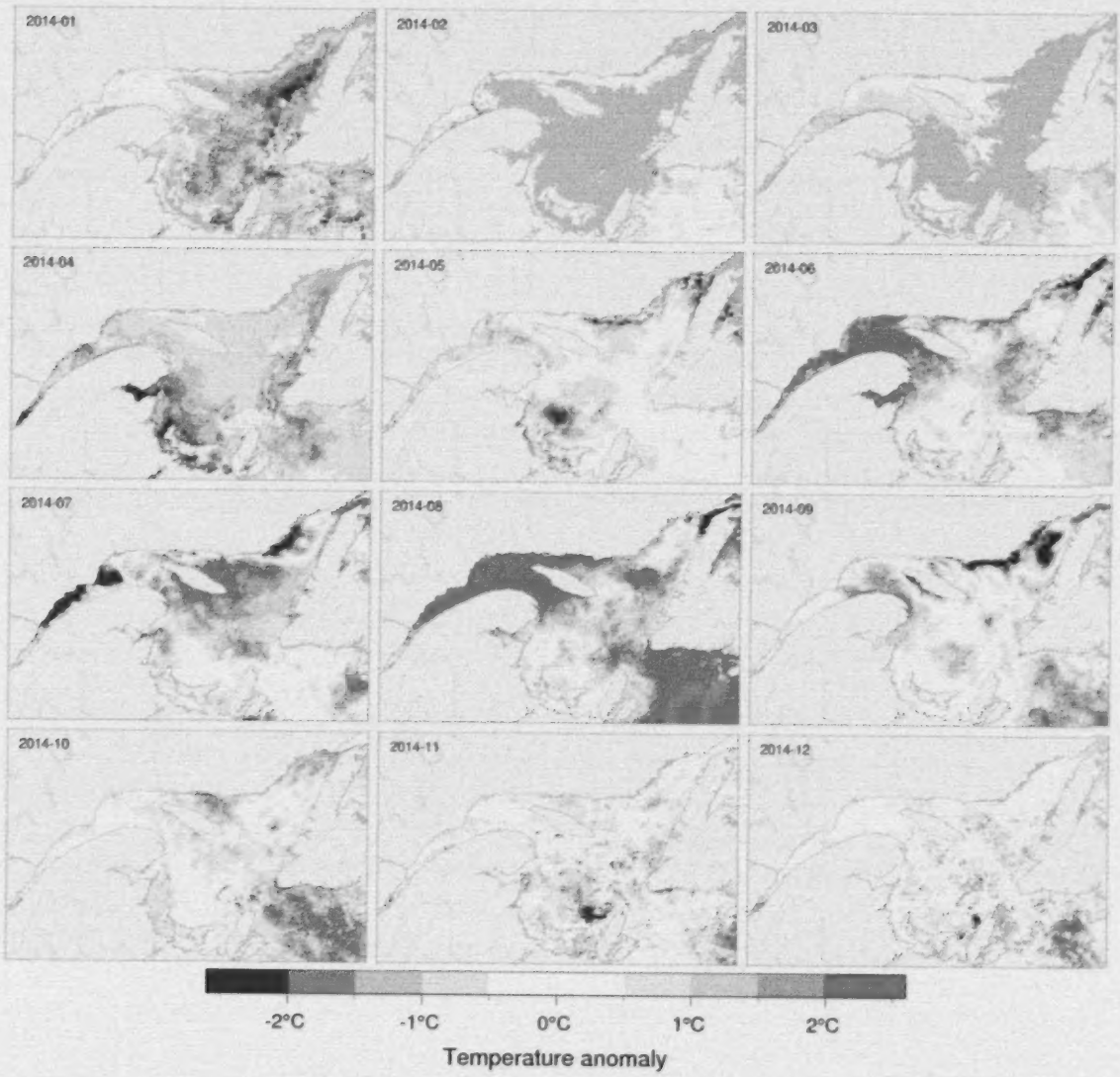

Fig. 13. Sea-surface temperature monthly anomalies based on monthly climatologies calculated for the 1999–2010 period observed with AVHRR remote sensing. Note that box average anomalies in subsequent figures use a 1985-2010 climatology from a different dataset.

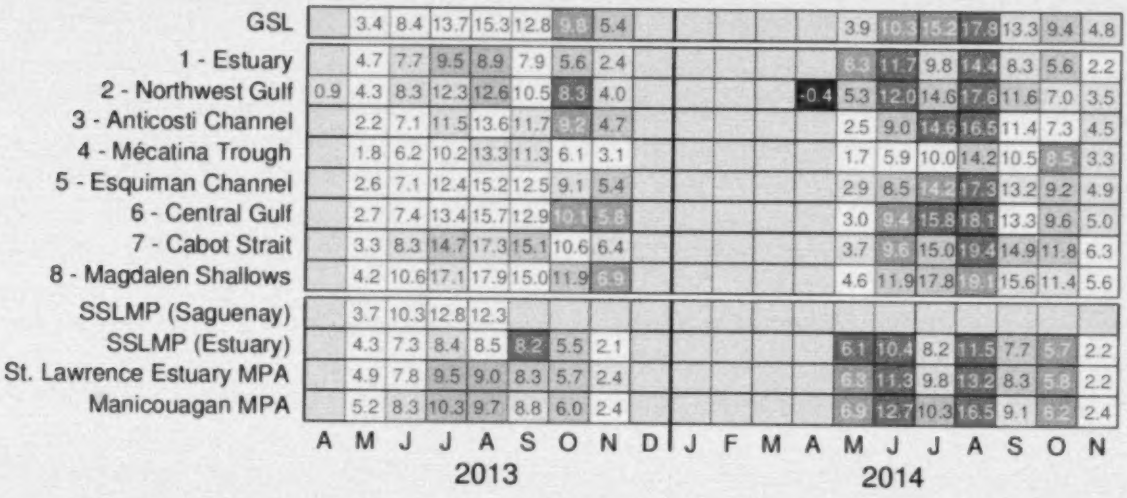

Fig. 14. AVHRR SST May to November monthly anomalies averaged over the Gulf, the eight regions of the Gulf, and management regions of the St. Lawrence Estuary for 2013 and 2014 (April results are also shown for the Northwest Gulf). The scorecards are colour-coded according to the monthly normalized anomalies based on the 1985–2010 climatologies for each month, but the numbers are the monthly average temperatures.

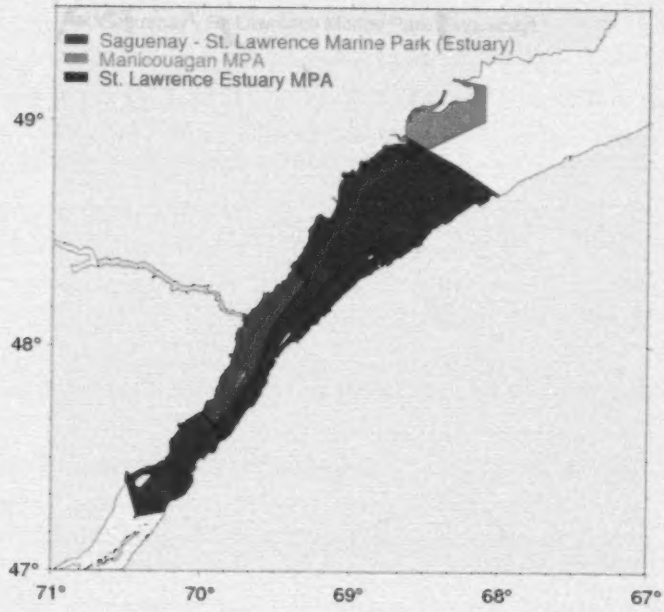

Fig. 15. Map showing the proposed Manicouagan MPA, the proposed St. Lawrence Estuary MPA, and the Saguenay – St. Lawrence Marine Park for the purpose of SST extraction from NOAA imagery (Fig. 14).

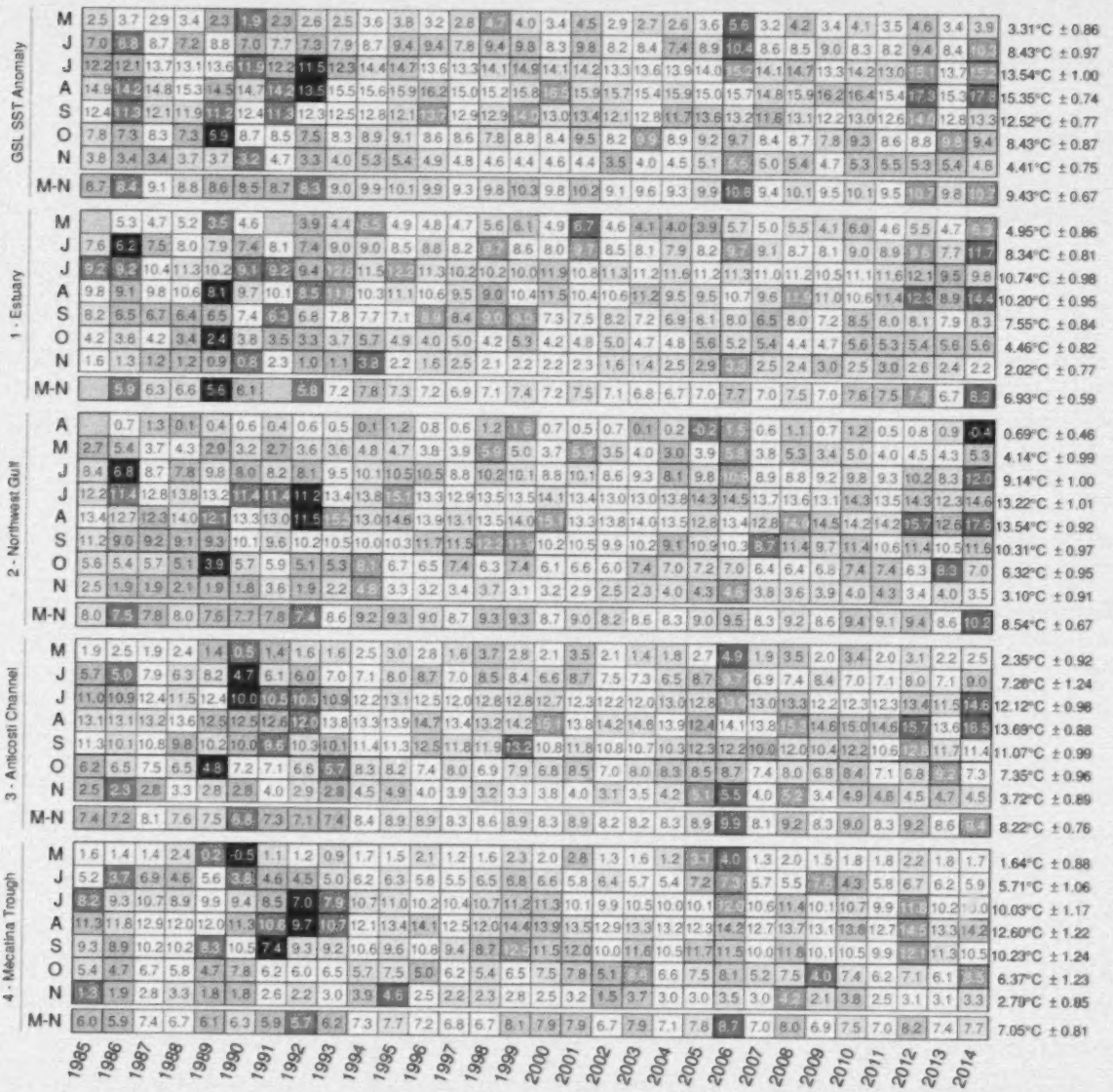

Fig. 16. AVHRR SST May to November monthly anomalies averaged over the Gulf of St. Lawrence and over the first four regions of the Gulf. The scorecards are colour-coded according to the monthly normalized anomalies based on the 1985–2010 climatologies for each month, but the numbers are the monthly average temperatures in °C. The 1985-2010 mean and standard deviation are indicated for each month on the right side of the table. April anomalies are included for the Northeast Gulf because those regions are typically ice-free by then. The May to November average is also included.

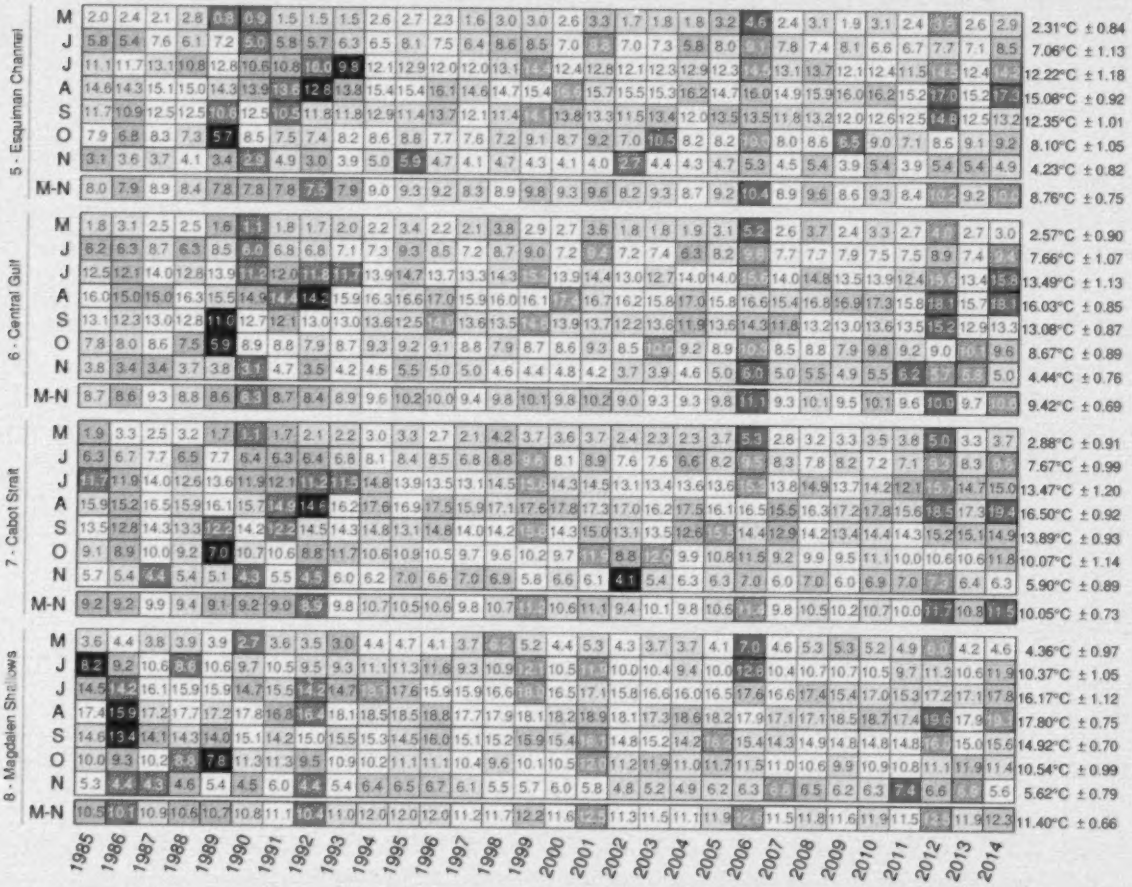

Fig. 17. AVHRR SST May to November monthly anomalies averaged over the remaining four regions of the Gulf. The scorecards are colour-coded according to the monthly normalized anomalies based on the 1985–2010 climatologies for each month, but the numbers are the monthly average temperatures in °C. The 1985-2010 mean and standard deviation are indicated for each month on the right side of the table. The May to November average is also included.

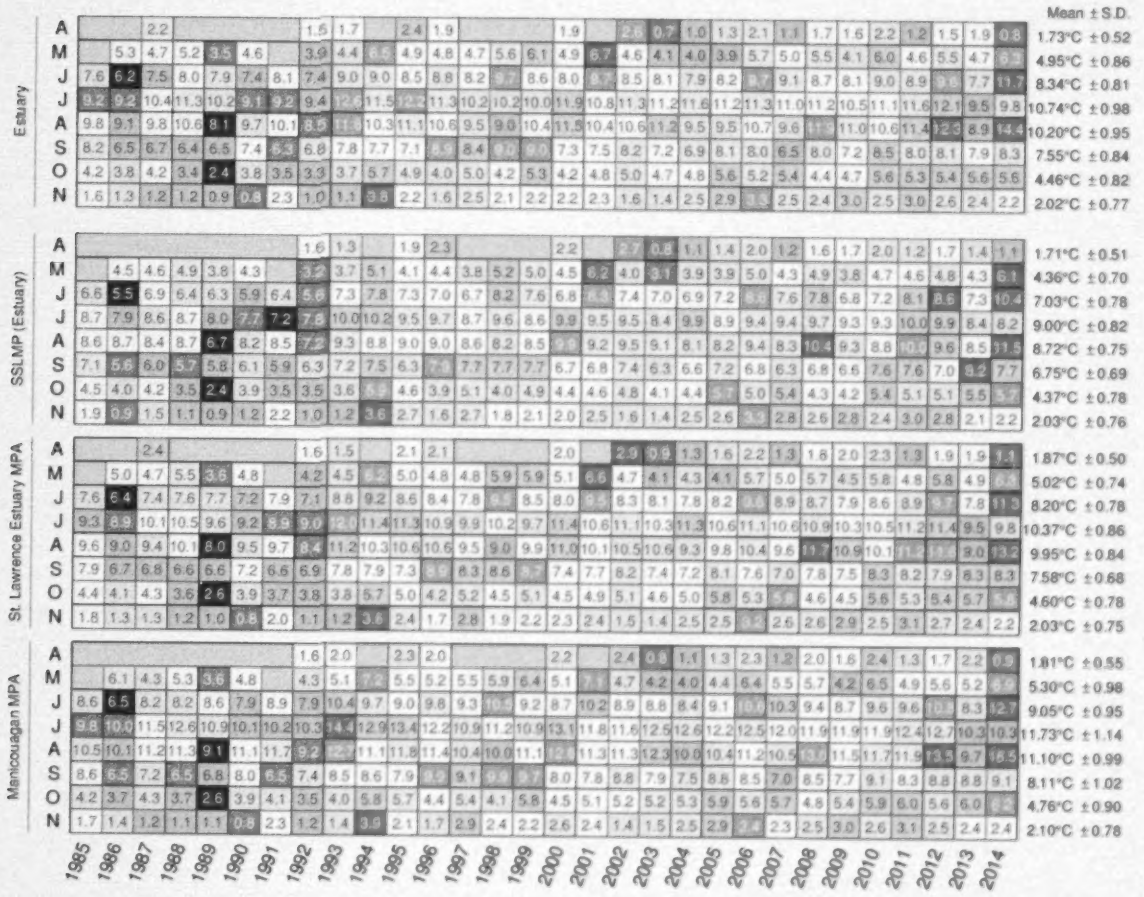

Fig. 18. AVHRR SST April to November monthly anomalies averaged over the Estuary (region 1 of the Gulf) and the Estuary subregion of the Saguenay – St. Lawrence Marine Park (PMSSL), the proposed St.Lawrence Estuary Marine Protected Area (MPA), and Manicouagan MPA. The scorecards are colour-coded according to the monthly normalized anomalies based on the 1985–2010 climatologies for each month, but the numbers are the monthly average temperatures in °C. The 1985-2010 mean and standard deviation are indicated for each month on the right side of the table.

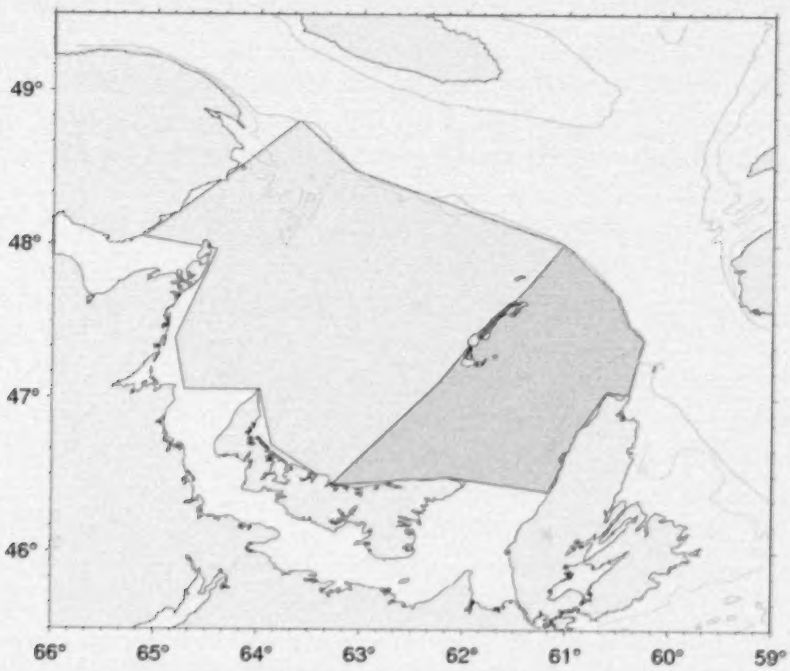

Fig. 19. Areas defined as the western and eastern Magdalen Shallows.

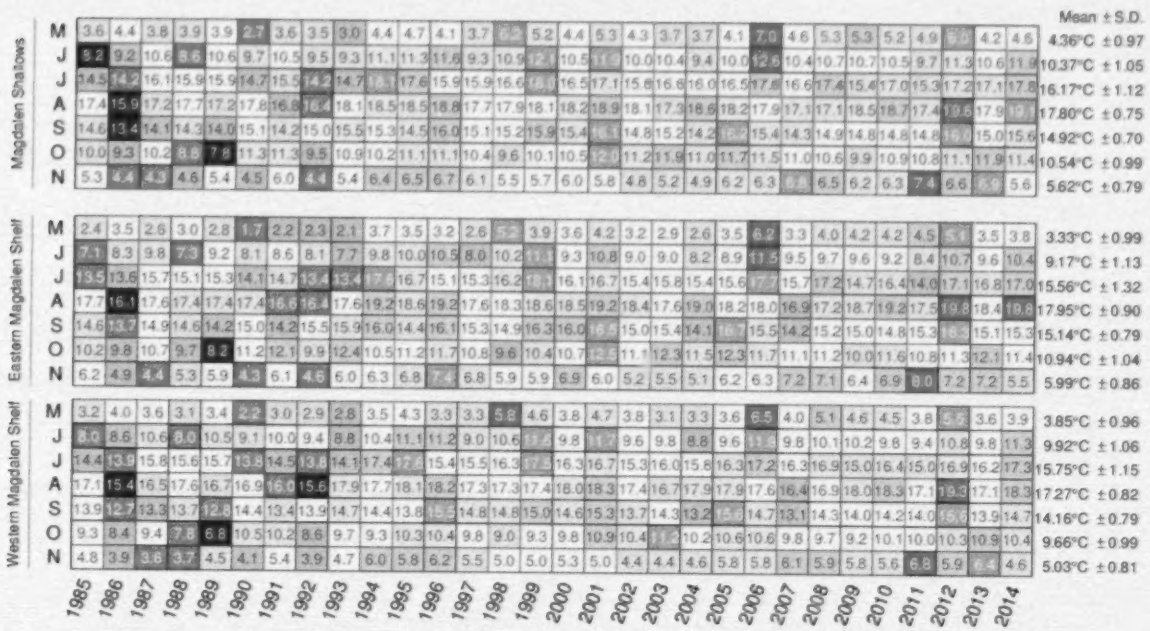

Fig. 20. AVHRR SST May to November monthly anomalies averaged over the Magdalen Shallows (region 8 of the Gulf) and the eastern and western subregions of the Magdalen Shallows. The scorecards are colour-coded according to the monthly normalized anomalies based on the 1985–2010 climatologies for each month, but the numbers are the monthly average temperatures in °C. The 1985-2010 mean and standard deviation are indicated for each month on the right side of the table.

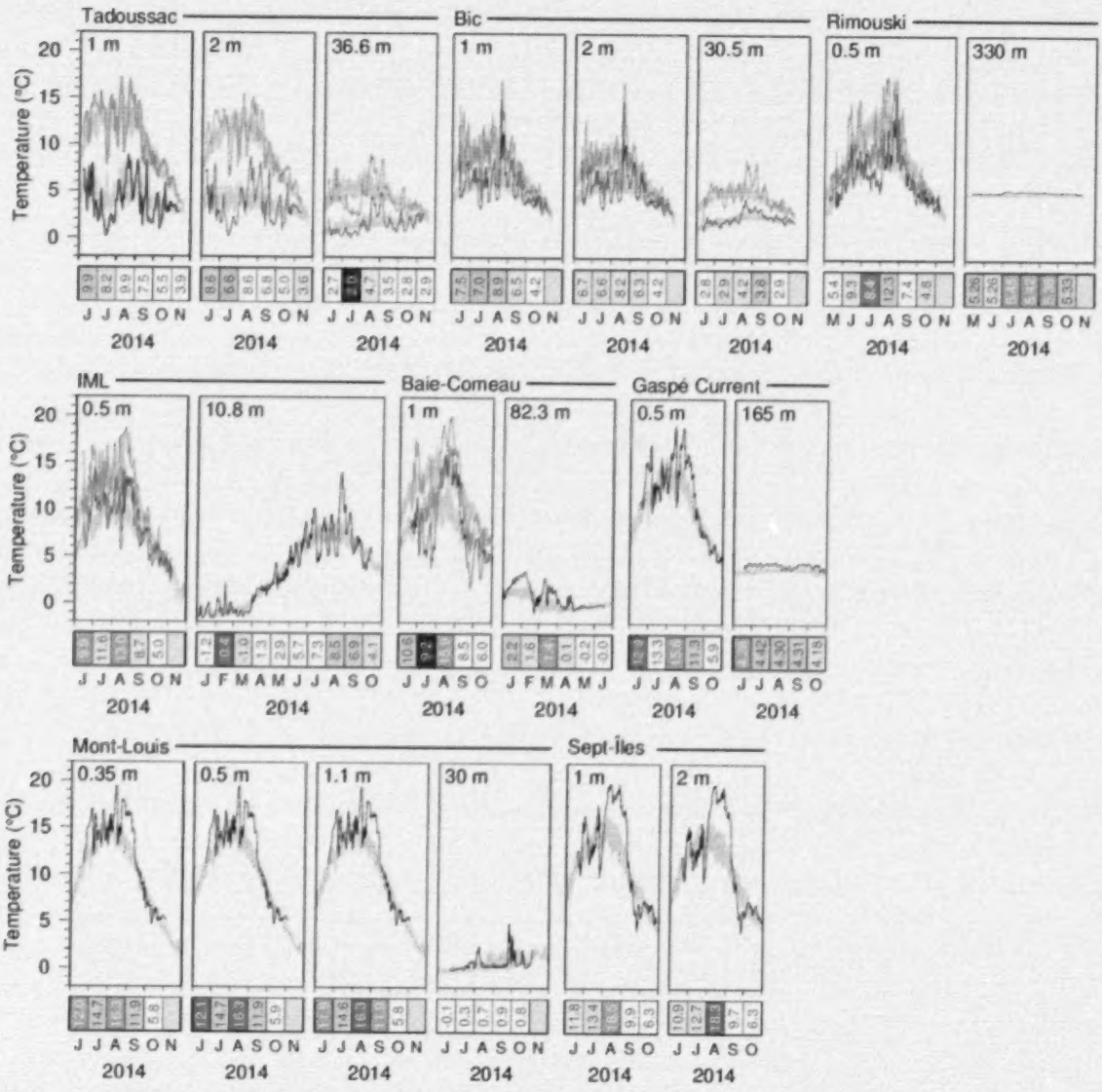

Fig. 21. Thermograph network data. Daily mean 2014 temperatures compared with the daily climatology (blue areas are daily averages ± 0.5 SD, orange areas are daily average maximums ± 0.5 SD and bright blue areas are daily average minimums ± 0.5 SD) for stations in the Estuary and northwestern Gulf. Scorecards show monthly average temperature.

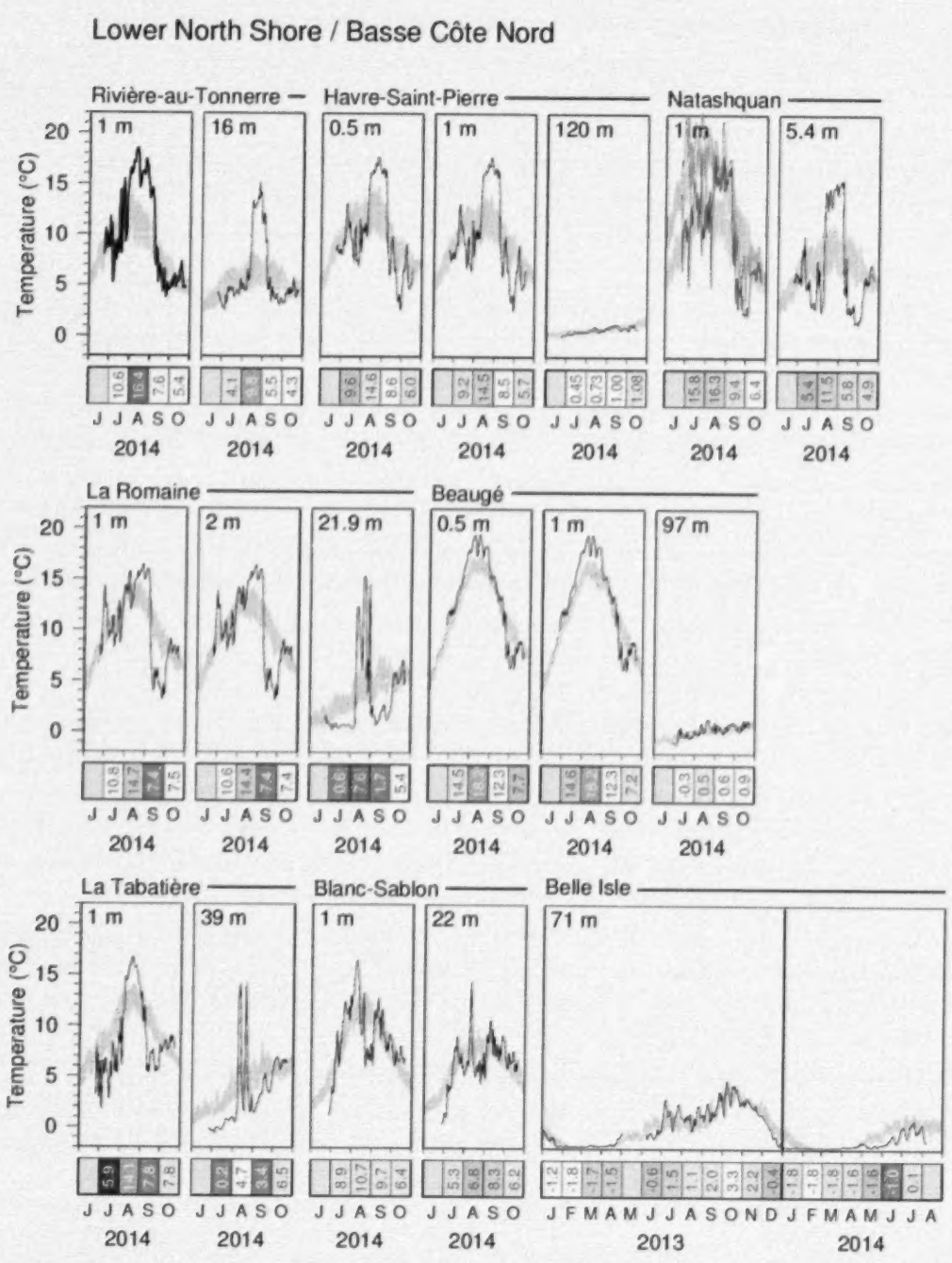

Fig. 22. Thermograph network data. Daily mean 2014 temperatures compared with the daily climatology (blue areas are daily averages ± 0.5 SD, orange areas are daily average maximums ± 0.5 SD and bright blue areas are daily average minimums ± 0.5 SD) for stations of the lower north shore.

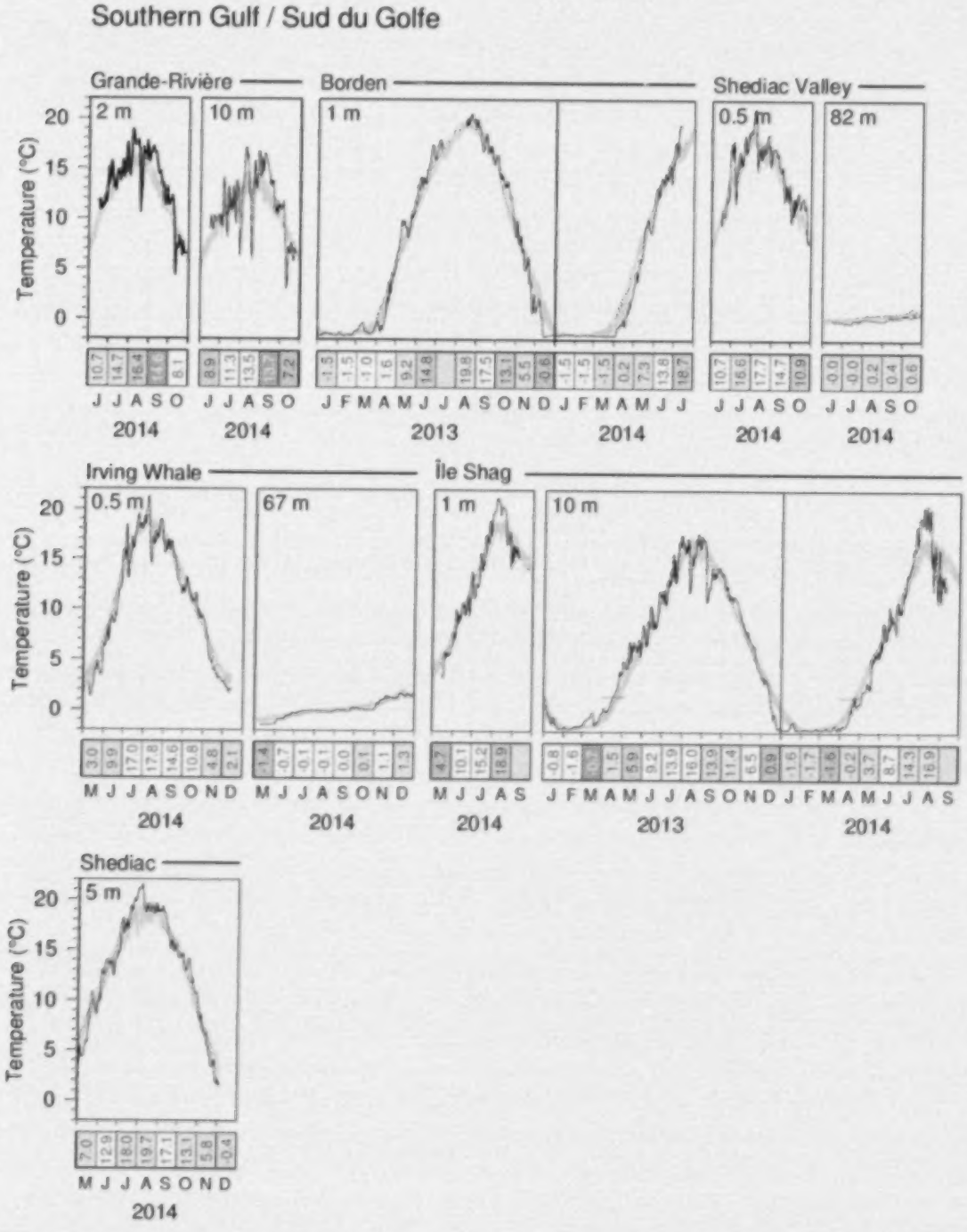

Fig. 23. Thermograph network data. Daily mean 2014 temperatures compared with the daily climatology (daily averages ± 0.5 SD; blue area) for stations of the southern Gulf. Data from 2013 are included if they were not all shown in last year's report. Red lines in the Île Shag panel span the historical dates when spring temperature increased over 1.5°C, a temperature associated with increased lobster mobility.

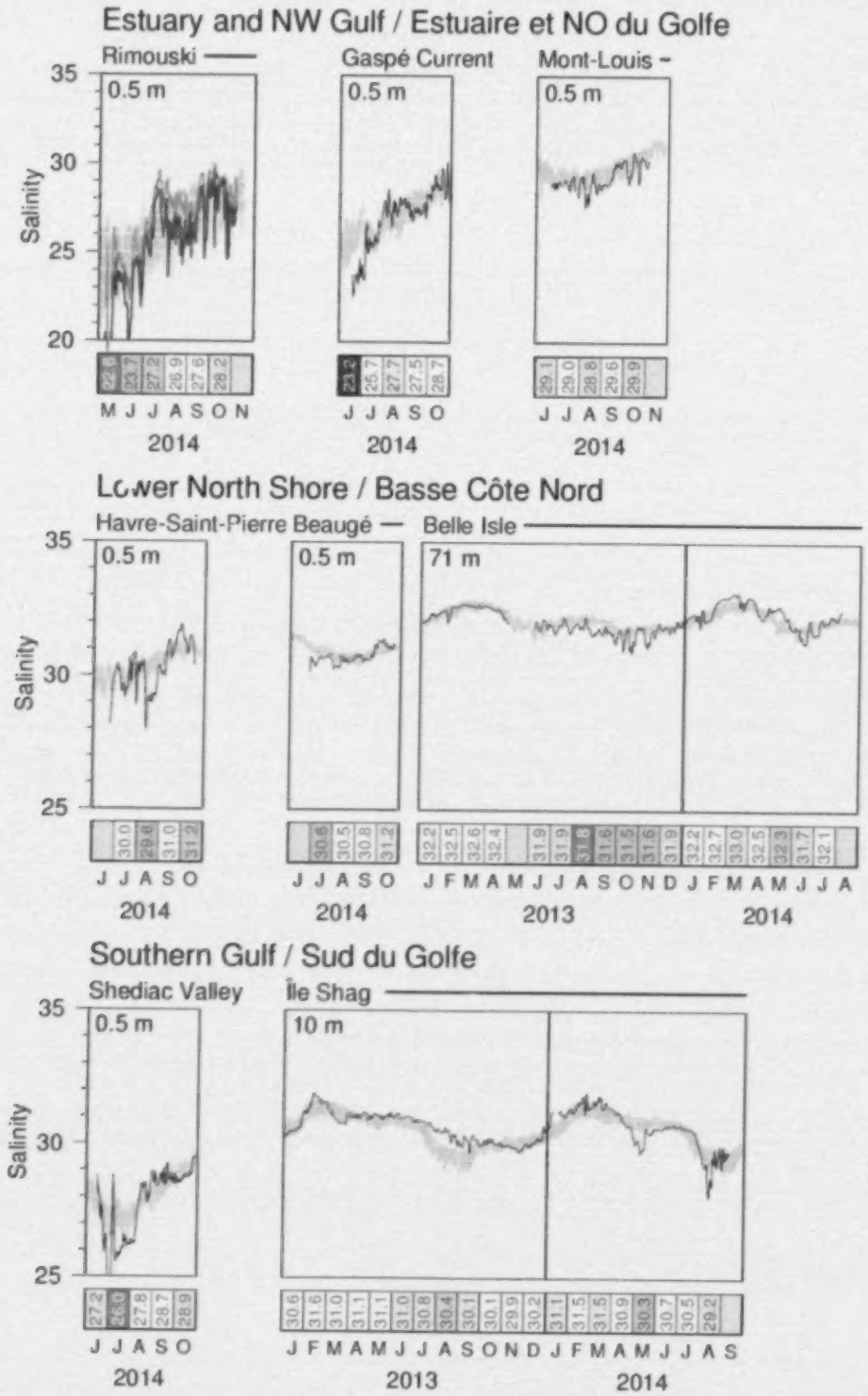

Fig. 24. Thermograph network data. Daily mean 2014 salinities compared with the daily climatology (daily averages ± 0.5 SD; blue area) computed from all available stations.

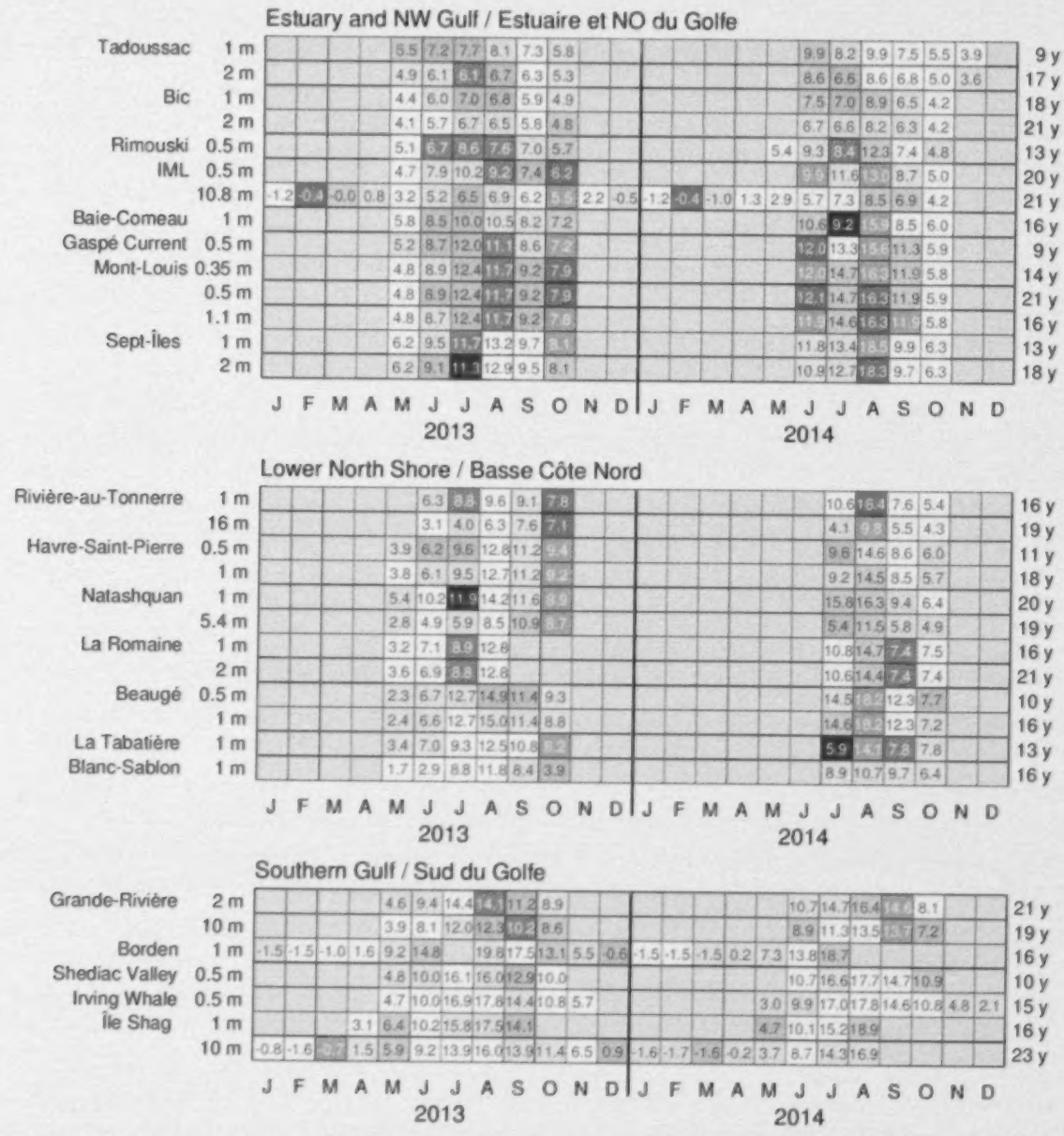
Estuary and NW Gulf / Estuaire et NO du Golfe
Tadoussac 1 m 9 y
2 m 17 y
Bic 1 m 18 y
2 m 21 y
Rimouski 0.5 m 13 y
IML 0.5 m 20 y
10.8 m 21 y
Baie-Comeau 1 m 16 y
Gaspé Current 0.5 m 9 y
Mont-Louis 0.35 m 14 y
0.5 m 21 y
1.1 m 16 y
Sept-Îles 1 m 13 y
2 m 18 y
J F M A M J J A S O N D J F M A M J J A S O N D
2013 2014
Lower North Shore / Basse Côte Nord
Rivière-au-Tonnerre 1 m 16 y
16 m 19 y
Havre-Saint-Pierre 0.5 m 11 y
1 m 18 y
Natashquan 1 m 20 y
5.4 m 19 y
La Romaine 1 m 16 y
2 m 21 y
Beaugé 0.5 m 10 y
1 m 16 y
La Tabatière 1 m 13 y
Blanc-Sablon 1 m 16 y
J F M A M J J A S O N D J F M A M J J A S O N D
2013 2014
Southern Gulf / Sud du Golfe
Grande-Rivière 2 m 21 y
10 m 19 y
Borden 1 m 16 y
Shediac Valley 0.5 m 10 y
Irving Whale 0.5 m 15 y
Île Shag 1 m 16 y
10 m 23 y
J F M A M J J A S O N D J F M A M J J A S O N D
2013 2014

Fig. 25. Monthly mean temperatures at all shallow sensors of the Maurice Lamontagne Institute thermograph network in 2013 and 2014. The number of years that each station and depth has been monitored is indicated on the far right. The colour-coding is according to the temperature anomaly relative to the climatology of each station for each month. Numbers are monthly average temperatures.

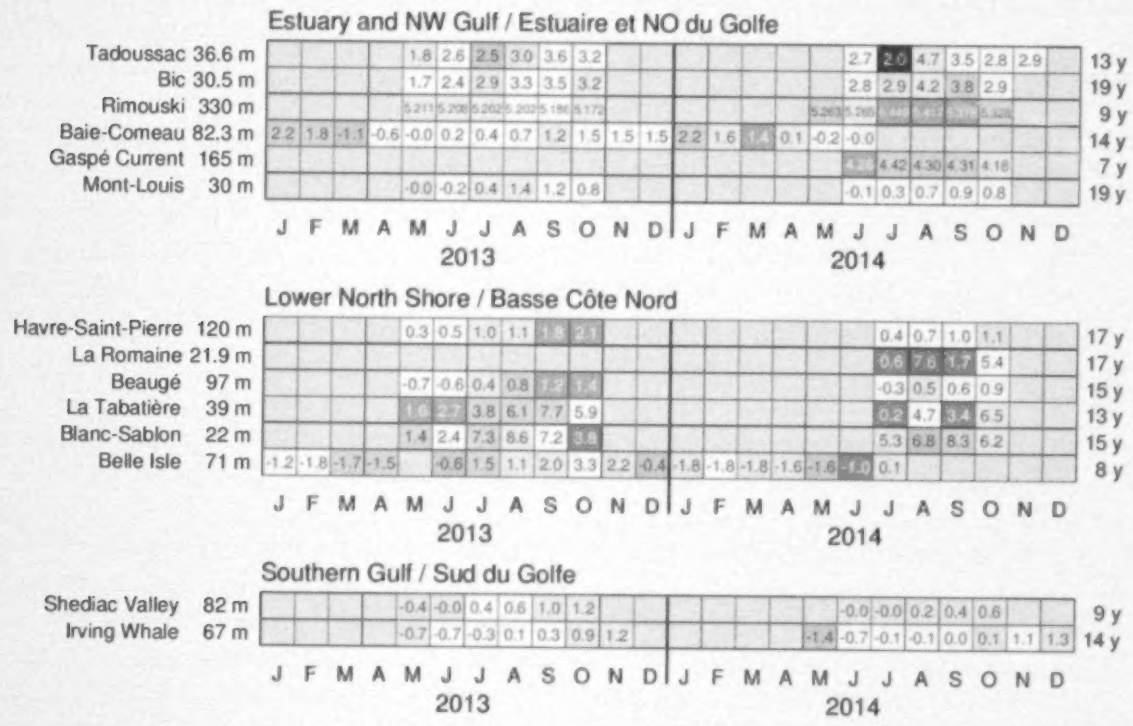
Estuary and NW Gulf / Estuaire et NO du Golfe
Tadoussac 36.6 m
Bic 30.5 m
Rimouski 330 m
Baie-Comeau 82.3 m
Gaspé Current 165 m
Mont-Louis 30 m
13 y
19 y
9 y
14 y
7 y
19 y
J F M A M J J A S O N D J F M A M J J A S O N D
2013
2014
Lower North Shore / Basse Côte Nord
Havre-Saint-Pierre 120 m
La Romaine 21.9 m
Beaugé 97 m
La Tabatière 39 m
Blanc-Sablon 22 m
Belle Isle 71 m
17 y
17 y
15 y
13 y
15 y
8 y
J F M A M J J A S O N D J F M A M J J A S O N D
2013
2014
Southern Gulf / Sud du Golfe
Shediac Valley 82 m
Irving Whale 67 m
9 y
14 y
J F M A M J J A S O N D J F M A M J J A S O N D
2013
2014

Fig. 26. Monthly mean temperatures at all sensors deeper than 20 m of the Maurice Lamontagne Institute thermograph network in 2013 and 2014. The number of years that each station and depth has been monitored is indicated on the far right. The colour-coding is according to the temperature anomaly relative to the climatology of each station for each month. Numbers are monthly average temperatures, with greater number of significant digits included when variance is lower.

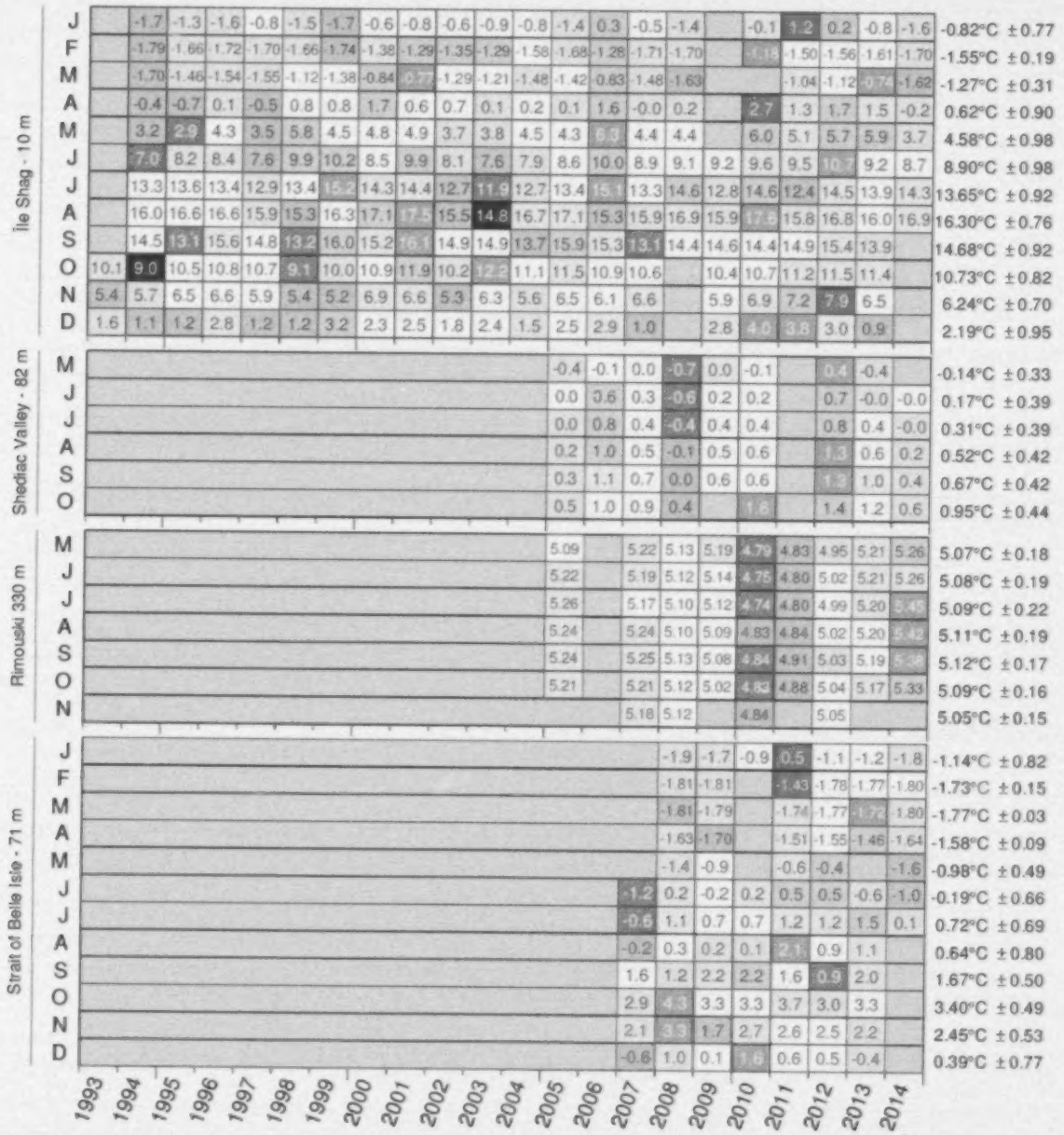

Fig. 27. Time series of the monthly averaged temperature anomalies for selected stations of the thermograph network. The colour-coding is according to the temperature anomaly relative to the climatology of each station for each month. Numbers are monthly average temperatures. The mean and standard deviation are indicated for each month on the right side of the figure.

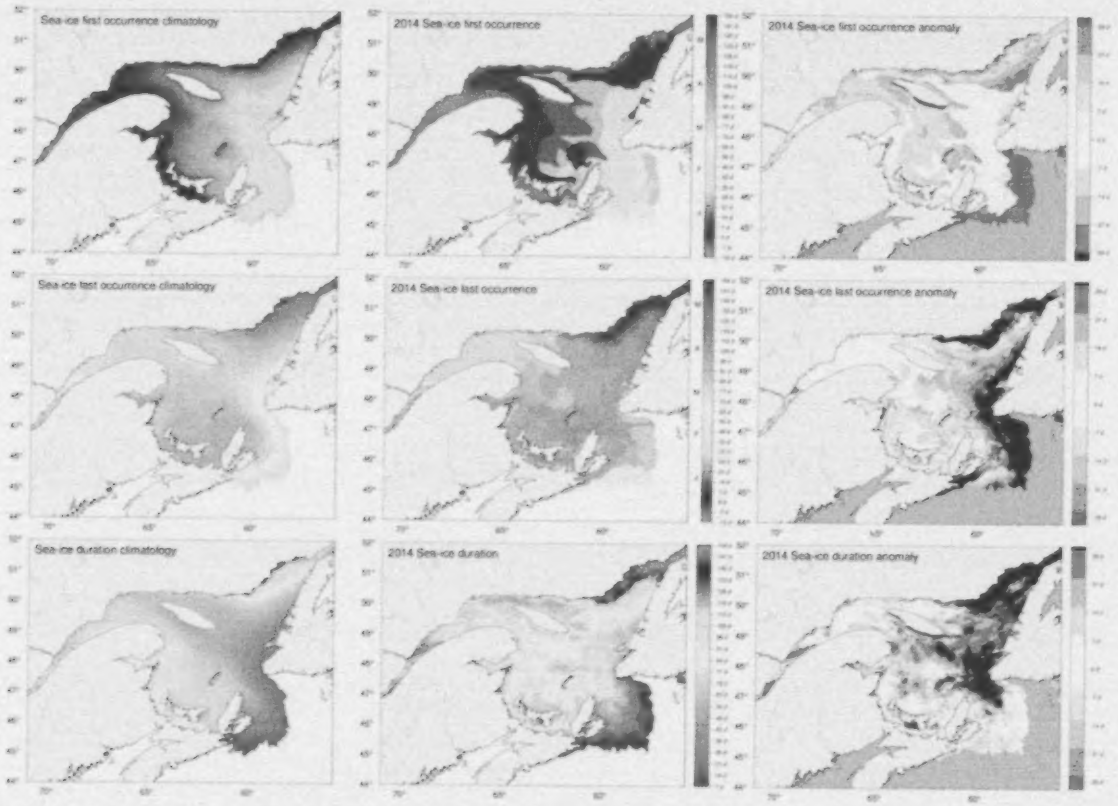
Sea-ice first occurrence climatology
2014 Sea-ice first occurrence
2014 Sea-ice first occurrence anomaly
Sea-ice last occurrence climatology
2014 Sea-ice last occurrence
2014 Sea-ice last occurrence anomaly
Sea-ice duration climatology
2014 Sea-ice duration
2014 Sea-ice duration anomaly

Fig. 28. First and last occurrence of ice and ice season duration based on weekly data. The 1981-2010 climatologies are shown (left) as well as the 2014 values (middle) and anomalies (right). First and last occurrence is defined here as the first and last weekly chart in which any amount of ice is recorded for each pixel and are illustrated as day-of-year. Ice duration sums the number of weeks (× 7 days) with ice cover for each pixel. Climatologies are shown for pixels that had at least 15 years out of the 30 with occurrence of sea-ice, and therefore also show the area with 50% likelihood of having some sea-ice at any time during any given year.

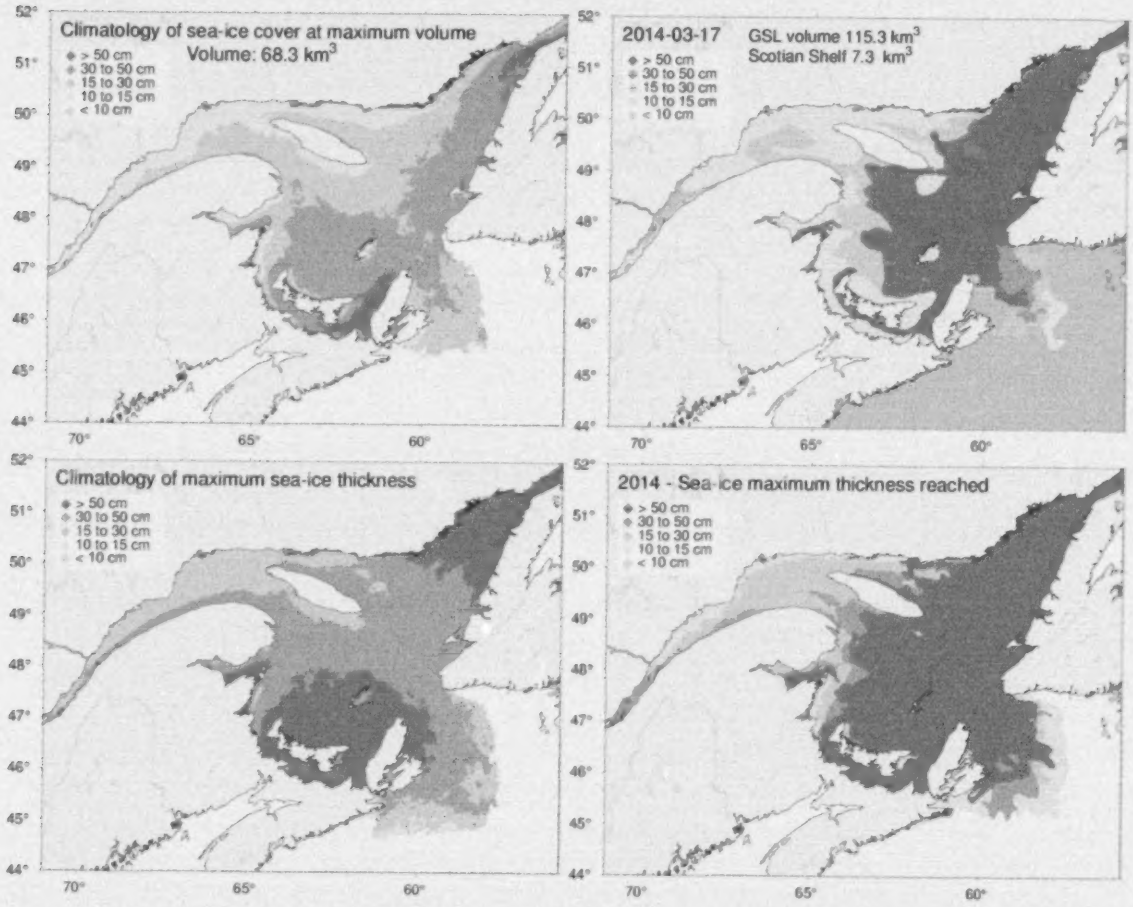

Fig. 29. Ice thickness map for 2014 for the day of the year with the maximum annual volume including the portion covering the Scotian Shelf (upper right panel) and similarly for the 1981-2010 climatology of the weekly maximum (upper left panel). Note that these maps reflect the ice thickness distribution on that day or week, and not the maximum observed at any given location during the year. That information is shown by the lower panels, showing the 1981-2010 climatology and 2014 distribution of the thickest ice recorded during the season at any location.

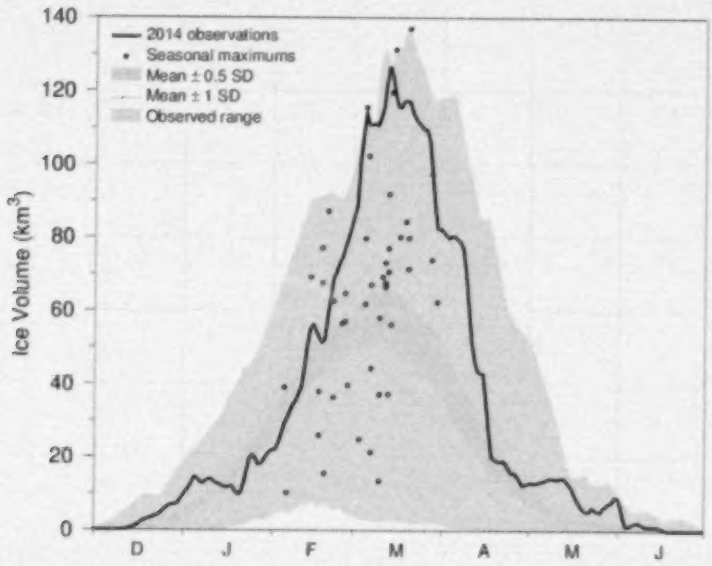

Fig. 30. Time series of the 2013-2014 daily mean ice volume for the Gulf of St. Lawrence and Scotian Shelf (black line), the 1981-2010 climatological mean volume plus and minus 0.5 and 1 SD (dark blue area and dashed line), the minimum and maximum span of 1969-2014 observations (light blue) and the date and volumes of 1969-2014 seasonal maximums (blue dots).

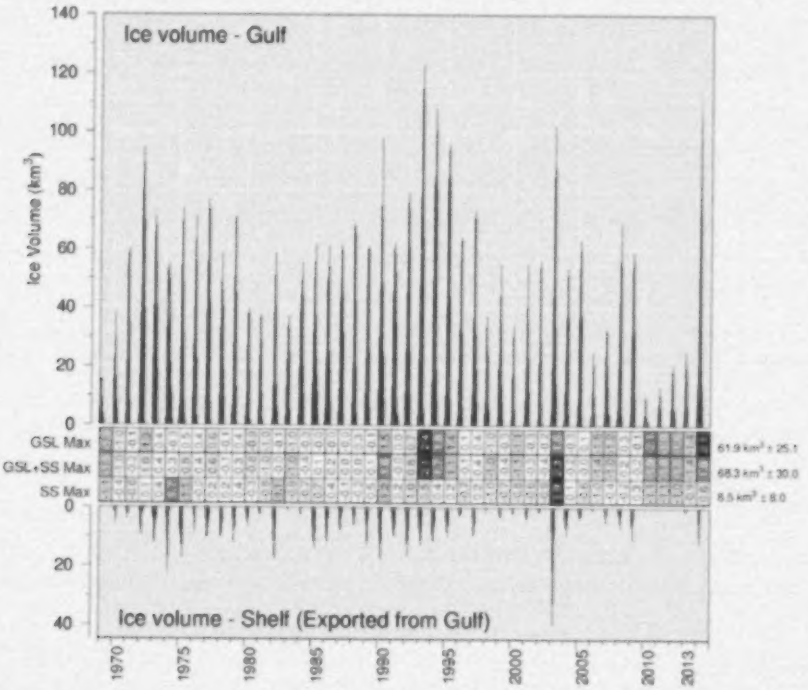

Fig. 31. Estimated ice volume in the Gulf of St. Lawrence (upper panel) and on the Scotian Shelf seaward of Cabot Strait (lower panel). Scorecards show numbered normalized anomalies for the Gulf, combined Gulf and Shelf and Shelf-only annual maximum volumes. Daily values from 1998 onward were filtered using a 3-day running mean prior to calculating the seasonal maximum. The mean and standard deviation are indicated on the right side using the 1981–2010 climatology.

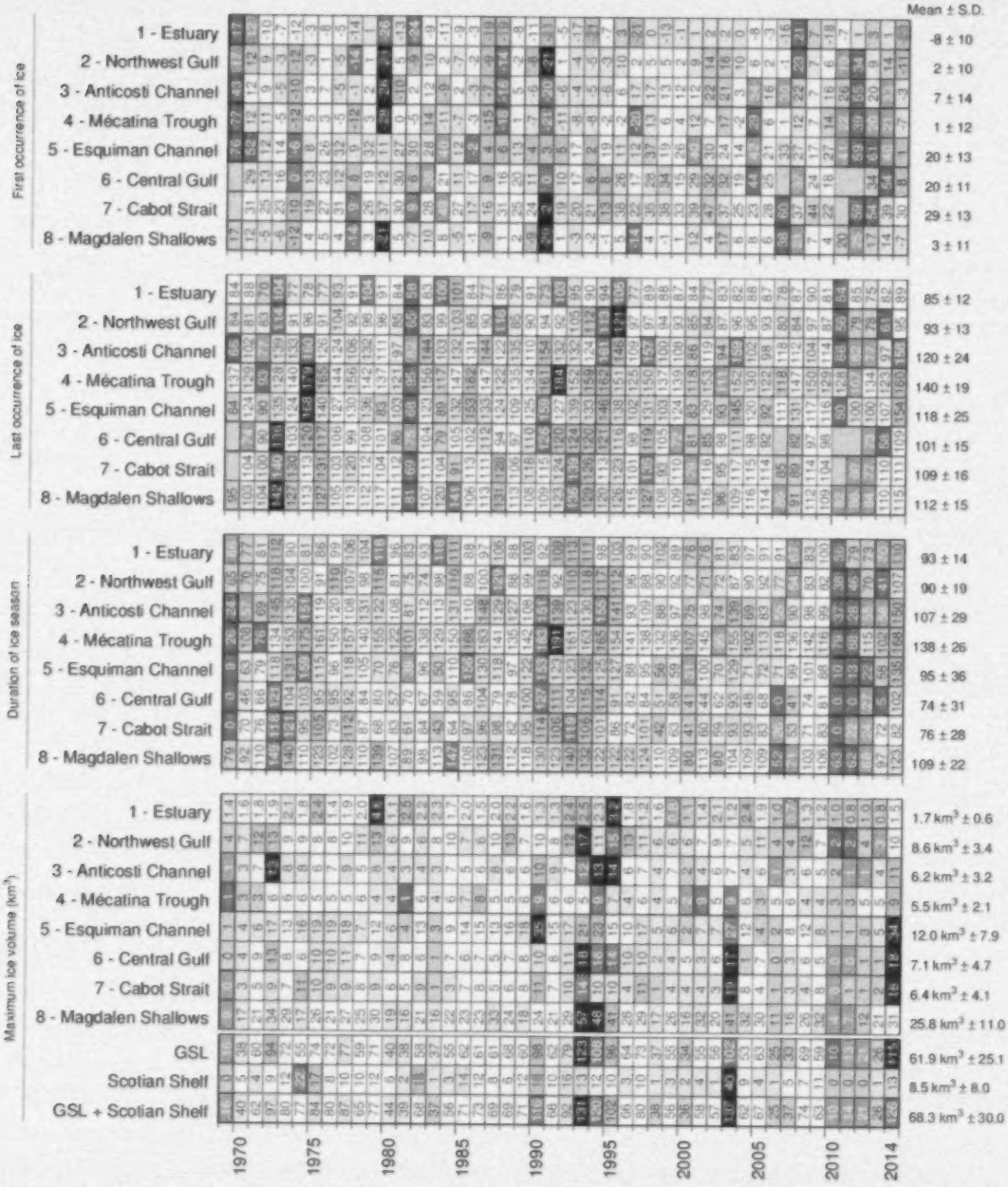

Fig. 32. First and last day of ice occurrence, ice duration, and maximum seasonal ice volume by region. The time when ice was first and last seen in days from the beginning of each year is indicated for each region, and the colour code expresses the anomaly based on the 1981–2010 climatology, with blue representing earlier first occurrence and later last occurrence. The threshold is 5% of the largest ice volume ever recorded in the region. Numbers in the table are the actual day of the year or volume, but the colour coding is according to normalized anomalies based on the climatology of each region. Duration is the numbers of days that the threshold was exceeded. For the last three lines showing seasonal maximum volumes over the areas of the GSL, Scotian Shelf and the combination, daily values from 1998 onward were filtered using a 3-day running mean prior to calculating the seasonal maximums; all prior data are based on weekly data.

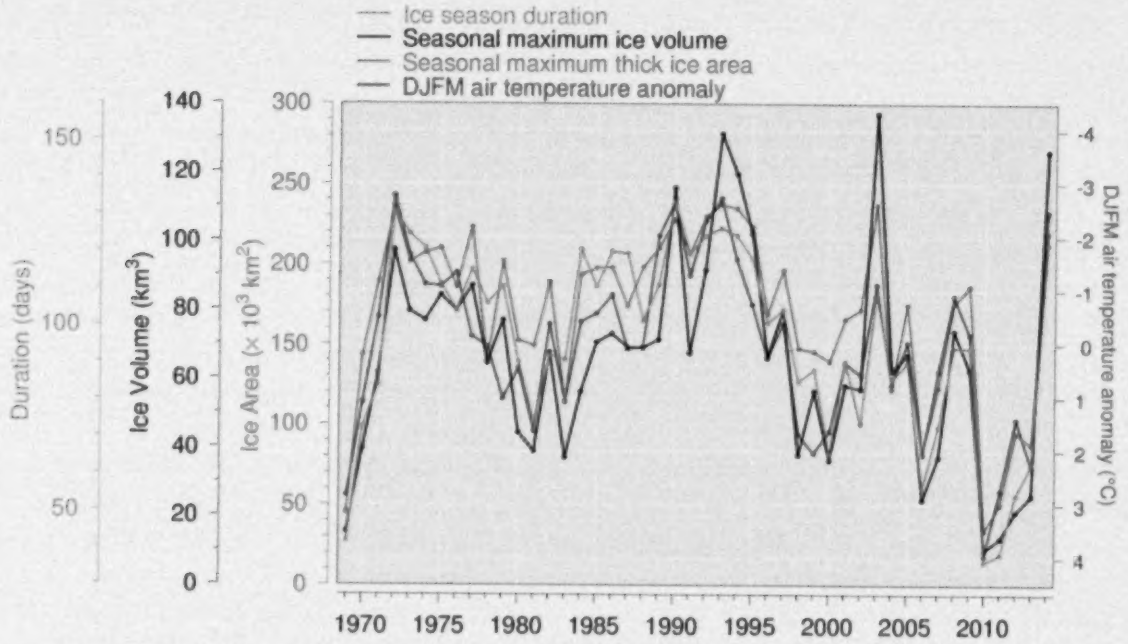

Fig. 33. Seasonal maximum ice volume and area including the portion on the Scotian Shelf (excluding ice less than 15 cm thick), ice season duration and December-to-March air temperature anomaly (Figure adapted from Hammill and Galbraith 2012, but here not excluding small floes and adding February and March data to the air temperature anomalies). Linear relations indicate losses of 17 km^3, 30,000 km^2 and 14 days of sea-ice season for each 1°C increase in winter air temperature (R^2 of 0.74, 0.79 and 0.78 respectively).

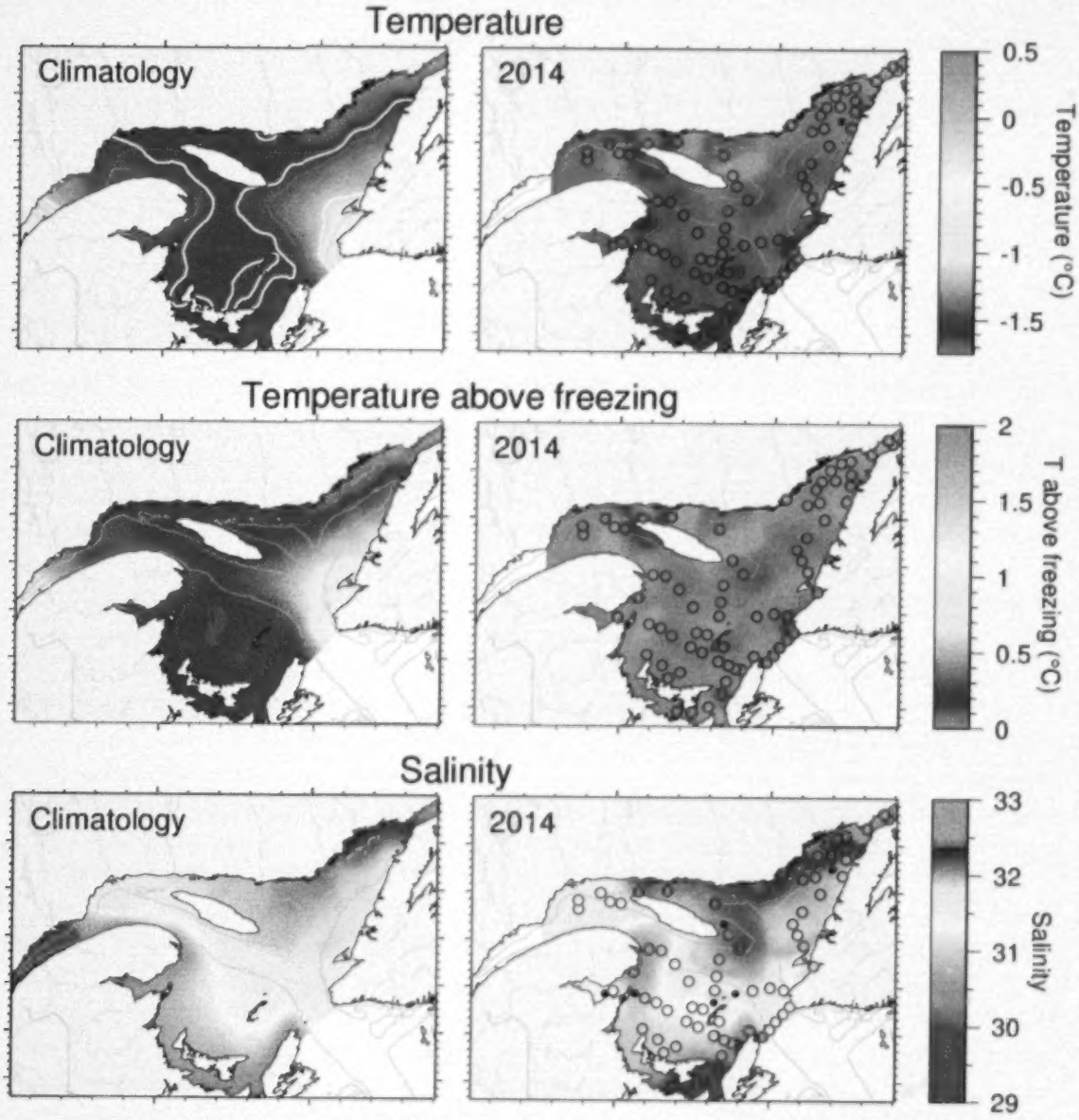

Fig. 34. Winter surface layer characteristics from the March 2014 helicopter survey compared with climatological means: surface water temperature (upper panel), temperature difference between surface water temperature and the freezing point (middle panel), and salinity (lower panel). Symbols are coloured according to the value observed at the station, using the same colour palette as the interpolated image. A good match is seen between the interpolation and the station observations where the station colours blend into the background. Black symbols indicate missing or bad data. The climatologies are based on 1996-2014 for salinity but excludes 2010 as an outlier for temperature and temperature above freezing.

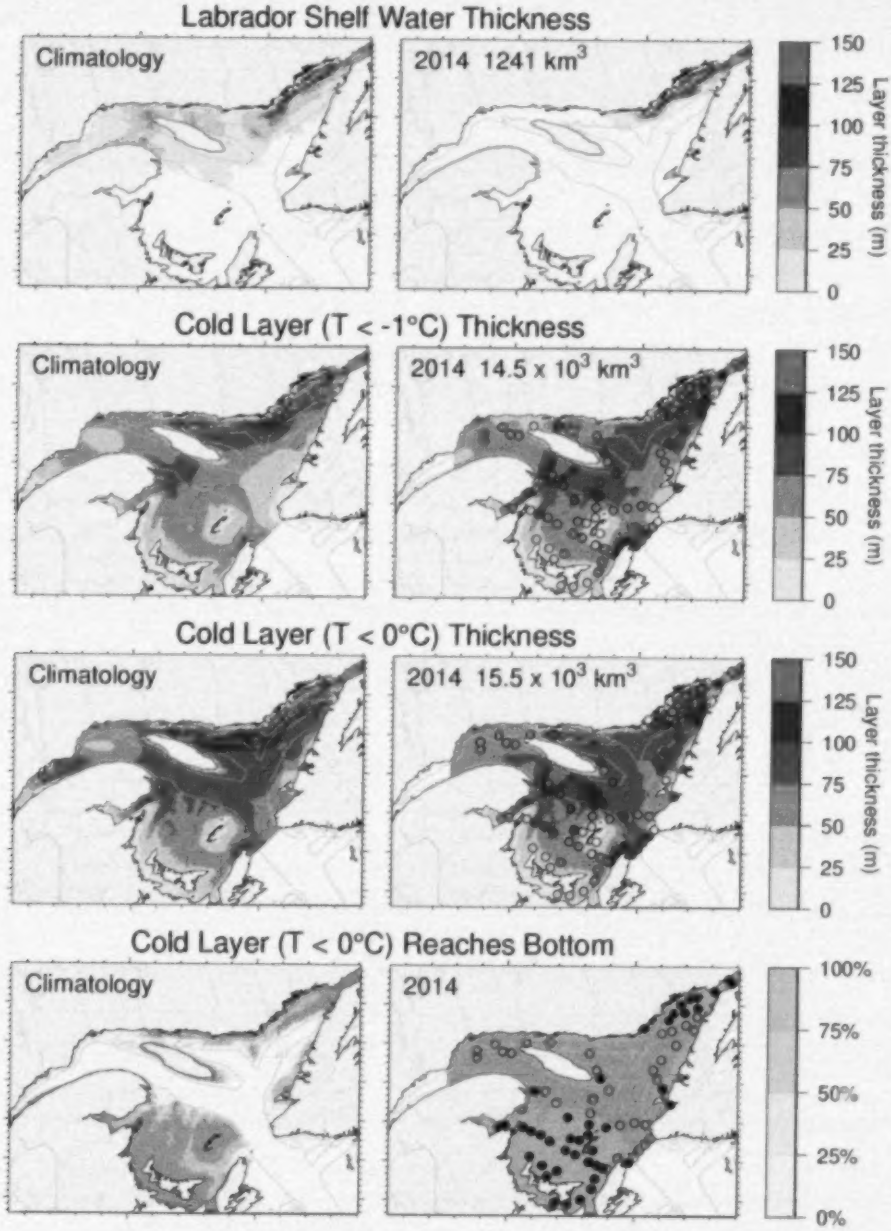

Fig. 35. Winter surface layer characteristics from the March 2014 helicopter survey compared with climatological means: estimates of the thickness of the Labrador Shelf water intrusion (upper panels), cold layer (T<-1°C, T<0°C) thickness (middle panels), and maps indicating where the cold layer (T<0°C) reaches the bottom (in brown; lower panels). Station symbols are coloured according to the observed values as in Fig. 34. For the lower panels, the stations where the cold layer reached the bottom are indicated with filled circles while open circles represent stations where the layer did not reach the bottom. Integrated volumes are indicated for the first six panels (including an approximation for the Estuary but excluding the Strait of Belle Isle). The climatologies are based on 1997-2014 for the Labrador Shelf water intrusion, 1996-2014 for the cold layer (T<0°C) but excludes 2010 for T<-1°C.

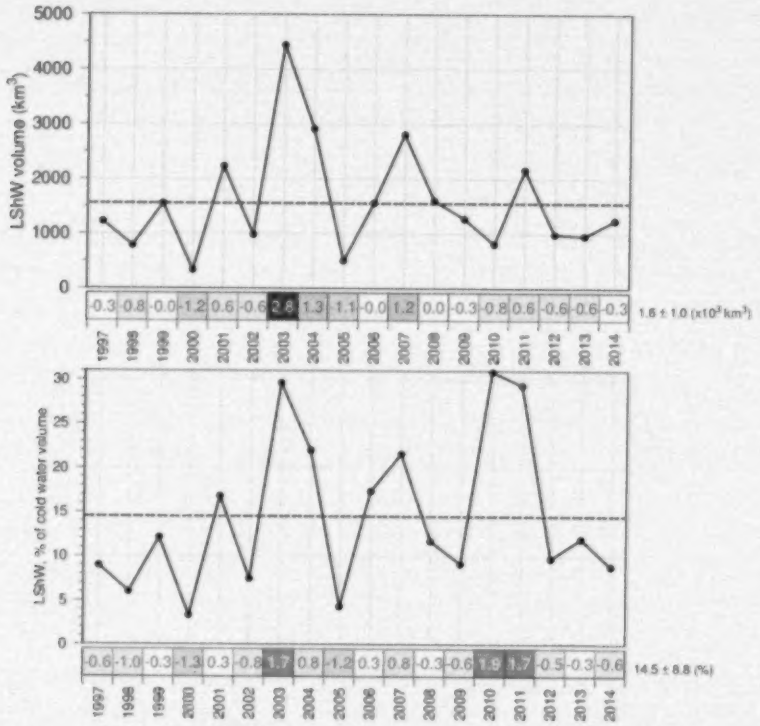

Fig. 36. Estimated volume of cold and saline Labrador Shelf water that flowed into the Gulf over the winter through the Strait of Belle Isle. The bottom panel shows the volume as a percentage of total cold-water volume (<-1°C). The numbers in the boxes are normalized anomalies.

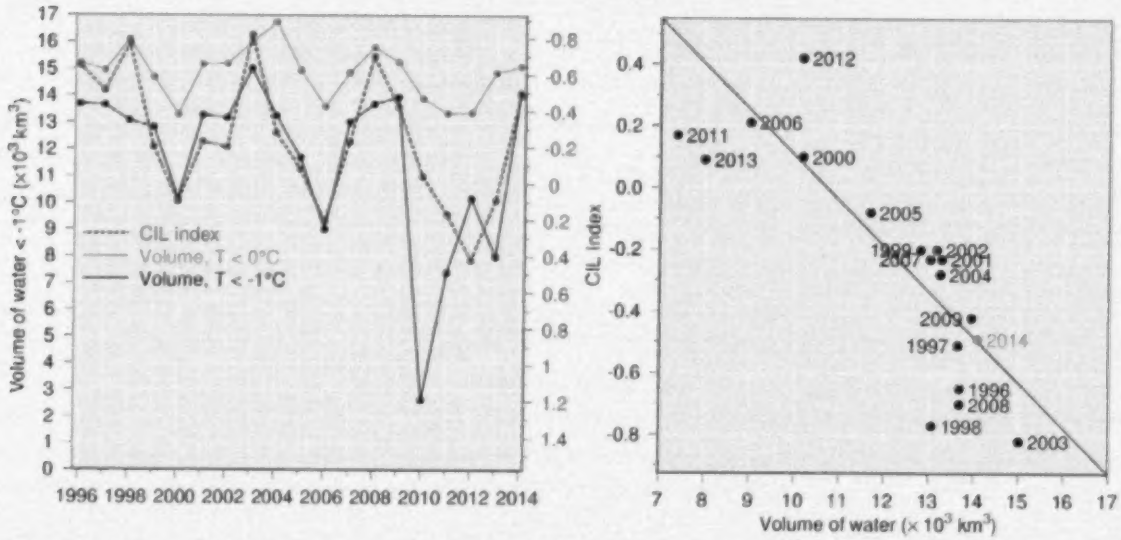

Fig. 37. Left panel: winter surface cold (T<-1°C and T<0°C) layer volume (excluding the Estuary and the Strait of Belle Isle) time series (black and grey lines) and summer CIL index (blue dashed line). Right panel: Relation between summer CIL index and winter cold-water volume with T<-1°C (regression for 1996-2014 data pairs, excluding 1998 [see Galbraith 2006] as well as the 2010 and 2011 mild winters). Note that the CIL scale in the left panel is reversed.

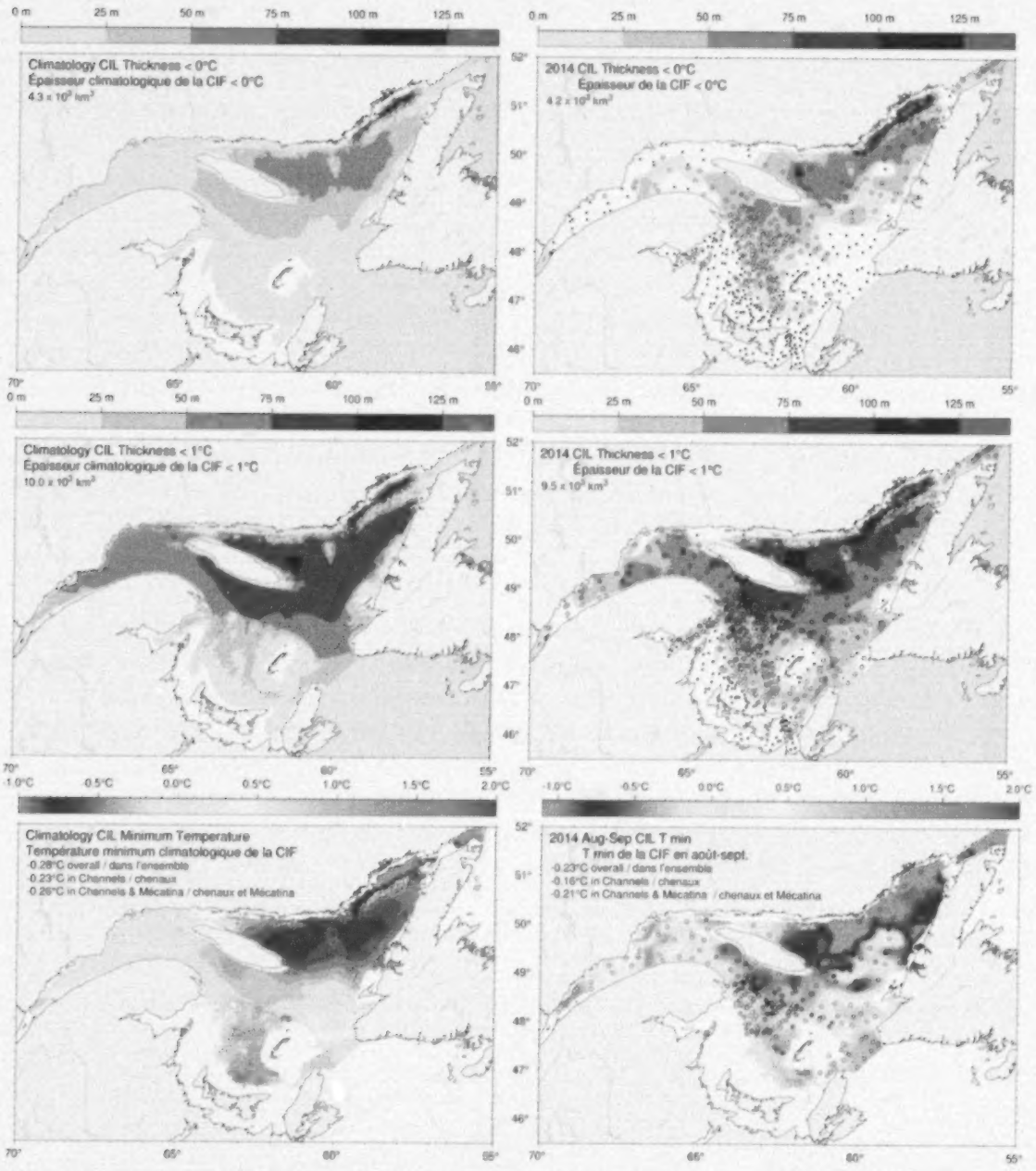
0 m 25 m 50 m 75 m 100 m 125 m
Climatology CIL Thickness < 0°C
Épaisseur climatologique de la CIF < 0°C
4.3 x 10³ km²
2014 CIL Thickness < 0°C
Épaisseur de la CIF < 0°C
4.2 x 10³ km²
Climatology CIL Thickness < 1°C
Épaisseur climatologique de la CIF < 1°C
10.0 x 10³ km²
2014 CIL Thickness < 1°C
Épaisseur de la CIF < 1°C
9.5 x 10³ km²
-1.0°C -0.5°C 0.0°C 0.5°C 1.0°C 1.5°C 2.0°C
Climatology CIL Minimum Temperature
Température minimum climatologique de la CIF
-0.26°C overall / dans l'ensemble
-0.23°C in Channels / chenaux
-0.26°C in Channels & Mécatina / chenaux et Mécatina
2014 Aug-Sep CIL T min
T min de la CIF en août-sept.
-0.23°C overall / dans l'ensemble
-0.16°C in Channels / chenaux
-0.21°C in Channels & Mécatina / chenaux et Mécatina
70° 65° 60° 55°
46° 47° 48° 49° 50° 51° 52°

Fig. 38. Cold intermediate layer thickness (T<0°C, top panels; T<1°C, middle panels) and minimum temperature (bottom panels) in August and September 2014 (right) and 1985-2010 climatology (left). Station symbols are colour-coded according to their CIL thickness and minimum temperature. Numbers in the upper and middle panels are integrated CIL volumes and in the lower panels are monthly average temperatures.

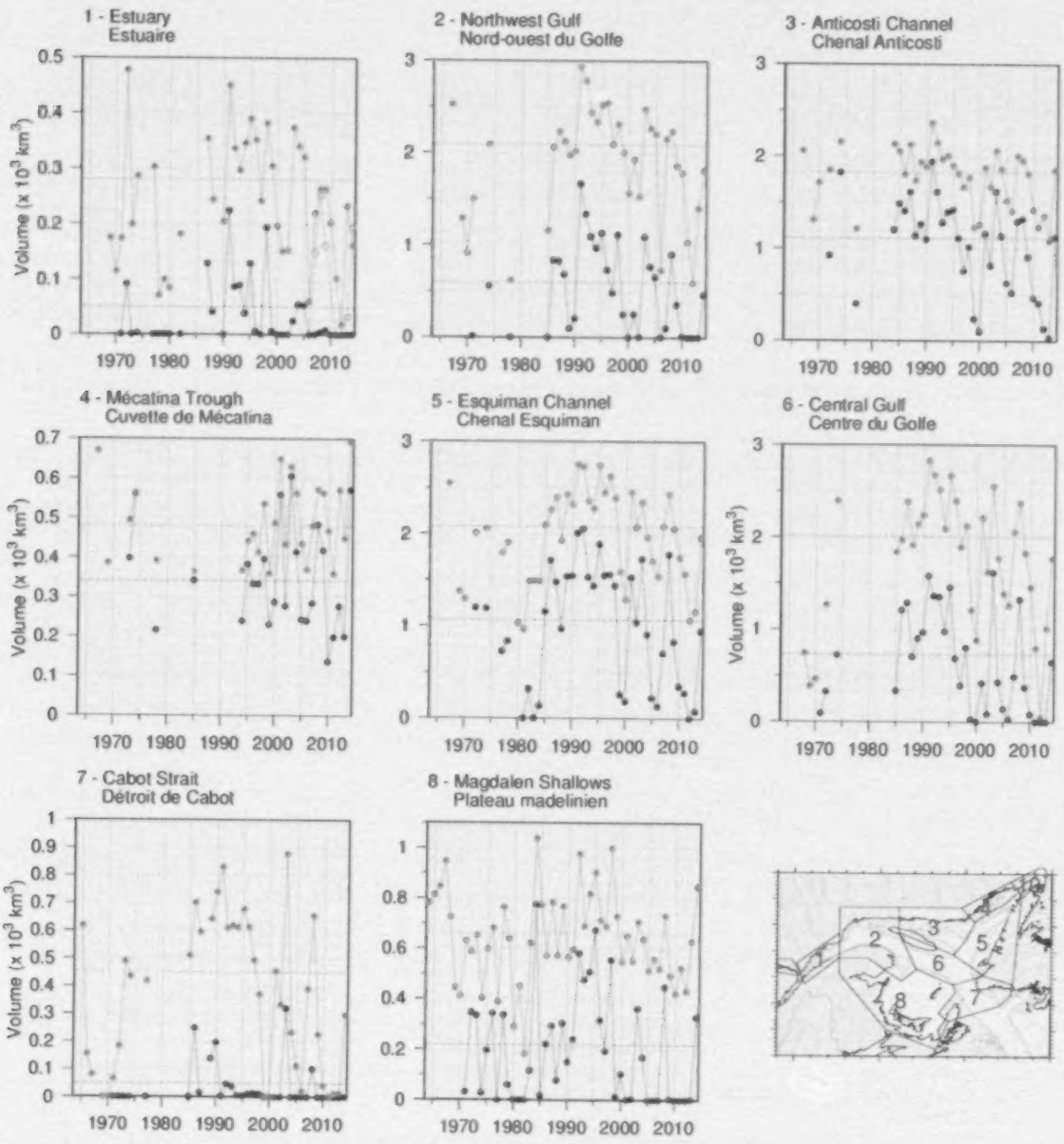

Fig. 39. Volume of the CIL colder than 0°C (blue) and colder than 1°C (red) in August and September (primarily region 8 in September). The volume of the CIL colder than 1°C in November for available years since 2006 is also shown for the St. Lawrence Estuary (dashed line).

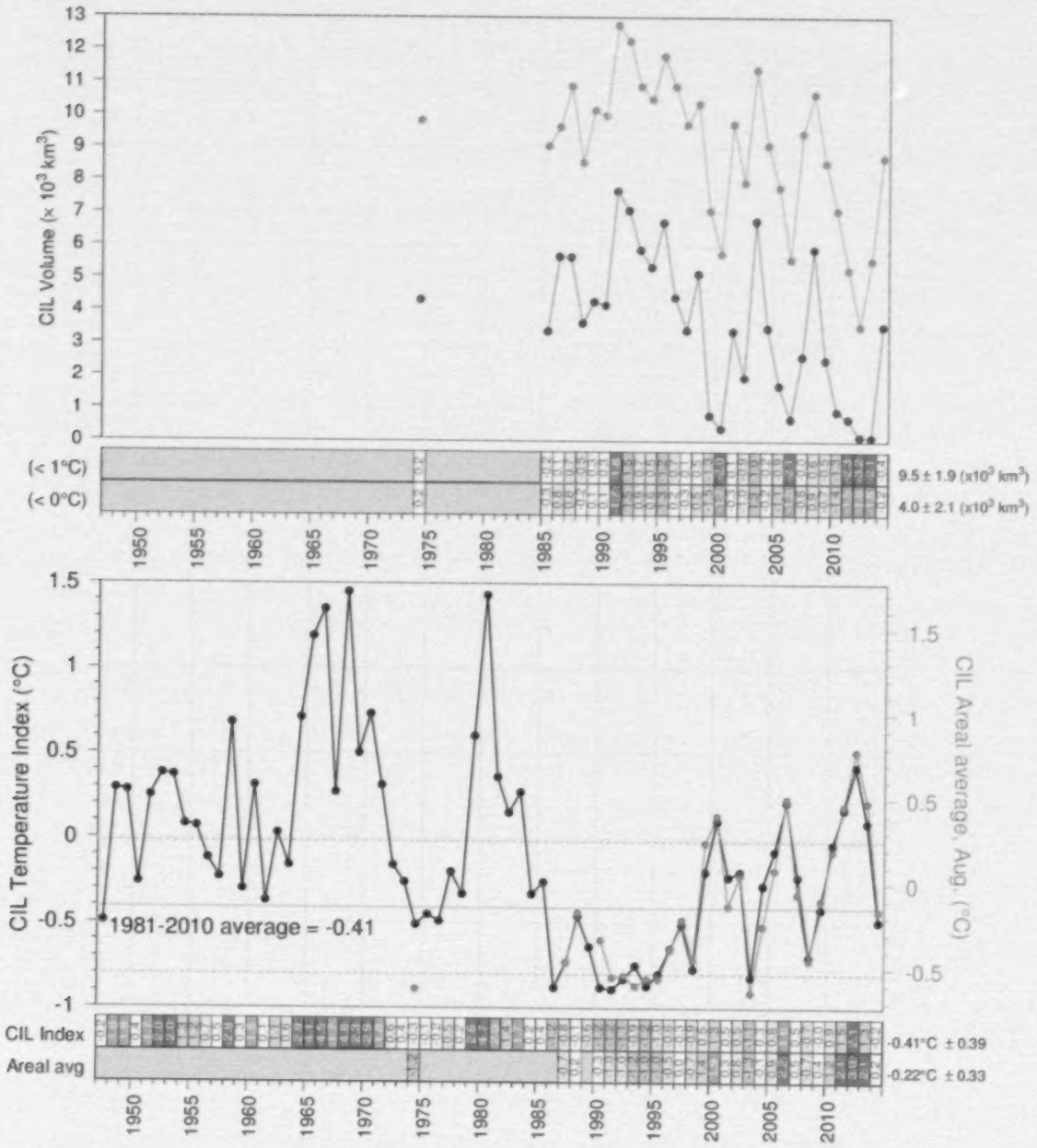

Fig. 40. CIL volume (top panel) delimited by 0°C (in blue) and 1°C (in red), and minimum temperature index (bottom panel) in the Gulf of St. Lawrence. The volumes are integrals of each of the annual interpolated thickness grids such as those shown in the top panels of Fig. 38 excluding Mécatina Trough and the Strait of Belle Isle. In the lower panel, the black line is the updated Gilbert and Pettigrew (1997) index interpolated to 15 July and the green line is the spatial average of each of the annual interpolated grid such as those shown in the two bottom panels of Fig. 38, excluding Mécatina Trough, the Strait of Belle Isle and the Magdalen Shallows. The numbers in the boxes are normalized anomalies relative to 1980-2010 climatologies constructed using all available years.

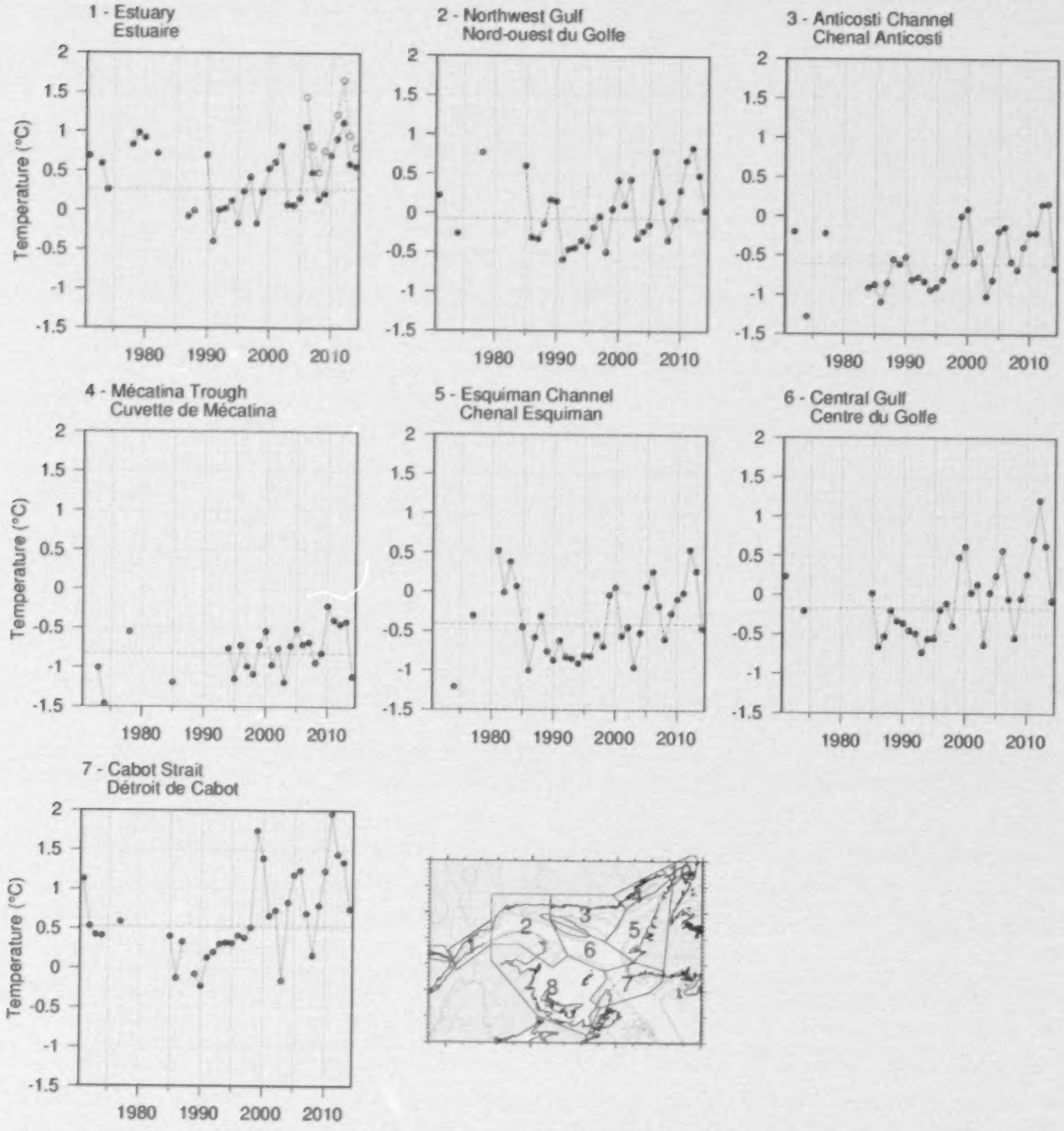

Fig. 41. Temperature minimum of the CIL spatially averaged for the seven areas where the CIL minimum temperature can be clearly identified. The spatial average of the November CIL temperature minimum for available years since 2006 is also shown for the St. Lawrence Estuary (dashed line).

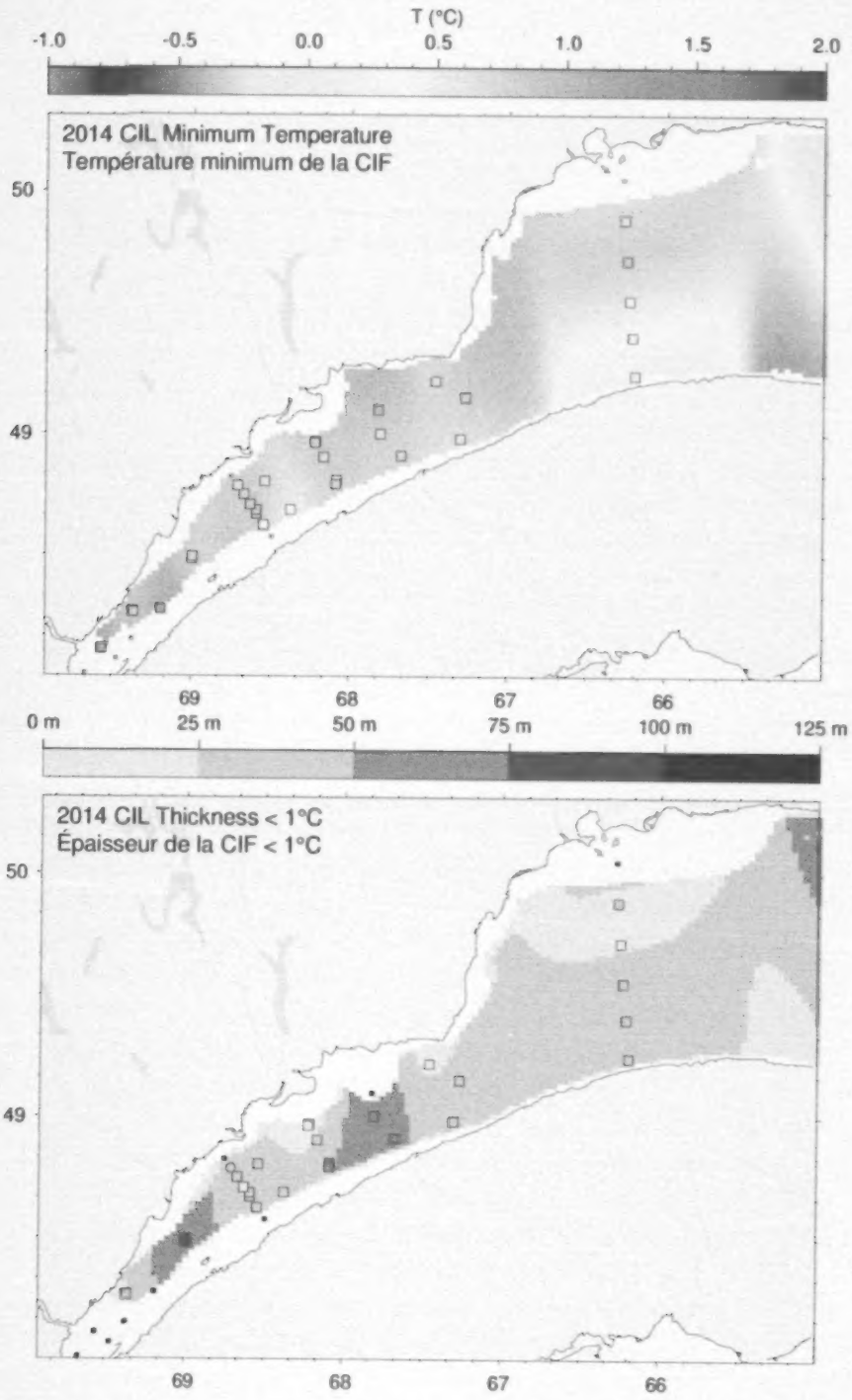

Fig. 42. Cold intermediate layer minimum temperature and thickness (T<1°C) in November 2014 in the St. Lawrence Estuary.

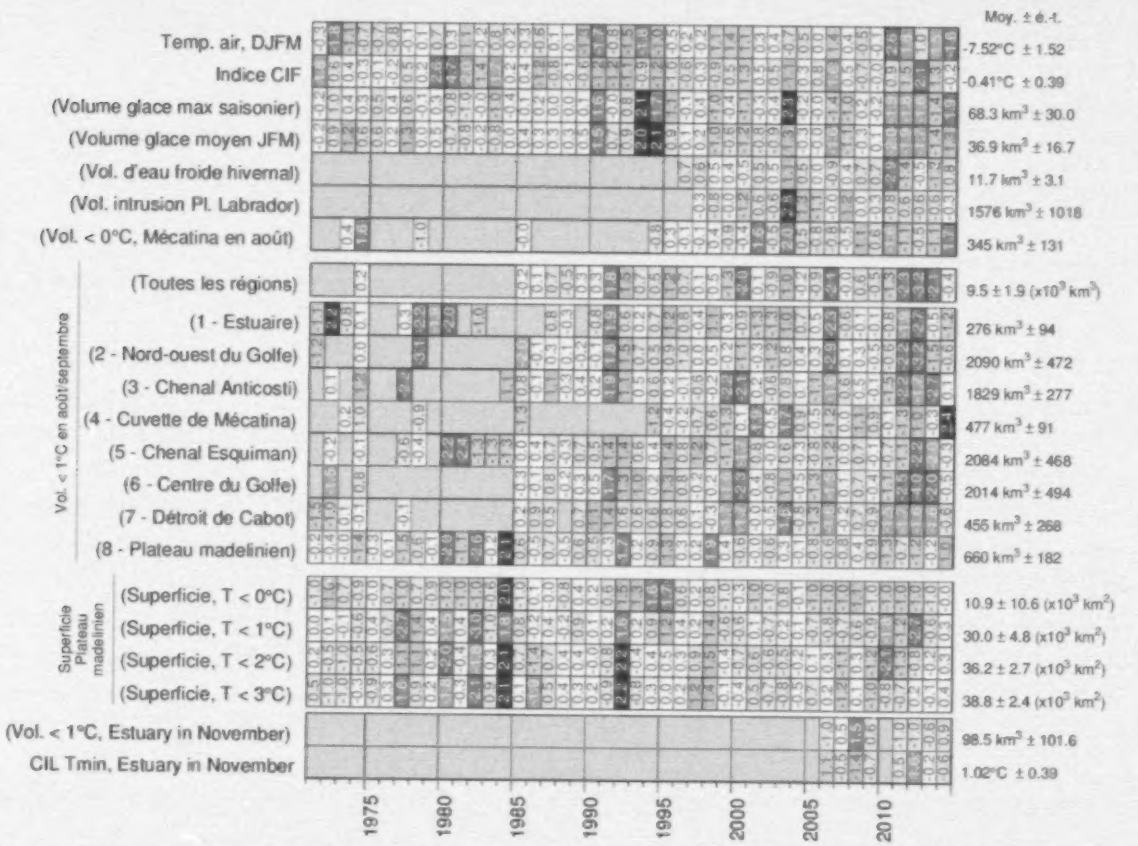

Fig. 43. Winter and summertime CIL related properties. The top block shows the scorecard time series for Dec-Jan-Feb-March air temperature (Fig. 5), the Gilbert and Pettigrew (1997) CIL index, yearly maximum sea-ice volume (Gulf + Scotian Shelf), Dec-Jan-Feb average sea-ice volume, winter (March) cold-layer (<-1°C) volume, volume of Labrador Shelf Water intrusion into the Gulf observed in March, and the August–September volume of cold water (<0°C) observed in the Mécatina Trough. Labels in parentheses have their colour coding reversed (blue for high values). The second block shows scorecard time series for August–September CIL volumes (<1°C) for all eight regions and for the entire Gulf when available. The third block shows the scorecard time series for the bottom areas of the Magdalen Shallows covered by waters colder than 0, 1, 2, and 3°C during the September survey. The last block shows the November survey CIL volume (<1°C) and average CIL minimum temperature in the Estuary.

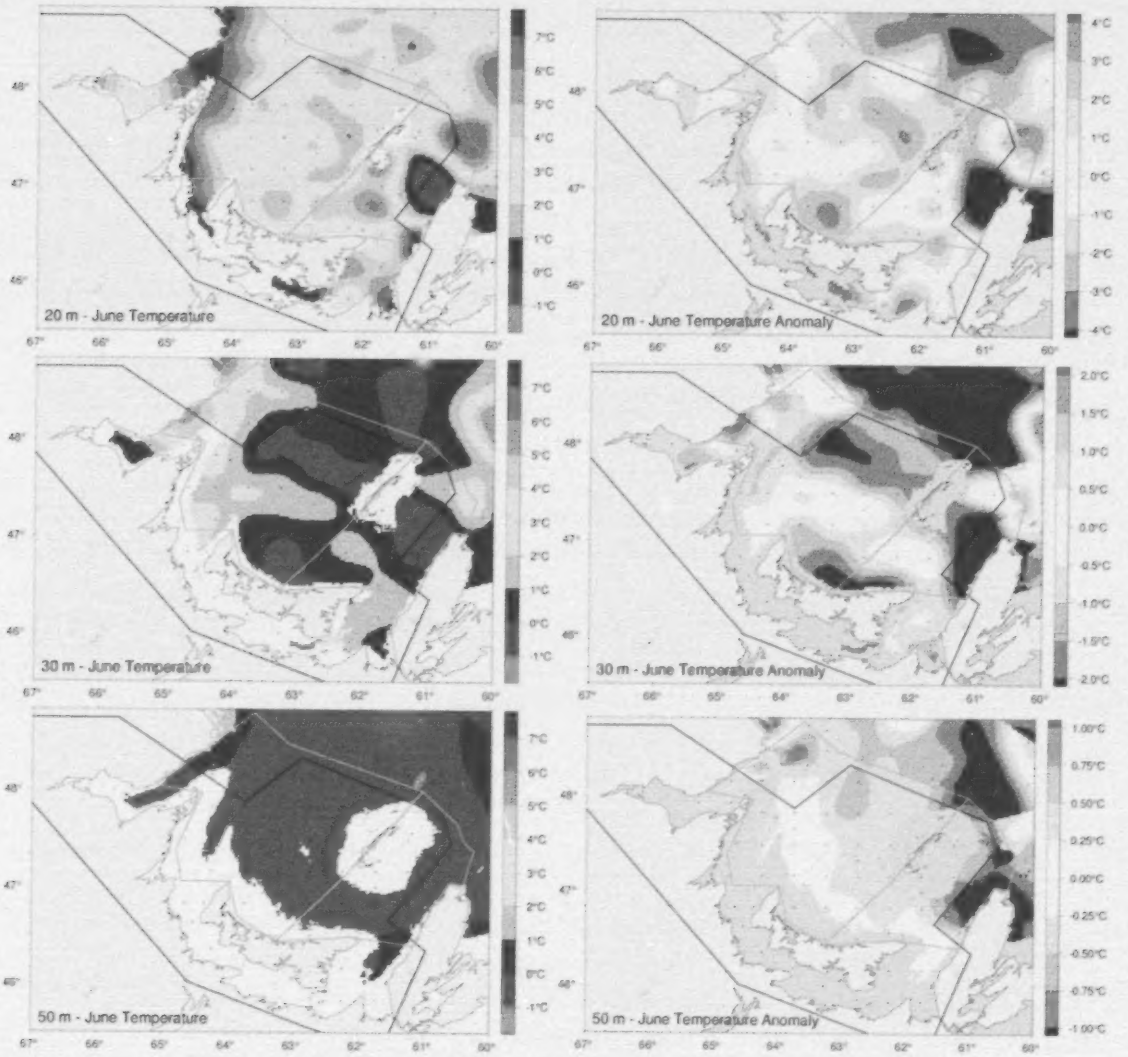
20 m - June Temperature
20 m - June Temperature Anomaly
30 m - June Temperature
30 m - June Temperature Anomaly
50 m - June Temperature
50 m - June Temperature Anomaly

Fig. 44. June depth-layer temperature and anomaly fields on the Magdalen Shallows at 10, 20 and 50 m. Anomalies are based on 1971-2010 climatologies for all available years (appearing on Fig. 45) The black outline delimits Region 8 (Fig. 2) and the gray outlines delimit western and eastern regions of the Magdalen Shallows (Fig. 19).

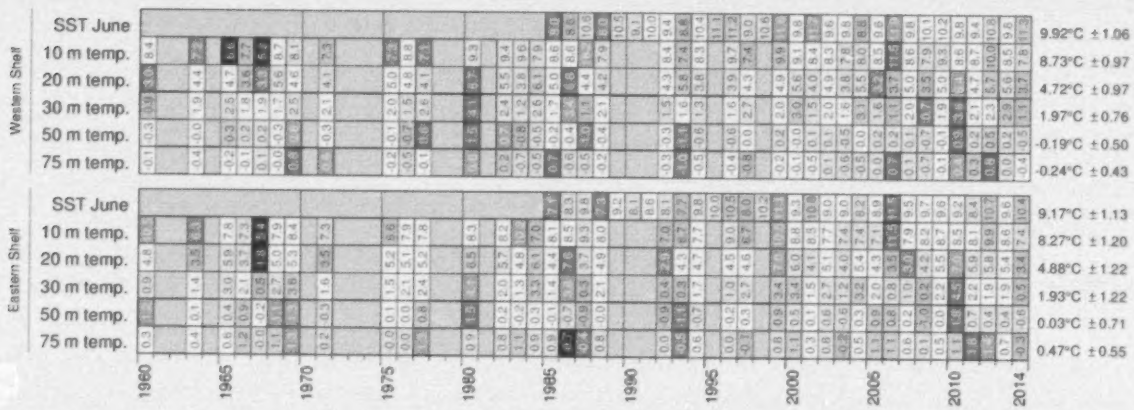

Fig. 45. Depth-layer average temperature anomalies for western and eastern Magdalen Shallows for the June mackerel survey. The SST data are June averages from NOAA remote sensing repeated from Fig. 20. The SST colour-coding is based on the 1985-2010 climatology and the numbers are mean temperatures in °C. The colour-coding of the 10 to 75 m lines are according to normalized anomalies based on the 1981-2010 climatologies, but the numbers are mean temperatures in °C.

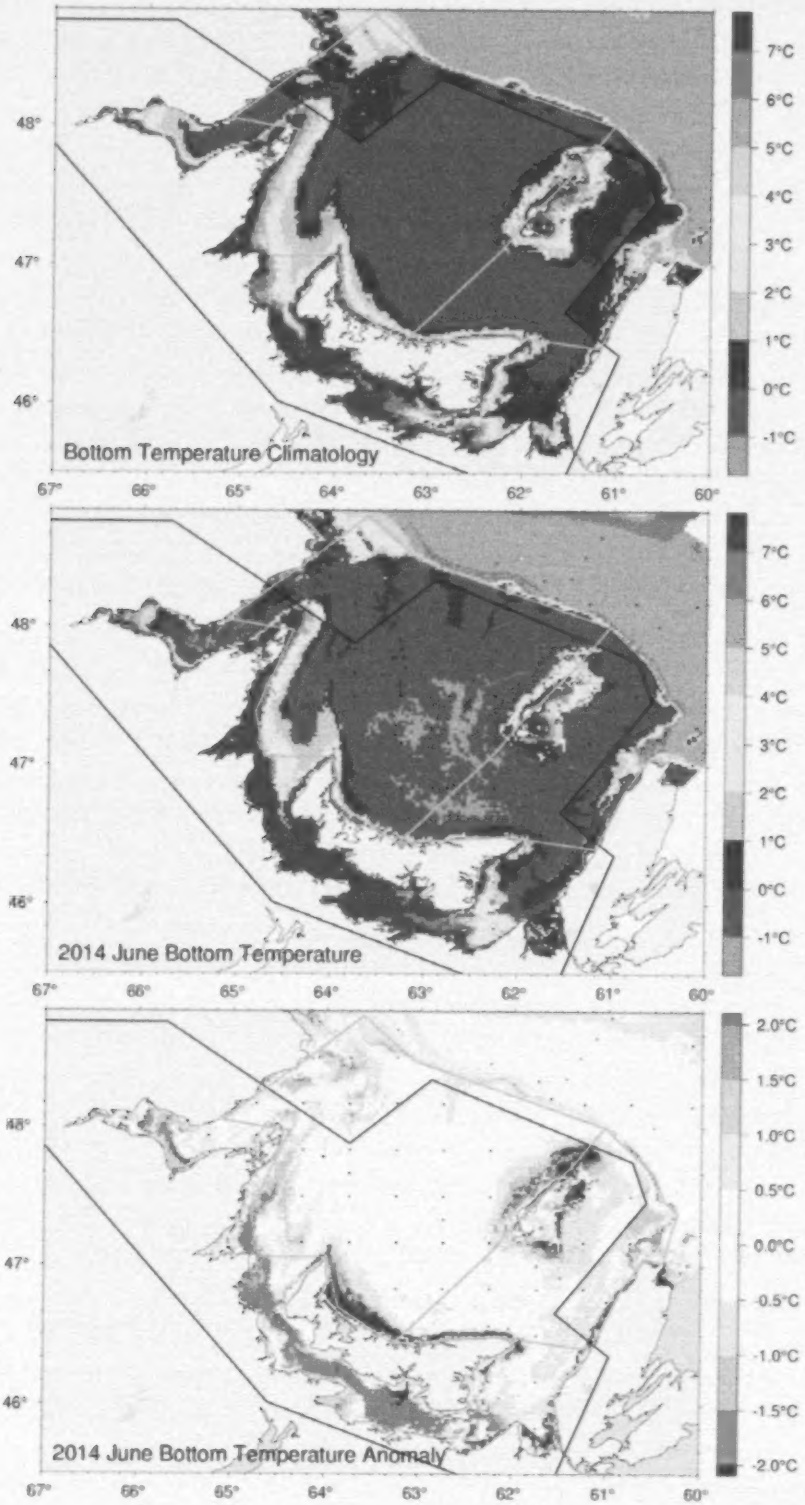

Fig. 46. June bottom temperature climatology (top), 2014 observations (middle) and anomaly (bottom).

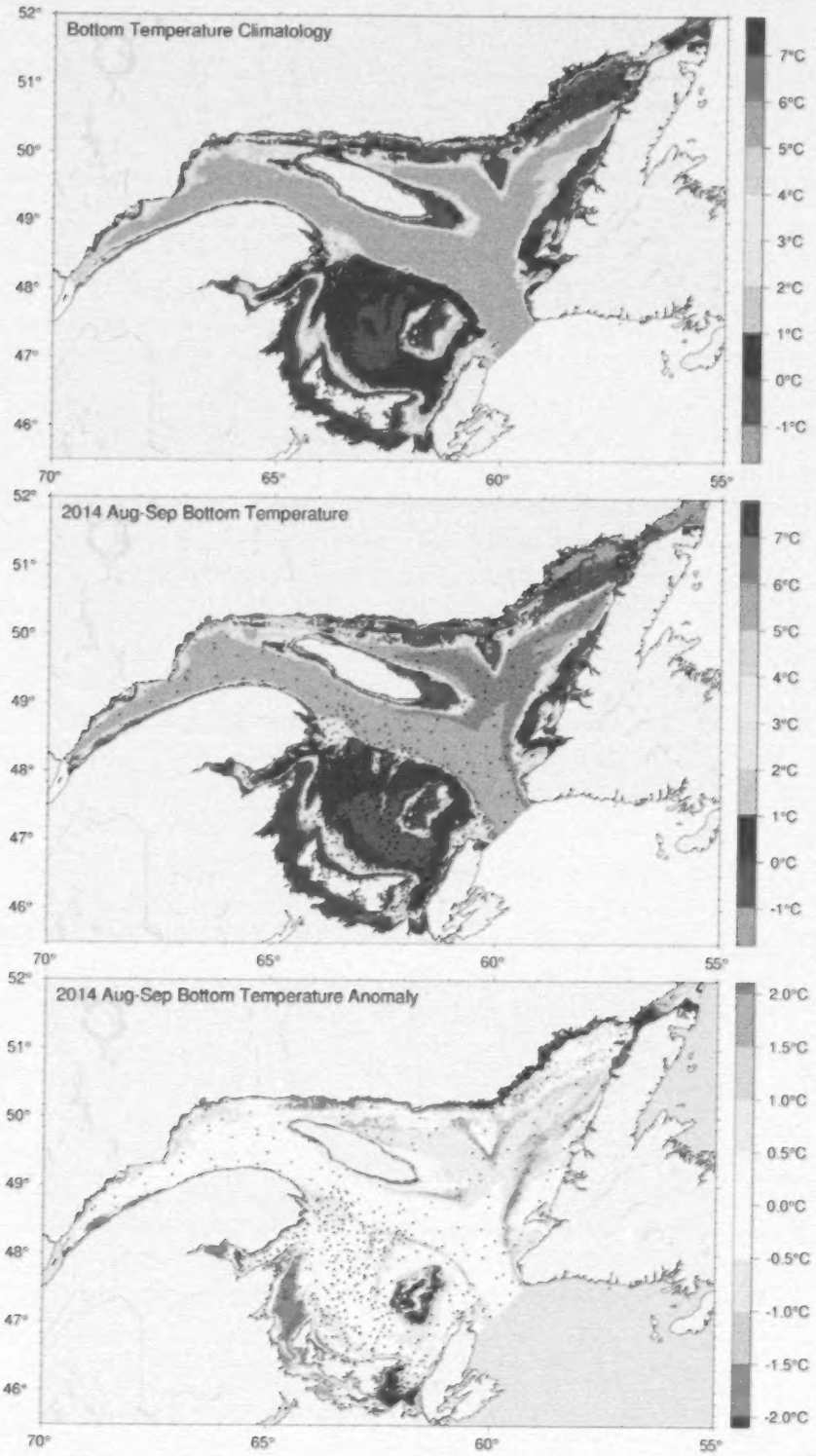

Fig. 47. August-September bottom temperature climatology (top), 2014 observations (middle) and anomaly (bottom).

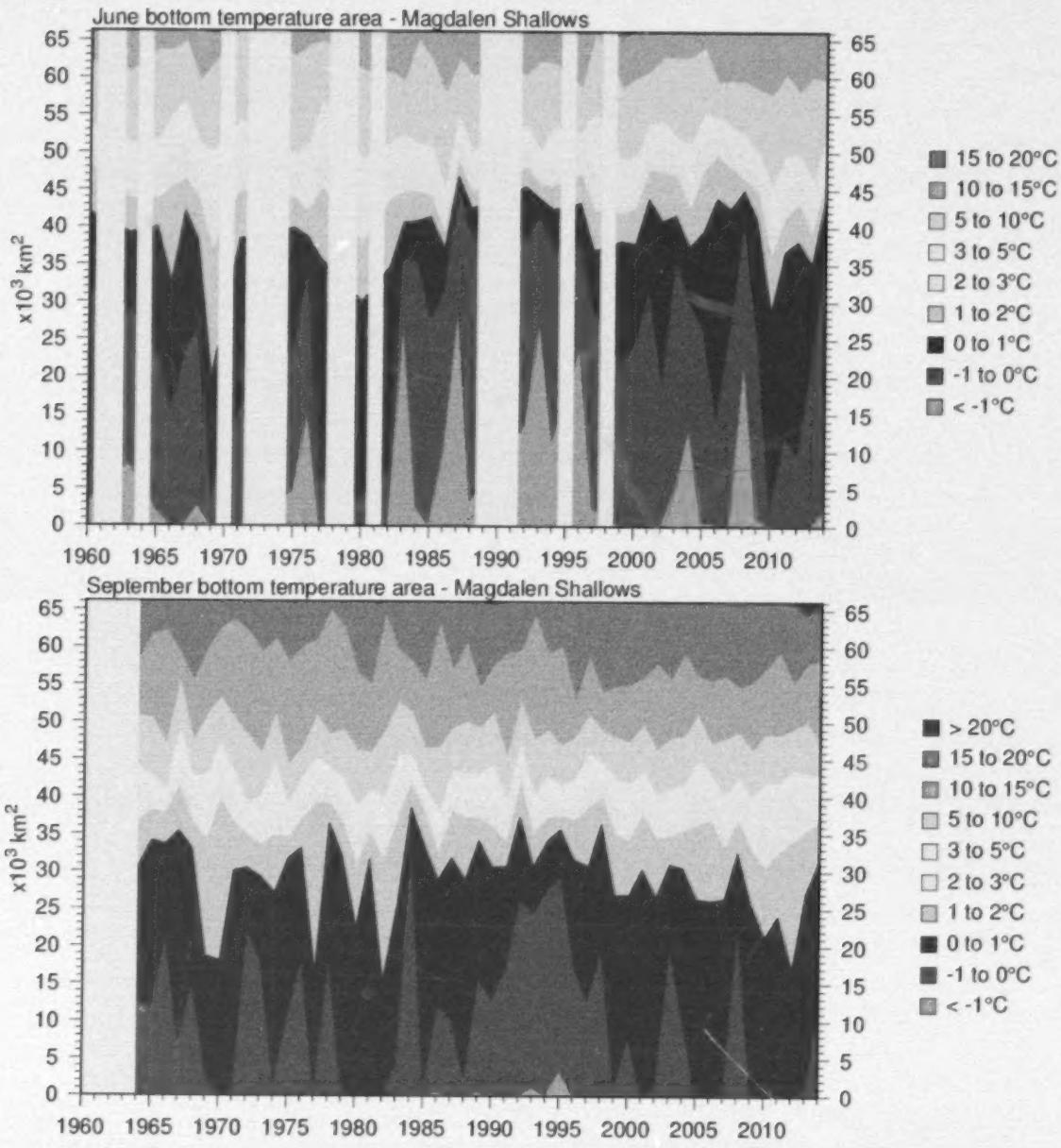

Fig. 48. Time series of the bottom areas covered by different temperature bins in June (top) and August-September (bottom) for the Magdalen Shallows (region 8). Data are mostly from September for the bottom panel.

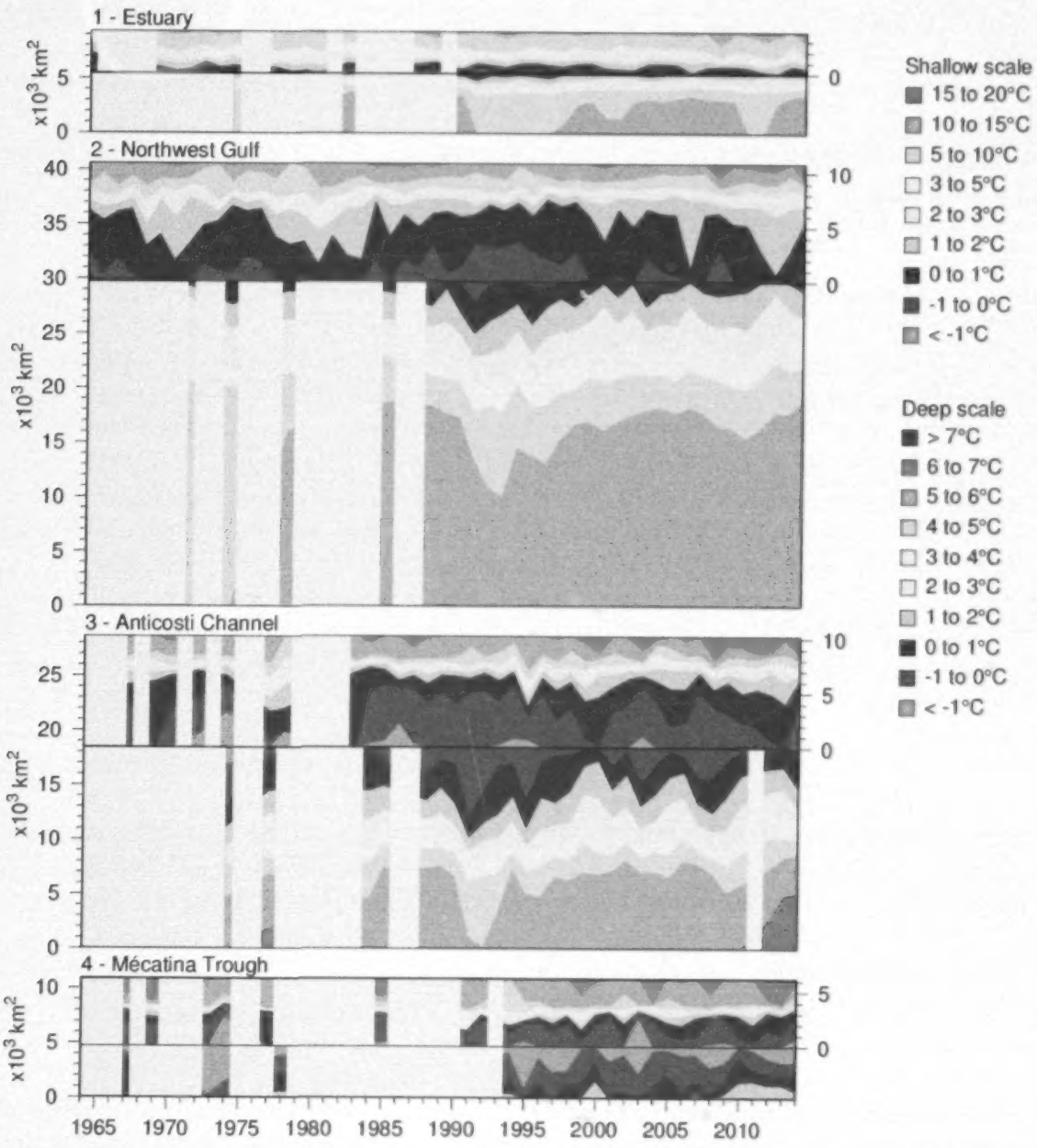

Fig. 49. Time series of the bottom areas covered by different temperature bins in August and September for regions 1 to 4. The panels are separated by a black horizontal line into shallow (<100m) and deep (>100 m) areas to distinguish between warmer waters above and below the CIL. The shallow areas are shown on top using the area scale on the right-hand side and have warmer waters shown starting from the top end. The deep areas are shown below the horizontal line and have warmer waters starting at the bottom end. The CIL areas above and below 100 m meet near the horizontal line.

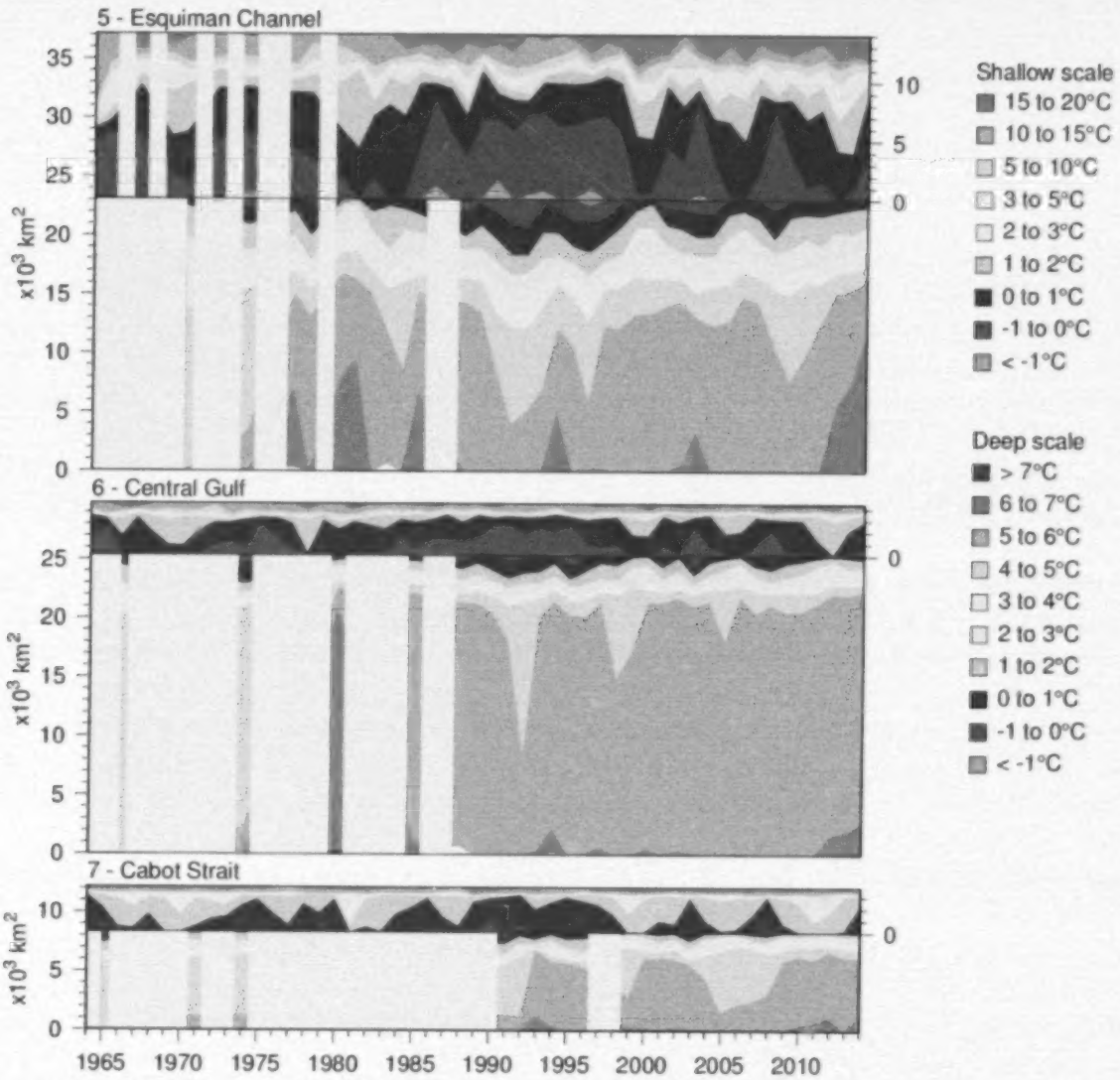

Fig. 50. Time series of the bottom areas covered by different temperature bins in August and September for regions 5 to 7. The panels are separated into shallow (<100 m) and deep (>100 m) areas to distinguish between warmer waters above and below the CIL See Fig. 49 caption.

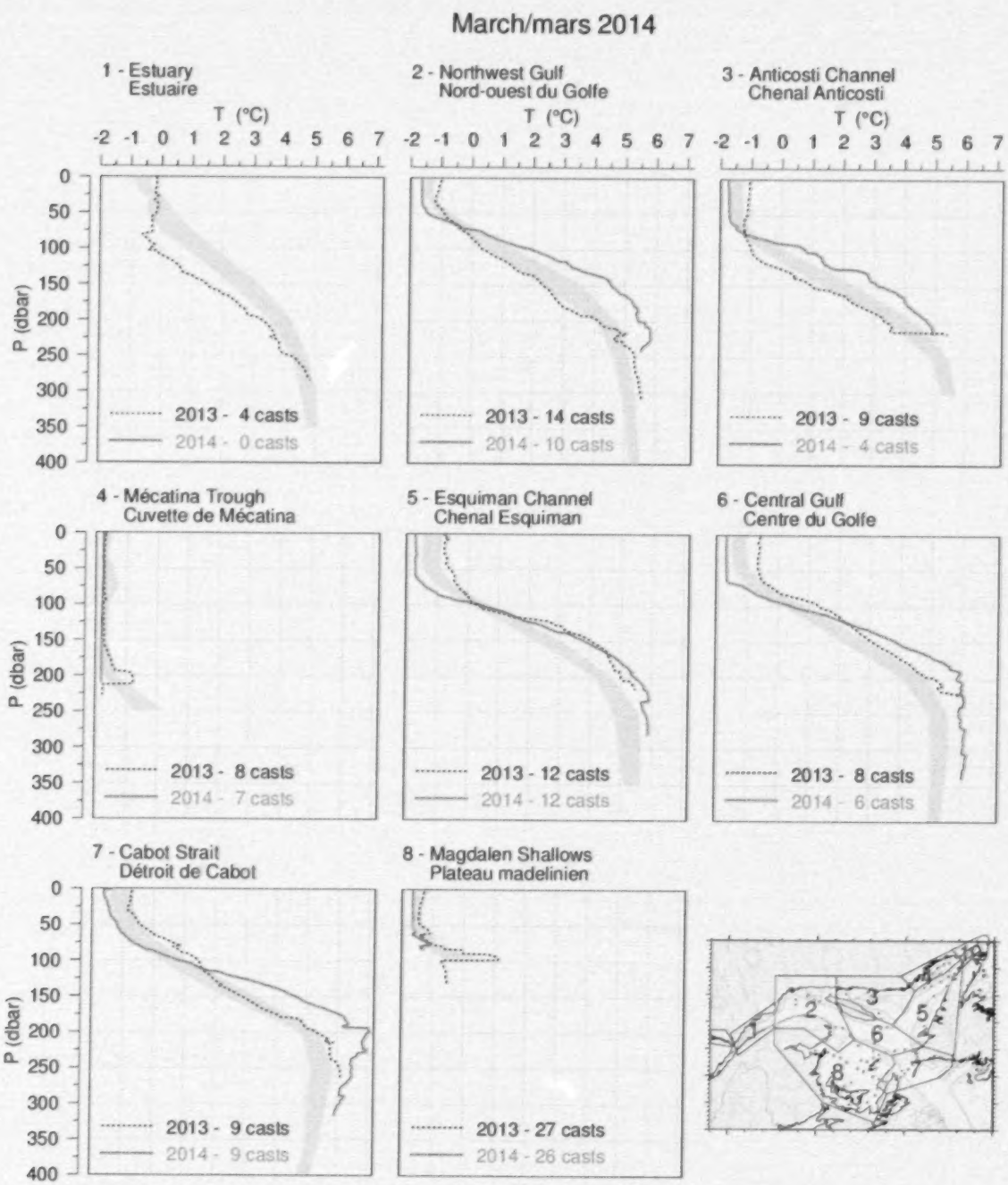

Fig. 51. Mean temperature profiles observed in each region of the Gulf during the March helicopter survey. The shaded area represents the 1981–2010 (but mostly 1996–2010) climatological monthly mean ± 0.5 SD. Mean profiles for 2013 are also shown for comparison.

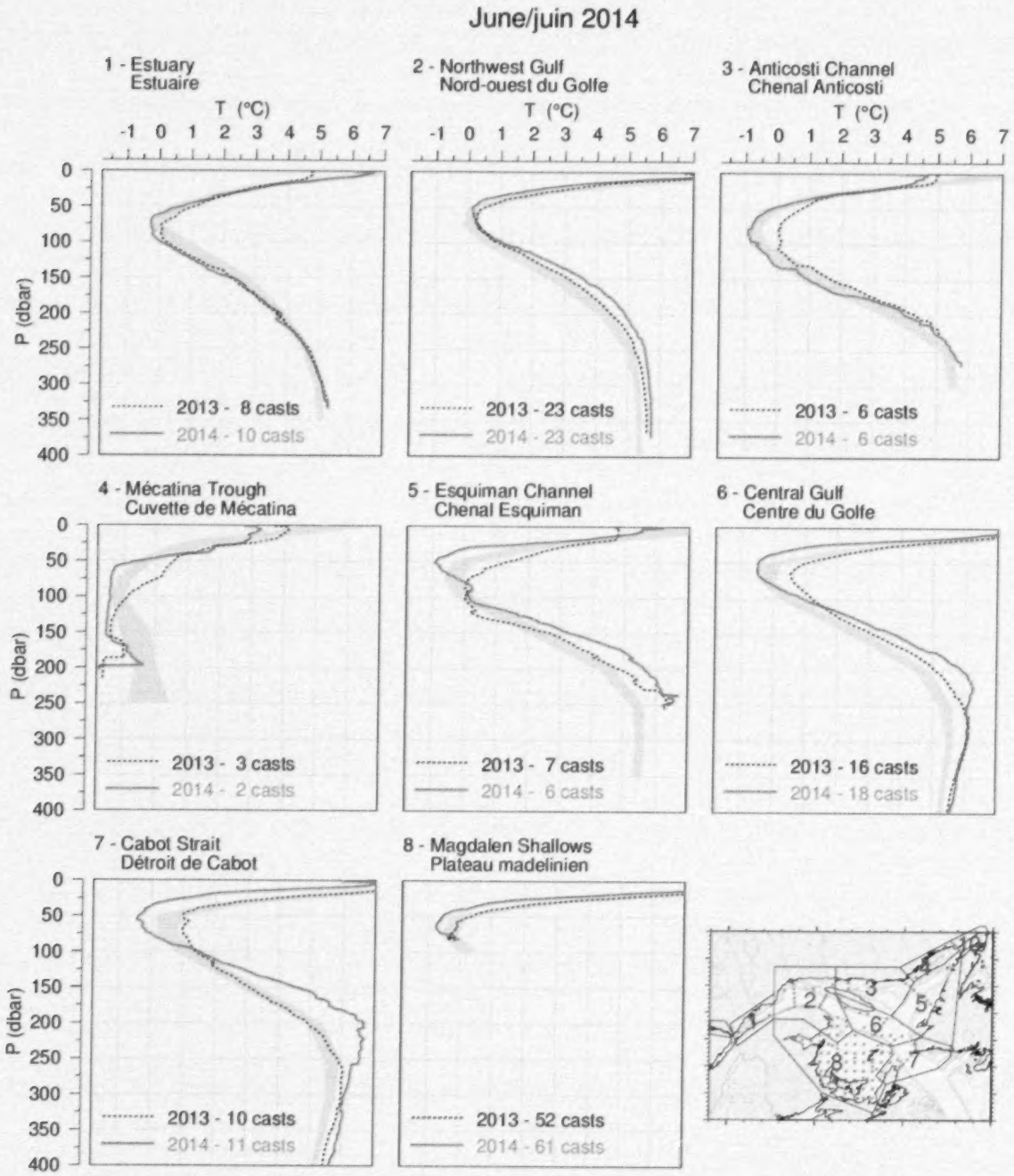

Fig. 52. Mean temperature profiles observed in each region of the Gulf during June. The shaded area represents the 1981–2010 climatological monthly mean ± 0.5 SD. Mean profiles for 2013 are also shown for comparison.

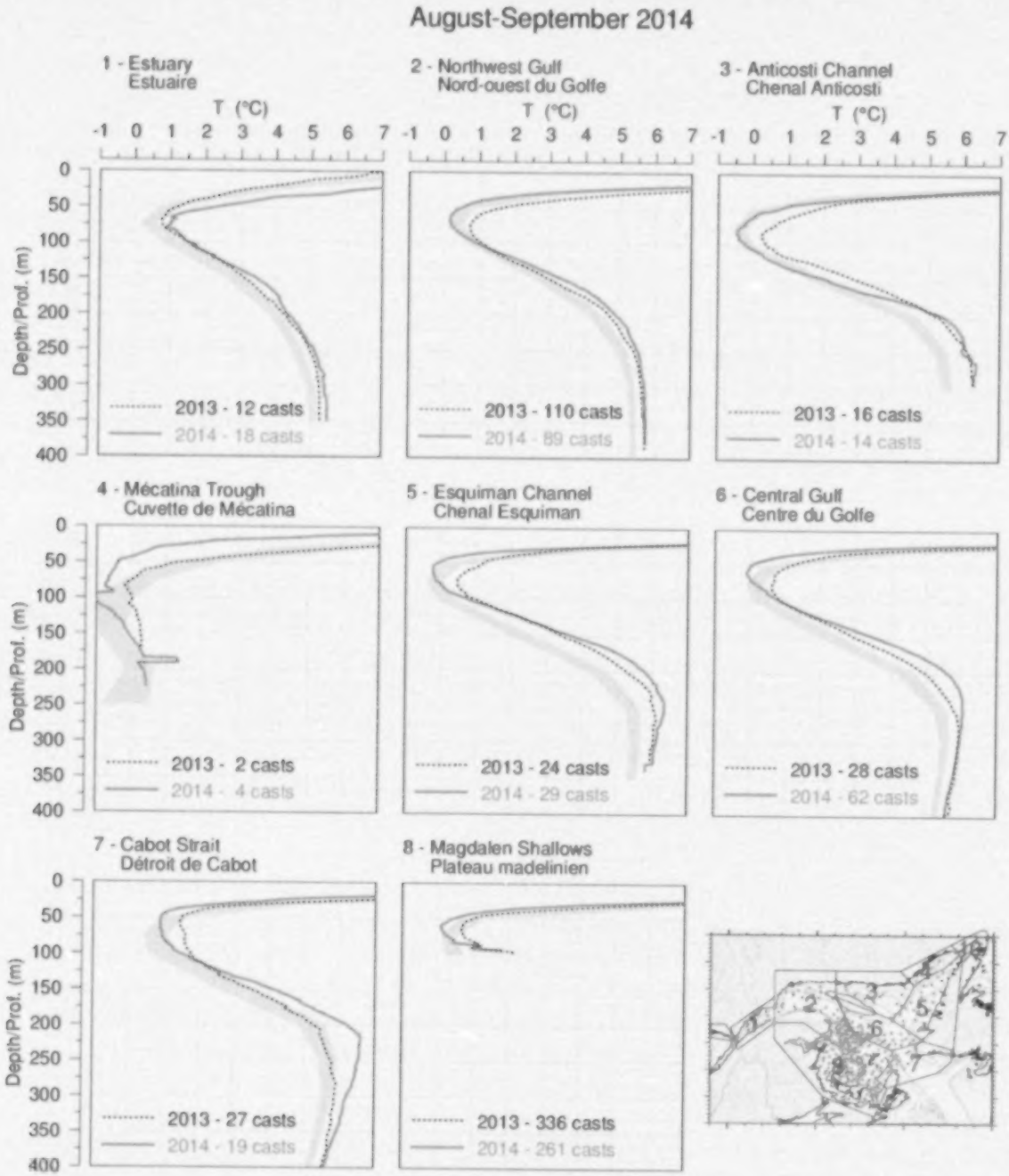

Fig. 53. Mean temperature profiles observed in each region of the Gulf during August and September. The shaded area represents the 1981–2010 climatological monthly mean ± 0.5 SD for August for regions 1 through 7 and for September for region 8. Mean profiles for 2013 are also shown for comparison.

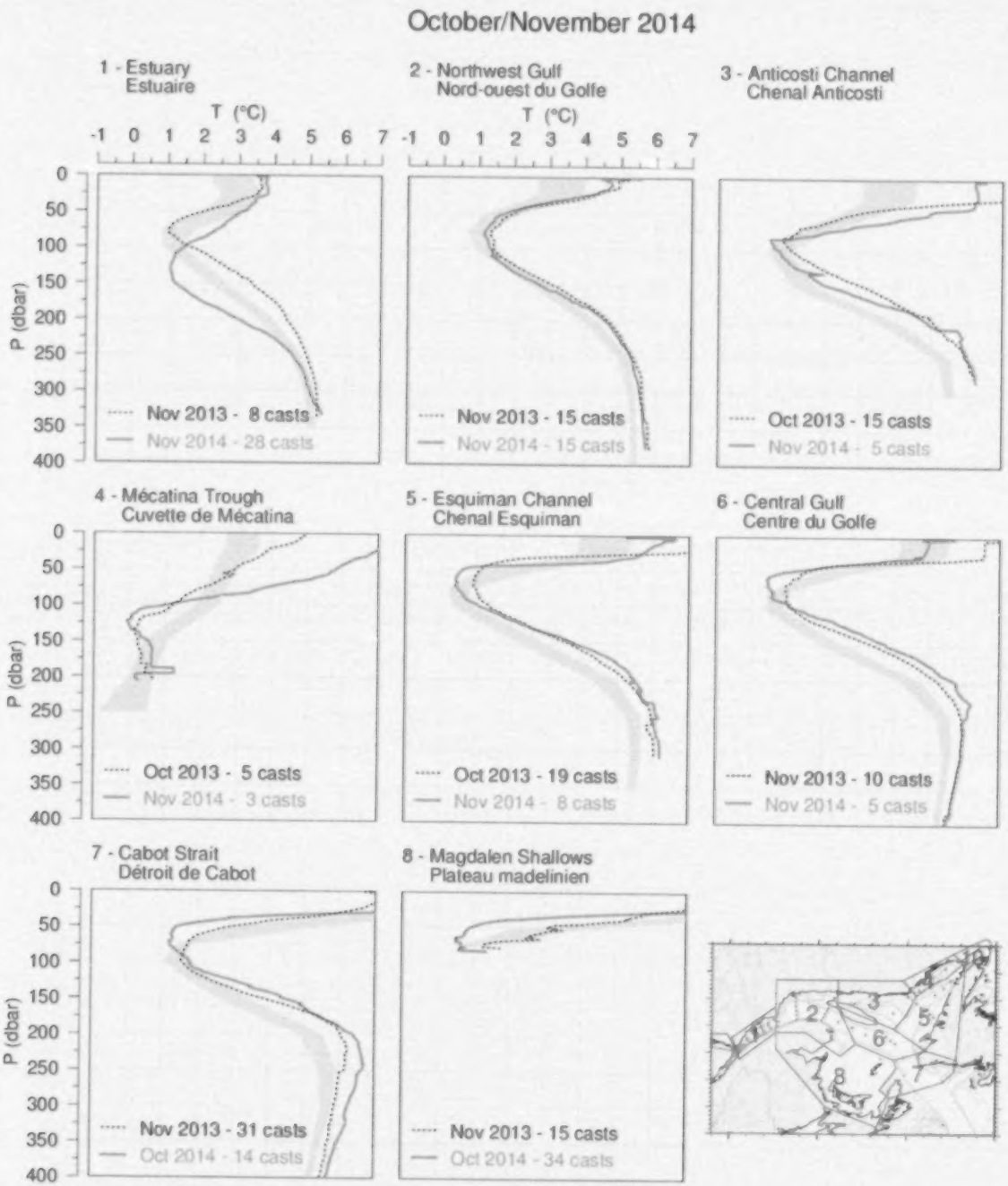

Fig. 54. Mean temperature profiles observed in each region of the Gulf during the October AZMP survey. The shaded area represents the 1981–2010 climatological monthly mean ± 0.5 SD. Mean profiles for 2013 are also shown for comparison.

1 - Estuary / Estuaire

	2013				2014		
	Mar	June	Aug	Oct	June	Aug	Nov
0 m	-0.29	5.3	7.0	4.0	6.9	13.6	3.8
10 m	-0.30	4.8	5.6	3.8	5.2	10.1	3.7
20 m	-0.35	3.4	4.3	3.5	3.7	7.9	3.8
30 m	-0.28	2.5	3.0	3.2	2.7	5.9	3.6
50 m	-0.29	1.0	1.4	2.4	0.7	2.4	3.1
75 m	0.44	-0.0	0.7	1.3	-0.3	1.0	2.4
100 m	-0.47	0.4	1.3	1.6	0.0	1.5	1.5
150 m	1.5	2.4	3.1	3.0	2.2	3.4	1.2
200 m	3.3	3.9	4.2	4.1	3.8	4.3	3.0
250 m	4.2	4.8	4.9	4.8	4.6	5.1	4.5
300 m	4.8	5.2	5.2	5.1	5.1	5.4	5.0
350 m		5.2	5.2	5.2	5.3	5.5	5.3

2 - Northwest Gulf / Nord-ouest du Golfe

	2013				2014			
	Mar	June	Aug	Nov	Mar	June	Aug	Nov
0 m	-0.99	7.6	14.3	4.9	-1.63	8.1	17.4	4.6
10 m	-1.06	6.4	12.7	4.9	-1.63	5.6	13.6	4.7
20 m	-1.11	3.7	8.2	4.5	-1.63	2.9	5.2	4.4
30 m	-1.20	2.2	4.6	3.8	-1.63	1.4	1.9	3.5
50 m	-0.90	0.5	1.6	2.0	-1.35	0.1	0.3	1.7
75 m	-0.25	0.3	0.7	1.3	0.3	0.3	0.2	1.2
100 m	0.4	0.9	1.1	1.4	2.0	1.0	1.0	1.3
150 m	2.3	3.1	3.0	3.1	4.7	3.6	3.4	2.7
200 m	3.8	4.5	4.7	4.7	5.4	4.9	4.9	4.6
250 m	5.3	5.2	5.4	5.4	5.5	5.5	5.5	5.3
300 m	5.5	5.5	5.6	5.6		5.7	5.7	5.6
350 m		5.6	5.7	5.7		5.7	5.7	5.7
400 m			5.7	5.8			5.7	5.7

3 - Anticosti Channel / Chenal Anticosti

	2013				2014			
	Mar	June	Aug	Oct	Mar	June	Aug	Nov
0 m	-1.05	4.9	14.1	8.8	-1.74	4.8	16.2	6.2
10 m	-1.05	4.9	13.6	8.7	-1.74	4.3	14.8	6.2
20 m	-1.07	3.5	8.0	8.5	-1.73	3.4	7.5	6.3
30 m	-1.09	1.7	4.6	6.2	-1.73	1.6	3.9	6.2
50 m	-1.12	0.7	1.6	2.6	-1.70	-0.2	0.6	4.6
75 m	-1.21	0.1	0.4	1.2	-1.25	-0.8	-0.3	1.9
100 m	-0.98	0.1	0.4	1.1	0.9	-0.8	-0.2	0.7
150 m	1.0	1.8	2.1	3.2	3.3	1.0	2.2	2.2
200 m	3.5	4.4	5.2	5.2	4.8	4.1	5.5	4.9
250 m			6.1	6.0		5.5	6.0	5.0

4 - Mécatina Trough / Cuvette de Mécatina

	2013				2014			
	Mar	June	Aug	Oct	Mar	June	Aug	Nov
0 m	-1.68	4.1	15.1	5.1	-1.75	3.2	14.0	7.1
10 m	-1.70	4.0	15.5	5.0	-1.76	3.1	7.0	7.2
20 m	-1.72	3.6	11.1	4.5	-1.76	2.9	2.3	7.1
30 m	-1.73	1.8	5.8	4.2	-1.75	1.9	0.7	6.7
50 m	-1.74	0.6	1.5	3.3	-1.74	-0.4	-0.4	5.8
75 m	-1.73	0.1	0.0	2.4	-1.76	-1.4	-0.6	3.9
100 m	-1.69	-0.8	0.0	1.3	-1.78	-1.4	-0.7	1.1
150 m	-1.71	-1.4	0.2	0.2	-1.79	-1.5	-0.1	0.5
200 m	-1.27	-1.6		0.5	-1.80	-0.4	1.4	1.2

5 - Esquiman Channel / Chenal Esquiman

	2013				2014			
	Mar	June	Aug	Oct	Mar	June	Aug	Nov
0 m	-0.68	4.8	16.4	8.6	-1.71	5.5	18.1	6.6
10 m	-0.64	4.8	15.9	8.6	-1.71	5.2	15.7	6.2
20 m	-0.77	4.4	8.2	7.3	-1.70	3.2	7.9	5.8
30 m	-0.72	2.9	3.4	3.1	-1.68	0.1	2.4	5.4
50 m	-0.55	1.3	1.1	1.3	-1.71	-0.9	-0.1	0.6
75 m	-0.27	0.1	0.5	1.0	-1.34	-0.1	-0.1	0.5
100 m	0.3	0.0	1.1	1.4	0.3	0.2	0.8	1.1
150 m	4.1	2.7	3.4	3.6	3.8	3.4	3.7	3.5
200 m	5.0	4.9	5.3	5.2	5.5	5.6	5.7	5.5
250 m		6.4	6.0	5.9	5.8	6.2	6.4	6.1
300 m			6.0	6.0	5.9		6.1	6.2

6 - Central Gulf / Centre du Golfe

	2013				2014			
	Mar	June	Aug	Nov	Mar	June	Aug	Oct
0 m	-0.56	7.2	15.1	6.6	-1.68	7.2	18.7	9.1
10 m	-0.63	6.9	14.3	6.6	-1.69	6.4	16.6	9.1
20 m	-0.60	5.0	8.9	6.6	-1.69	3.0	5.8	8.7
30 m	-0.65	3.2	3.3	6.0	-1.68	0.6	2.0	6.9
50 m	-0.61	1.0	1.2	1.4	-1.67	-0.5	0.0	0.8
75 m	-0.10	0.7	0.6	1.0	-0.98	-0.2	0.2	0.4
100 m	1.4	1.3	0.8	1.2	0.6	0.9	1.0	0.7
150 m	3.2	3.2	3.0	3.5	4.0	3.7	3.7	3.3
200 m	4.9	5.2	5.0	5.3	5.9	5.9	5.7	5.5
250 m		6.0	5.9	5.9	5.9	6.1	6.0	6.2
300 m		6.1	6.0	5.9	6.0	6.0	5.9	6.0
350 m		5.8	5.8	5.7	6.1	5.8	5.8	5.8
400 m		5.5	5.6	5.6		5.6	5.6	5.6
450 m		5.5	5.4	5.4		5.5	5.5	5.5

7 - Cabot Strait / Détroit de Cabot

	2013				2014			
	Mar	June	Aug	Nov	Mar	June	Aug	Oct
0 m	-0.70	8.3	17.2	7.2	-1.61	7.0	18.9	12.0
10 m	-0.74	7.7	15.6	7.1	-1.60	5.6	13.6	11.7
20 m	-0.77	5.4	5.8	6.8	-1.50	1.8	4.2	10.7
30 m	-0.84	2.8	4.1	6.0	-1.45	0.4	2.3	6.4
50 m	-0.46	1.0	2.4	3.0	-1.18	-0.4	1.2	1.4
75 m	0.6	1.0	1.6	1.7	-0.67	-0.0	1.0	1.3
100 m	1.4	1.4	1.8	1.6	0.8	1.5	1.4	1.9
150 m	2.9	3.1	3.1	3.5	4.8	4.6	4.4	4.5
200 m	5.2	4.9	5.4	5.1	6.4	6.5	6.4	6.4
250 m	6.1	5.8	5.8	6.2	6.5	6.5	6.6	6.6
300 m		6.0	5.8	5.9	6.0	6.1	6.2	6.2
350 m		5.7	5.7	5.7		5.9	5.9	6.0
400 m		5.4	5.5	5.5		5.6	5.6	5.6
450 m		5.4	5.4	5.4		5.5	5.5	5.5
500 m			5.4				5.5	5.5

8 - Magdalen Shallows / Plateau madelinien

	2013				2014			
	Mar	June	Sep	Oct	Mar	June	Sep	Oct
0 m	-1.28	9.9	14.9	12.2	-1.65	9.6	15.2	11.7
10 m	-1.32	9.1	14.5	12.2	-1.65	7.9	15.0	11.3
20 m	-1.37	6.6	11.5	11.4	-1.65	4.2	11.4	9.6
30 m	-1.43	3.2	5.5	5.3	-1.66	1.2	5.3	4.7
50 m	-1.38	0.3	1.0	0.7	-1.66	-0.5	0.9	0.8
75 m	-1.08	-0.2	0.9	0.7	-1.22	-0.6	0.2	0.6
100 m	1.1		1.1				0.7	

Fig. 55. Depth-layer monthly average temperature summary for months during which the eight Gulf-wide oceanographic surveys took place in 2013 and 2014. The colour-coding is according to the temperature anomaly relative to the monthly 1981–2010 climatology of each region.

1 - Estuary / Estuaire

	2013				2014		
	Mar	June	Aug	Oct	June	Aug	Nov
Strat.	3.02	5.0	3.1	2.5	7.0	4.7	2.0
0 m	29.9	25.0	28.4	28.6	23.1	27.1	28.3
10 m	30.0	25.4	29.0	29.0	25.1	28.1	28.4
20 m	30.3	27.1	29.8	29.7	27.0	29.1	29.0
30 m	30.5	28.6	30.5	30.6	28.7	29.7	29.6
50 m	31.1	30.8	31.6	31.6	31.3	31.2	30.7
75 m	31.7	31.9	32.3	32.3	32.0	32.2	31.4
100 m	32.4	32.5	32.8	32.7	32.4	32.8	32.0
150 m	32.9	33.3	33.5	33.5	33.2	33.6	32.7
200 m	33.5	33.9	34.0	34.0	33.8	34.0	33.5
250 m	34.0	34.3	34.3	34.3	34.2	34.4	34.1
300 m	34.3	34.5	34.5	34.4	34.4	34.5	34.4
350 m		34.5	34.5	34.5	34.5	34.5	34.5

2 - Northwest Gulf / Nord-ouest du Golfe

	2013				2014			
	Mar	June	Aug	Nov	Mar	June	Aug	Nov
Strat.	0.54	3.0	4.1	1.2	0.25	3.8	5.1	1.8
0 m	31.3	28.8	28.7	30.8	31.4	28.2	28.6	30.0
10 m	31.4	29.4	29.2	30.8	31.4	29.4	29.3	30.2
20 m	31.5	30.4	30.2	31.0	31.5	30.6	30.7	30.4
30 m	31.6	31.0	30.9	31.3	31.6	31.2	31.4	31.1
50 m	32.0	31.8	31.7	31.9	31.8	32.0	32.0	31.9
75 m	32.3	32.2	32.2	32.3	32.4	32.4	32.4	32.3
100 m	32.6	32.6	32.6	32.7	33.0	32.8	32.8	32.6
150 m	33.3	33.5	33.4	33.5	34.0	33.7	33.6	33.4
200 m	33.8	34.0	34.1	34.1	34.4	34.2	34.1	34.0
250 m	34.4	34.4	34.5	34.5	34.6	34.5	34.5	34.4
300 m	34.6	34.6	34.6	34.7		34.7	34.6	34.6
350 m		34.7	34.7	34.7		34.7	34.7	34.6
400 m			34.8	34.8			34.7	34.7

3 - Anticosti Channel / Chenal Anticosti

	2013				2014			
	Mar	June	Aug	Oct	Mar	June	Aug	Nov
Strat.	0.03	1.7	2.8	1.6	0.05	1.7	3.6	0.5
0 m	32.0	30.2	30.5	30.8	32.1	30.3	30.2	31.0
10 m	32.0	30.3	30.6	30.8	32.1	31.0	30.4	31.1
20 m	32.0	31.3	31.1	30.9	32.1	31.3	31.2	31.1
30 m	32.0	31.6	31.5	31.2	32.1	31.6	31.5	31.2
50 m	32.0	31.9	31.8	31.9	32.1	32.0	32.0	31.4
75 m	32.0	32.1	32.1	32.2	32.2	32.3	32.3	32.0
100 m	32.1	32.4	32.5	32.6	32.7	32.4	32.5	32.5
150 m	32.8	33.0	33.4	33.5	33.4	33.0	33.3	33.1
200 m	33.5	33.9	34.2	34.2	34.0	33.8	34.2	34.0
250 m			34.6	34.6		34.3	34.5	34.5

4 - Mécatina Trough / Cuvette de Mécatina

	2013				2014			
	Mar	June	Aug	Oct	Mar	June	Aug	Nov
Strat.	0.21	1.7	3.0	0.8	0.01	1.3	3.4	0.4
0 m	32.2	30.1	30.9	30.8	32.4	30.3	30.1	31.0
10 m	32.3	30.1	30.9	30.9	32.4	30.4	31.1	31.0
20 m	32.3	31.3	31.2	31.2	32.4	31.3	31.5	31.1
30 m	32.4	31.5	31.6	31.3	32.4	31.4	31.8	31.2
50 m	32.5	31.9	32.0	31.5	32.4	31.6	32.1	31.3
75 m	32.5	32.1	32.3	31.8	32.4	32.3	32.3	31.7
100 m	32.6	32.4	32.5	32.1	32.6	32.5	32.5	32.2
150 m	32.6	32.5	32.8	32.5	32.9	32.6	32.8	32.7
200 m	32.7	32.6		32.6	33.0	32.9	33.0	32.9

5 - Esquiman Channel / Chenal Esquiman

	2013				2014			
	Mar	June	Aug	Oct	Mar	June	Aug	Nov
Strat.	0.22	0.5	3.2	1.8	0.09	1.2	3.9	1.3
0 m	31.9	31.6	30.8	31.0	31.9	31.0	30.5	31.2
10 m	31.9	31.6	30.9	31.1	31.9	31.1	30.7	31.3
20 m	31.9	31.6	31.5	31.3	31.9	31.4	31.2	31.4
30 m	32.0	31.7	31.7	31.8	32.0	31.7	31.6	31.4
50 m	32.2	31.9	32.0	32.2	32.0	31.9	32.0	32.2
75 m	32.3	32.2	32.4	32.5	32.1	32.3	32.3	32.4
100 m	32.5	32.5	32.7	32.7	32.5	32.4	32.7	32.7
150 m	33.7	33.3	33.5	33.6	33.6	33.4	33.6	33.6
200 m	34.1	34.0	34.2	34.2	34.2	34.2	34.2	34.2
250 m		34.6	34.5	34.5	34.4	34.5	34.6	34.5
300 m			34.6	34.5	34.5		34.7	34.6

6 - Central Gulf / Centre du Golfe

	2013				2014			
	Mar	June	Aug	Nov	Mar	June	Aug	Oct
Strat.	0.18	1.1	3.1	1.5	0.02	1.3	4.7	1.9
0 m	31.7	31.3	30.6	31.1	31.9	31.2	29.7	30.8
10 m	31.7	31.3	30.7	31.1	31.9	31.3	30.0	30.8
20 m	31.8	31.5	31.2	31.1	31.9	31.5	31.3	30.9
30 m	31.8	31.6	31.7	31.2	31.9	31.8	31.6	31.2
50 m	31.9	31.9	32.0	32.1	31.9	32.1	32.0	32.1
75 m	32.1	32.4	32.3	32.4	32.1	32.4	32.4	32.4
100 m	32.7	32.7	32.6	32.7	32.5	32.8	32.7	32.6
150 m	33.4	33.4	33.4	33.5	33.6	33.6	33.6	33.5
200 m	34.0	34.1	34.1	34.2	34.3	34.3	34.2	34.2
250 m		34.6	34.5	34.6	34.6	34.6	34.5	34.5
300 m		34.7	34.7	34.7	34.8	34.7	34.7	34.7
350 m		34.8	34.8	34.8	34.8	34.8	34.8	34.8
400 m		34.9	34.9	34.9		34.9	34.9	34.9
450 m		34.9	34.9	34.9		34.9	34.9	34.9

7 - Cabot Strait / Détroit de Cabot

	2013				2014			
	Mar	June	Aug	Nov	Mar	June	Aug	Oct
Strat.	0.62	1.6	3.3	1.1	0.35	1.5	4.3	3.1
0 m	30.9	30.5	31.0	31.2	31.1	30.6	30.2	29.6
10 m	31.0	30.7	31.1	31.2	31.2	30.7	30.7	29.8
20 m	31.2	31.0	31.7	31.3	31.3	31.1	31.6	30.2
30 m	31.4	31.3	31.9	31.5	31.4	31.3	31.9	30.8
50 m	31.7	31.7	32.2	32.0	31.5	31.6	32.1	31.8
75 m	32.2	32.1	32.4	32.5	31.8	32.2	32.3	32.4
100 m	32.6	32.5	32.7	32.7	32.4	32.8	32.6	32.8
150 m	33.3	33.4	33.4	33.6	33.8	33.8	33.7	33.8
200 m	34.1	34.1	34.2	34.4	34.4	34.5	34.4	34.4
250 m	34.5	34.5	34.5	34.6	34.6	34.6	34.6	34.6
300 m		34.7	34.7	34.7	34.7	34.7	34.7	34.7
350 m		34.9	34.8	34.8		34.8	34.8	34.8
400 m		34.9	34.9	34.9		34.9	34.9	34.9
450 m		34.9	34.9	34.9		34.9	34.9	34.9
500 m			34.9				34.9	34.9

8 - Magdalen Shallows / Plateau madelinien

	2013				2014			
	Mar	June	Sep	Oct	Mar	June	Sep	Oct
Strat.	0.52	2.5	4.1	2.9	0.31	2.9	4.0	3.1
0 m	30.7	29.5	28.7	29.5	30.8	28.9	28.9	29.5
10 m	30.8	29.7	28.8	29.4	30.9	29.7	29.0	29.7
20 m	31.0	30.2	29.4	29.6	30.9	30.4	29.5	30.0
30 m	31.1	30.7	30.4	30.5	30.9	31.0	30.5	30.8
50 m	31.4	31.3	31.5	31.4	31.2	31.4	31.6	31.8
75 m	31.7	31.8	32.2	31.9	31.6	31.9	32.1	32.3
100 m	32.6		32.3				32.6	

Fig. 56. Depth-layer monthly average stratification and salinity summary for months during whichthe eight Gulf-wide oceanographic surveys took place in 2013 and 2014. Stratification is defined as the density difference between 50 m and the surface and its colour-coding is reversed (blue for positive anomaly).

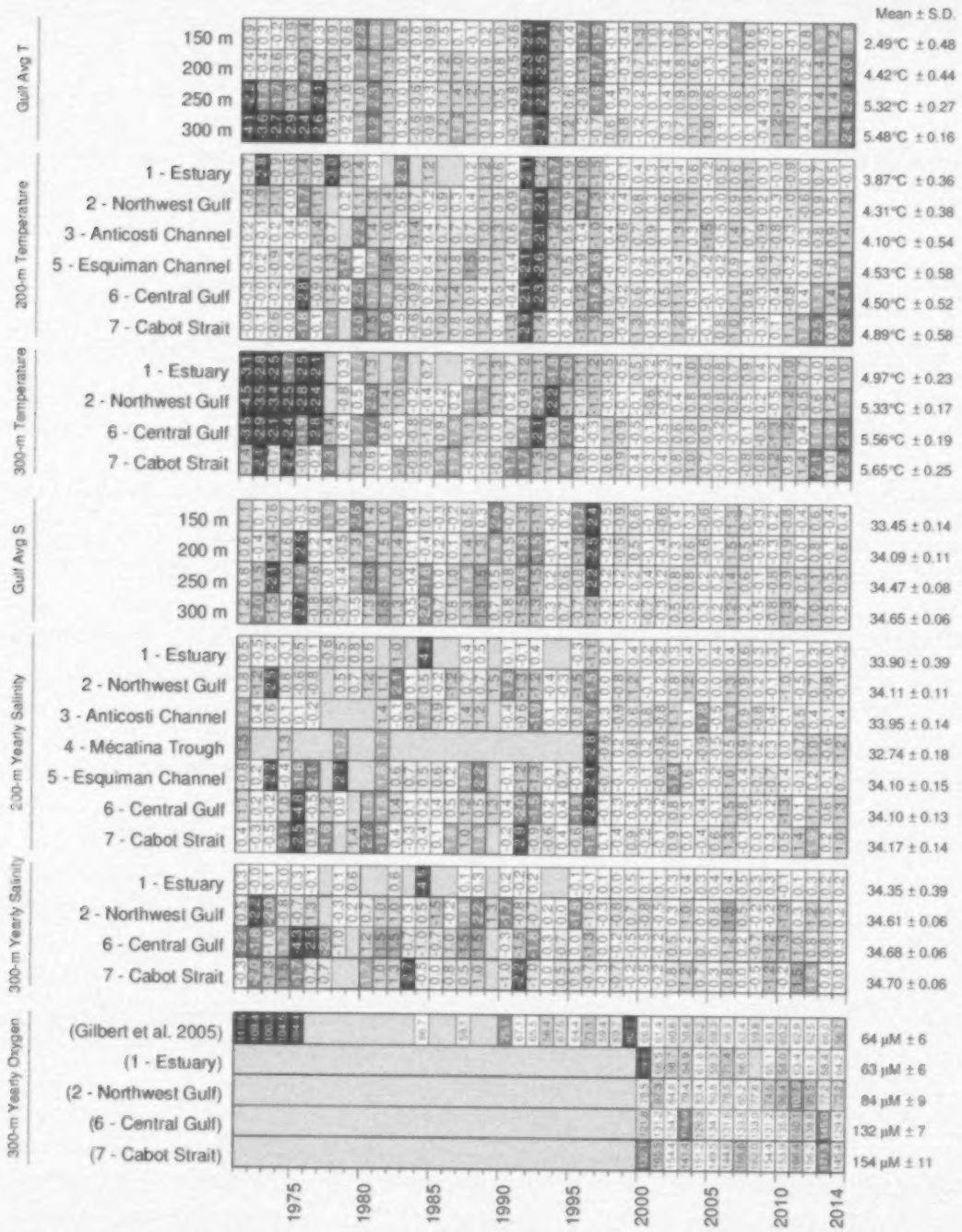

Fig. 57. Deep layer temperature, salinity, and dissolved oxygen. Gulf averages for temperature and salinity are shown for 150, 200, 250, and 300 m, and regional averages are shown for 200 and 300m. Dissolved oxygen is shown with an inverted colour scheme for the updated Gilbert et al. 2005 time series as well as recent regional averages at 300 m obtained using a Seabird SBE43 CTD sensor. The numbers on the right are the 1981–2010 climatological means and standard deviations. The numbers in the boxes are normalized anomalies, except for oxygen where physical values are shown for easier comparison between the Gilbert et al. 2005 time series and the CTD data.

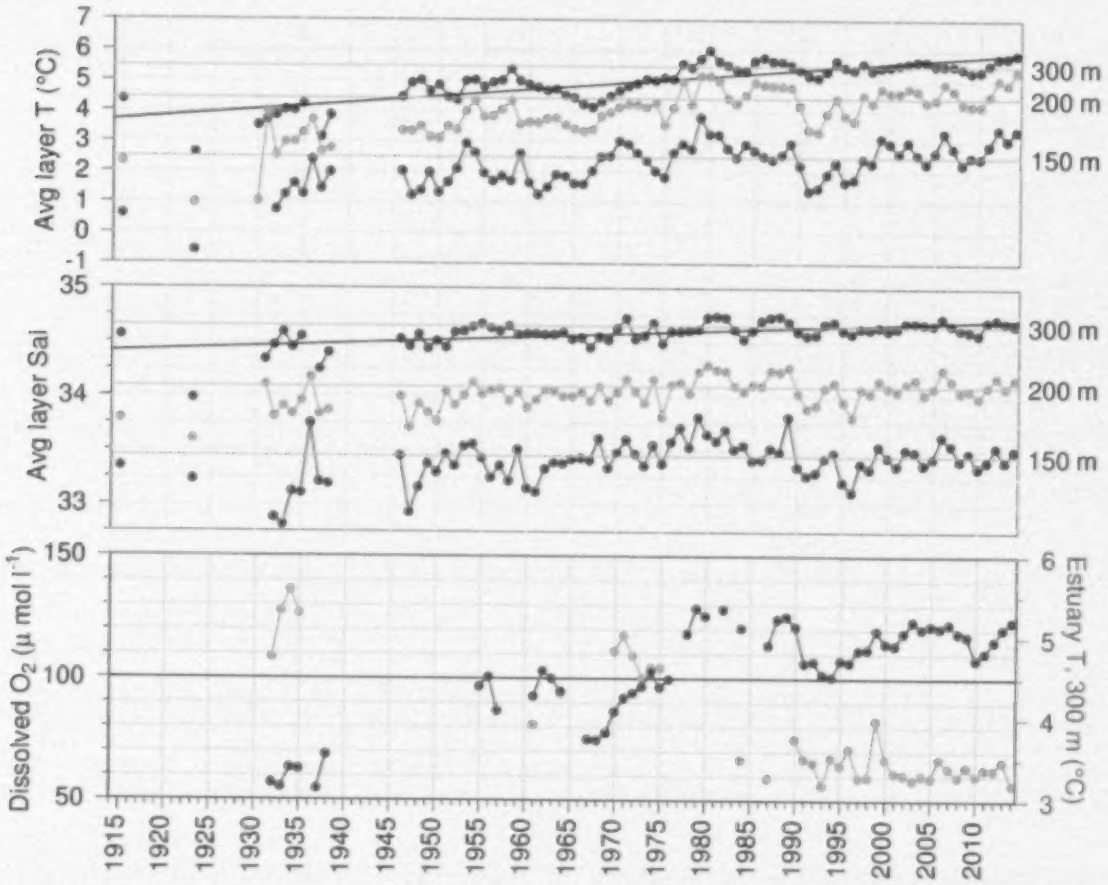

Fig. 58. Layer-averaged temperature and salinity time series for the Gulf of St. Lawrence and dissolved oxygen between 295 m and the bottom in the deep central basin of the St. Lawrence Estuary. The temperature and salinity panels show the 150 m, 200 m, and 300 m annual averages and the horizontal lines are 1981–2010 means. Sloped lines show linear regressions for temperature and salinity at 300 m of respectively 2.2°C and 0.3 per century. The horizontal line in the oxygen panel corresponds roughly to 30% saturation and marks the threshold of hypoxic conditions. In addition to the dissolved oxygen time series (light blue), the lower panel also shows temperature (dark blue) at 300 m in the Estuary.

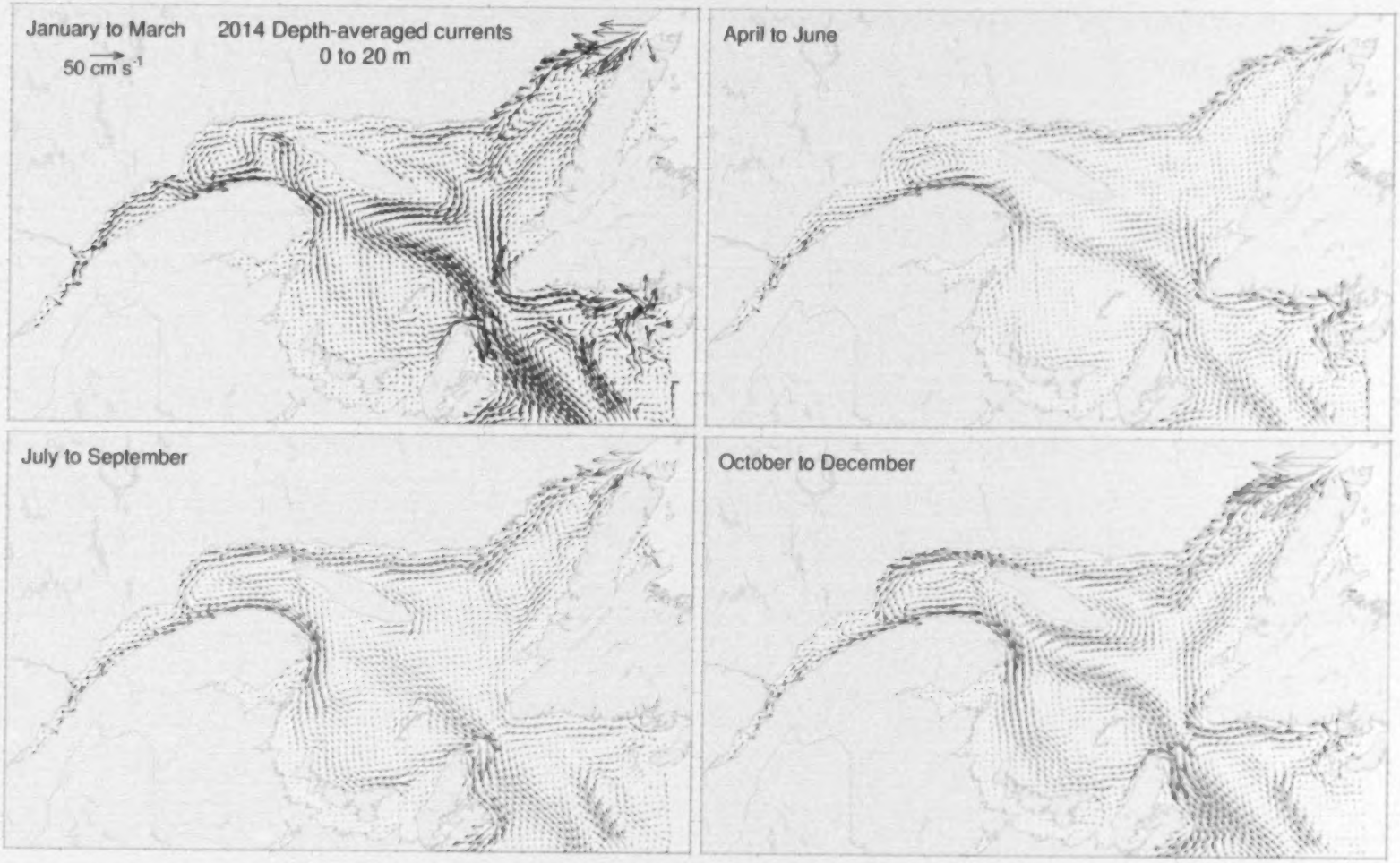

Fig. 59. Depth-averaged currents from 0 to 20 m for each three-month period of 2014.

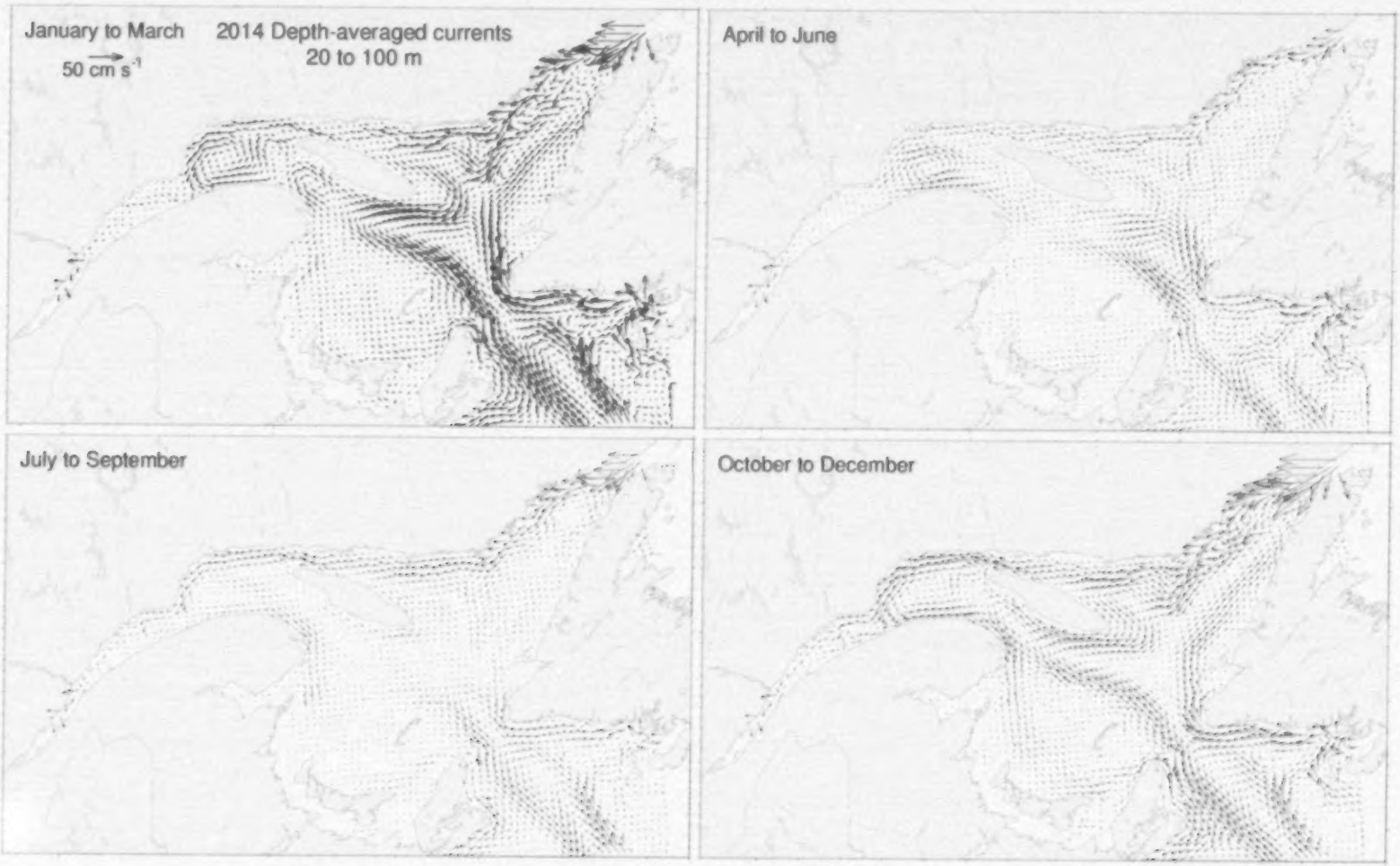

Fig. 60. Depth-averaged currents from 20 to 100 m for each three-month period of 2014.

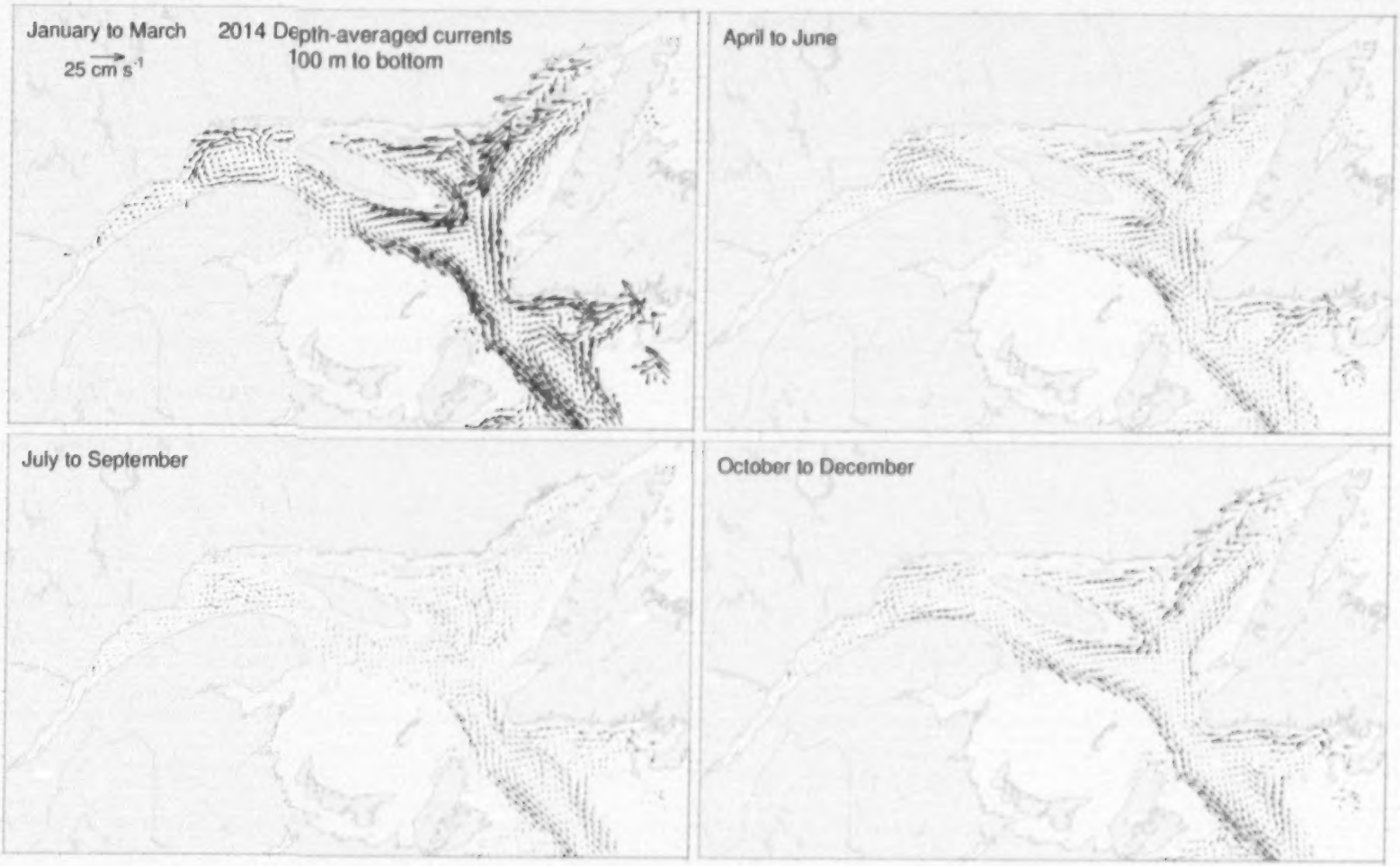

Fig. 61. Depth-averaged currents from 100 m to the bottom for each three-month period of 2014.

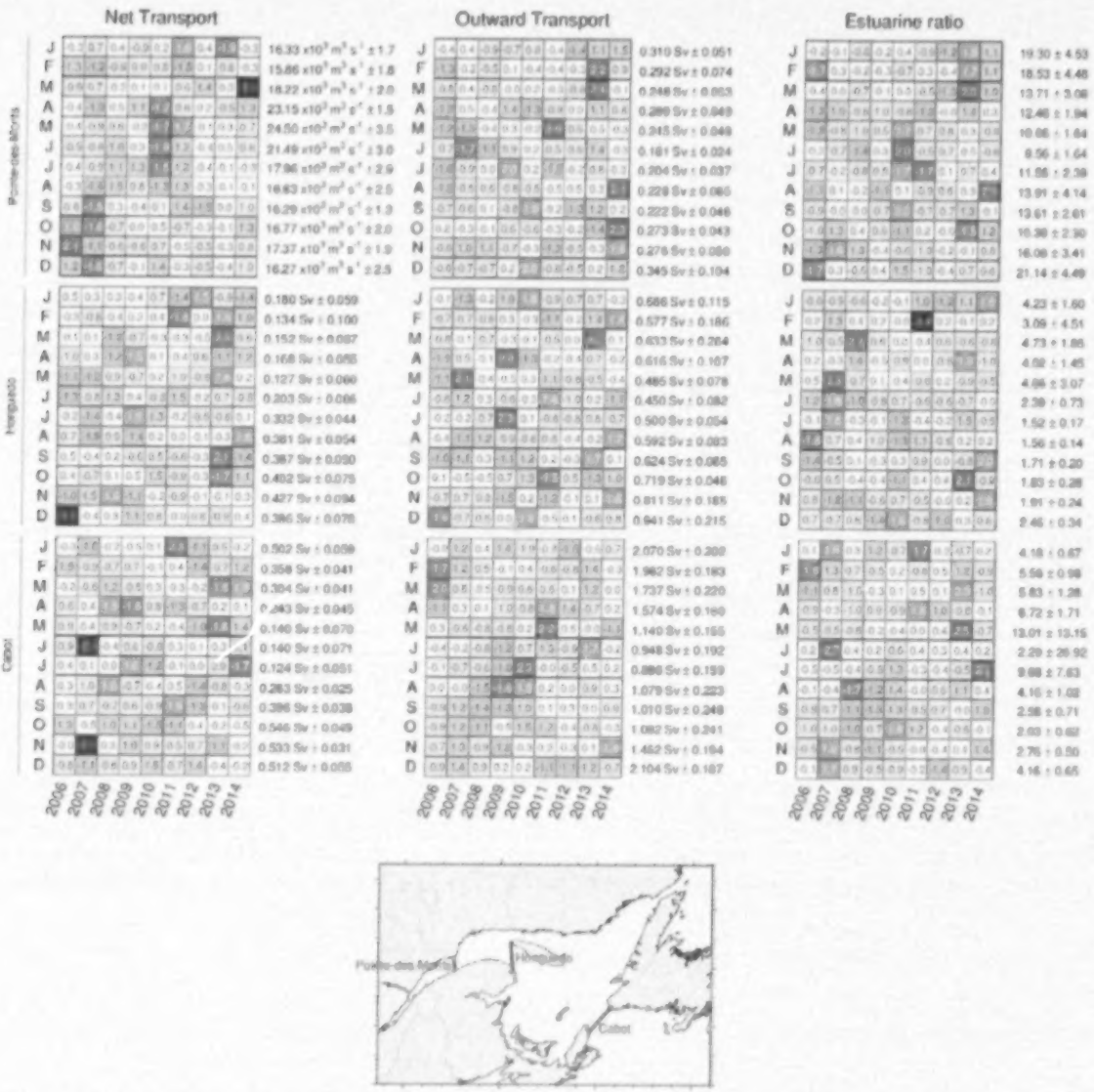

Fig. 62. Monthly averaged modelled transports and estuarine ratio across sections of the Gulf of St. Lawrence since 2006. The numbers on the right are the 2006–2014 means and standard deviations. The numbers in the boxes are normalized anomalies. Colours indicate the magnitude of the anomaly. Sv (Sverdrup) are units of transport equal to 10^6 $m^3 s^{-1}$.

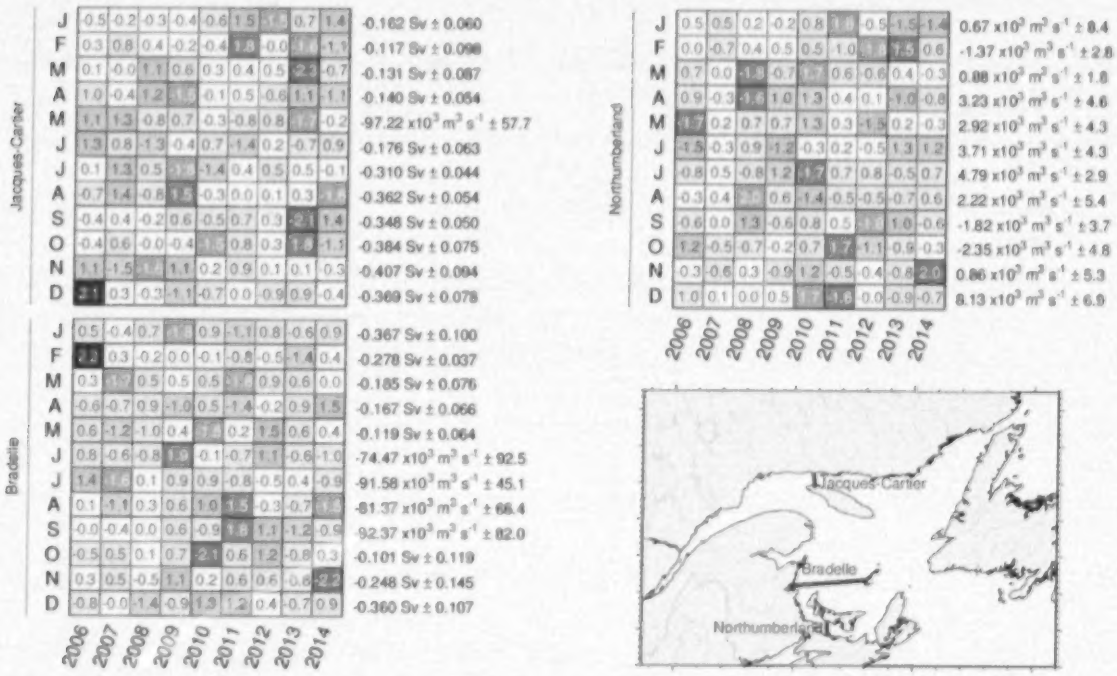

Fig. 63. Monthly averaged modelled transports across sections of the Gulf of St. Lawrence since 2006. The numbers on the right are the 2006–2014 means and standard deviations, with positive values toward east and north. The numbers in the boxes are normalized anomalies. Colours indicate the magnitude of the anomaly (e.g., negative anomalies are still shown in red when the mean transport is negative across the section).

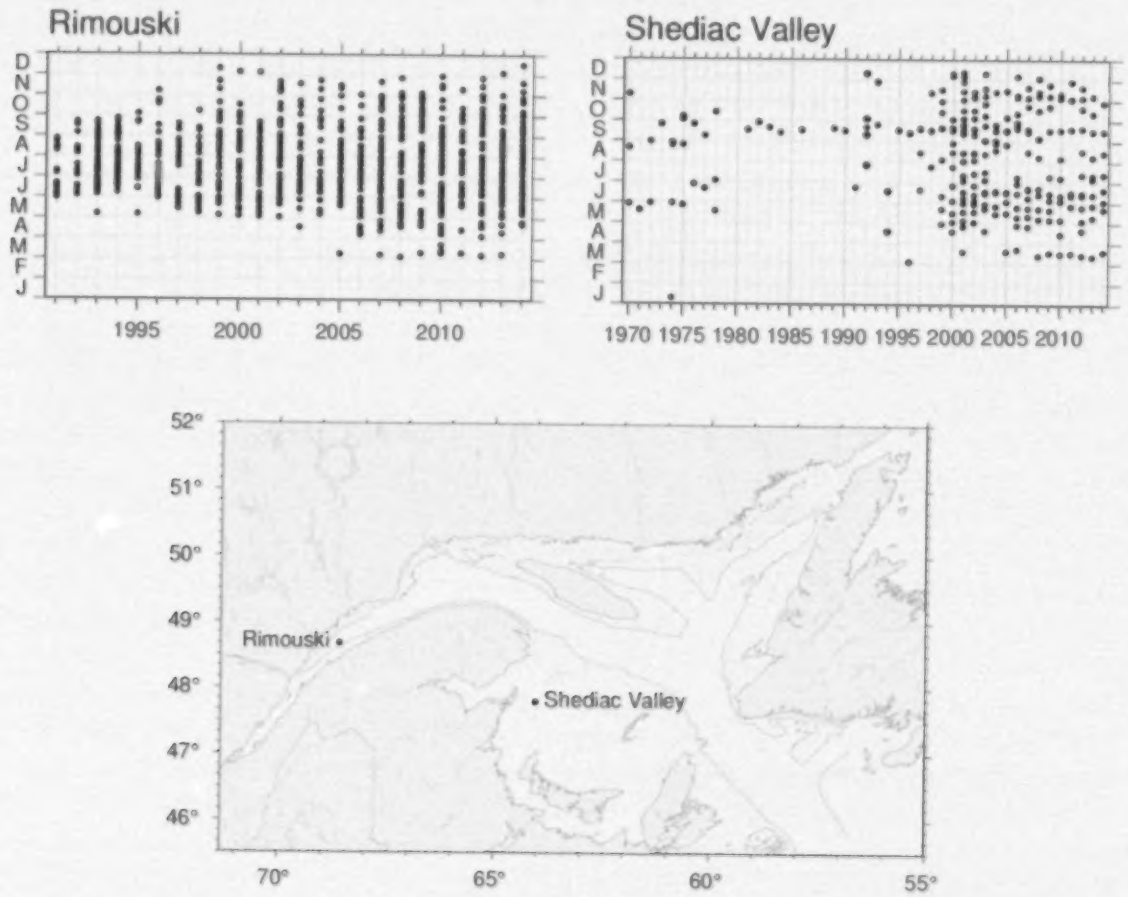

Fig. 64. Sampling frequency and positions of the AZMP stations Rimouski and Shediac Valley.

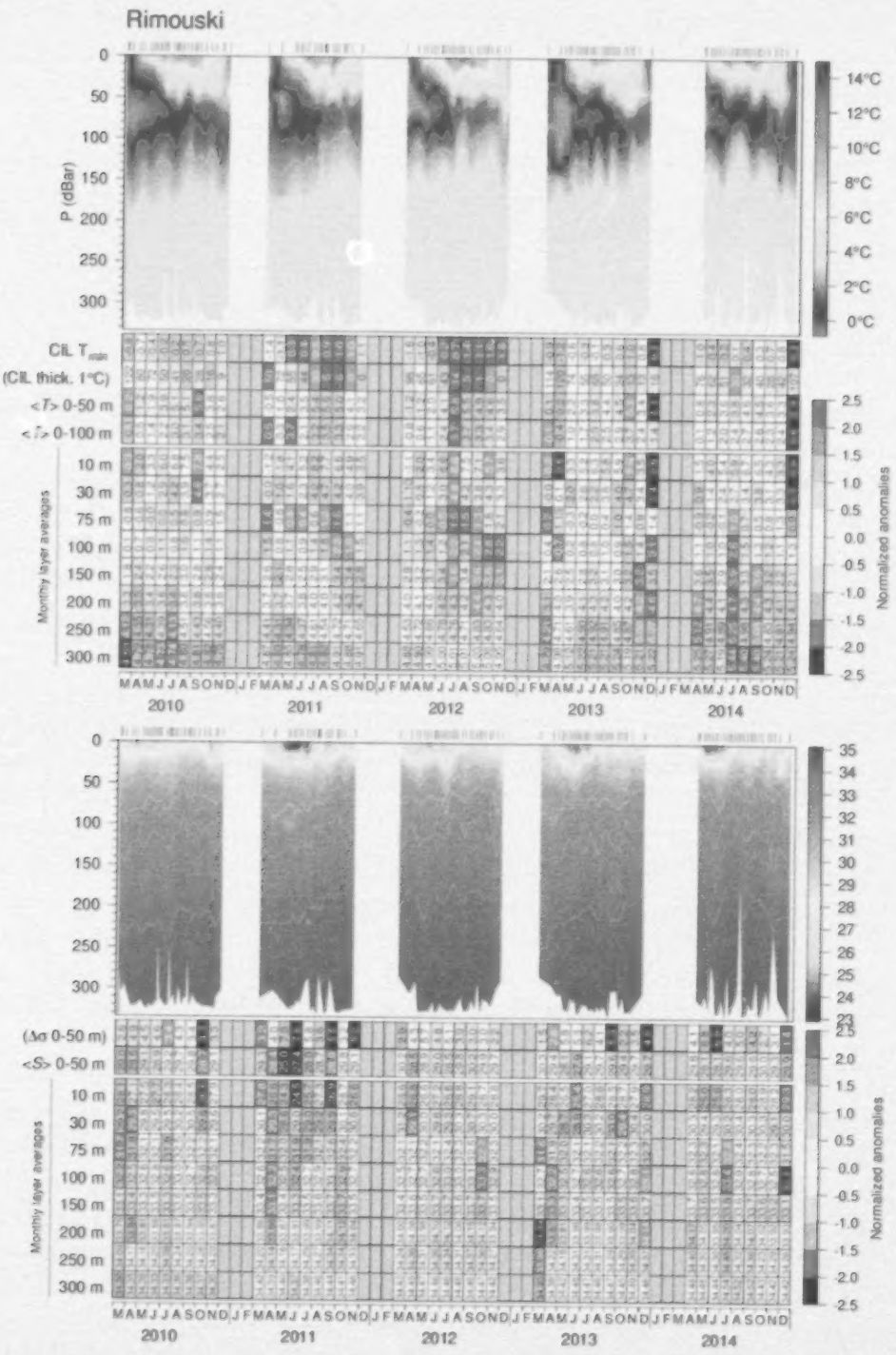

Fig. 65. Isotherm (top) and isohaline (bottom) time series at the Rimouski station; tick marks above indicate sample dates. The scorecard tables are monthly layer averages colour-coded according to the anomaly relative to the 1993–2010 monthly climatology for the station (yearly climatology for 250 m and deeper). Thickness of the CIL and stratification have reversed colour codes where red indicates thinner CIL (warmer water) and less stratification (higher surface salinity).

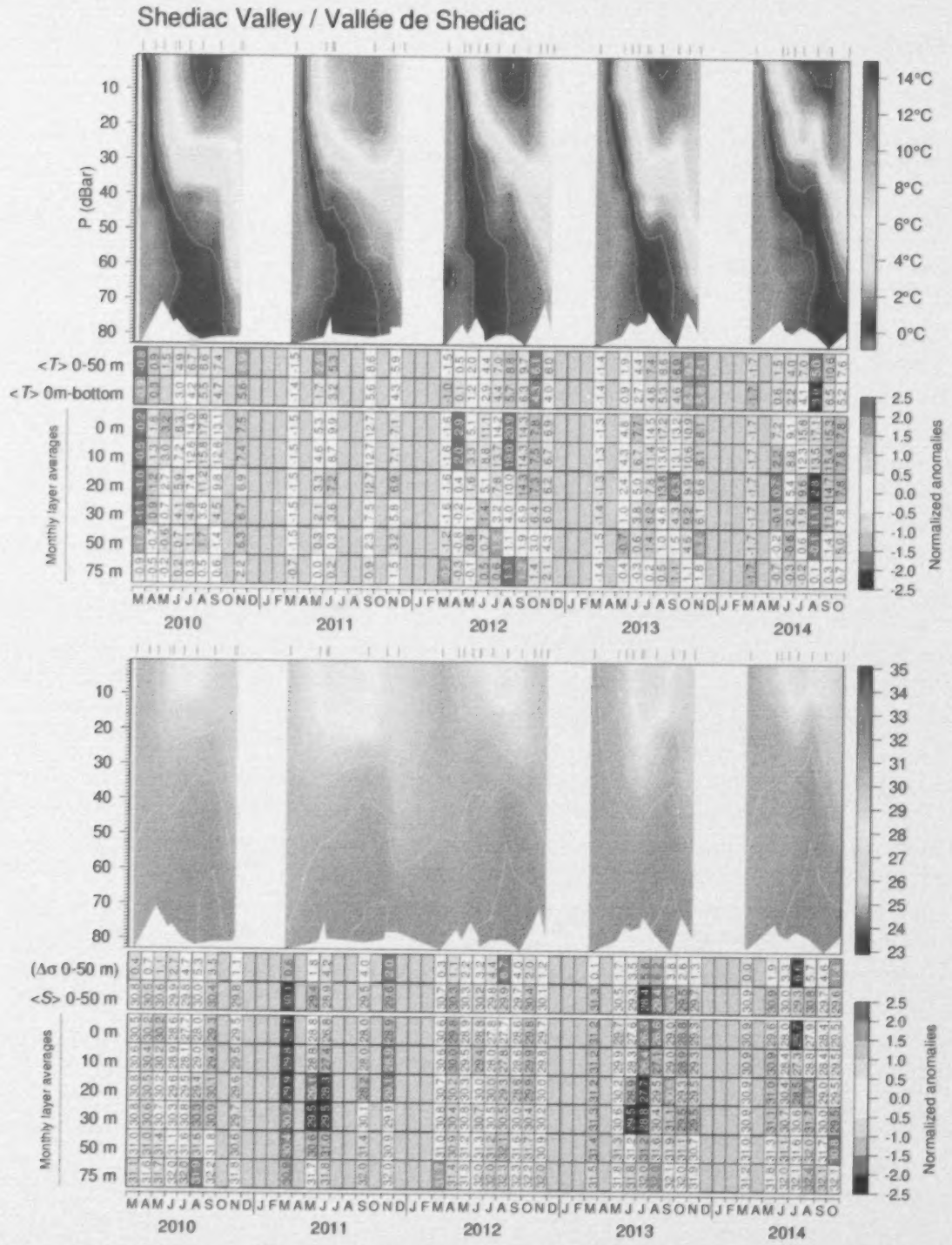

Fig. 66. Isotherm (top) and isohaline (bottom) time series at the Shediac Valley station; tick marks above indicate sample dates. Scorecard tables are monthly layer averages colour-coded according to the anomaly relative to the 1981–2014 monthly climatology for the station (input to climatology is sparse prior to 1999).

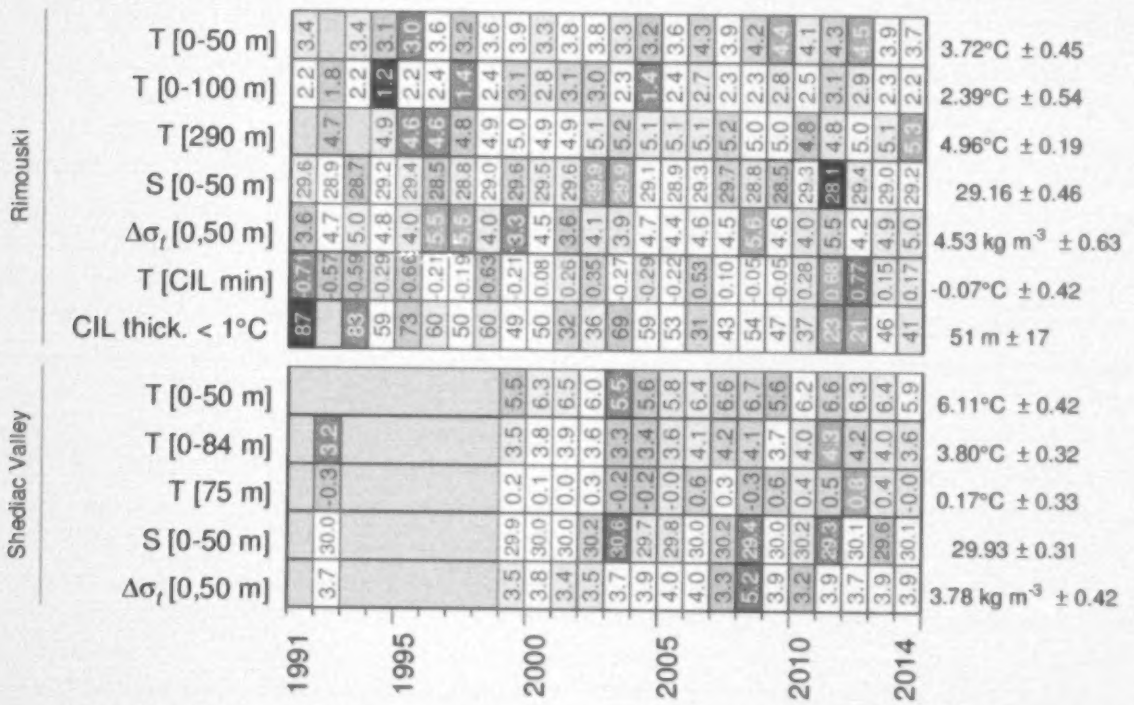

Fig. 67. May to October temperature and salinity layer averages, stratification expressed as the density difference between 0 and 50 m, and CIL temperature minimum and thickness (T<1°C) for the fixed monitoring stations. Numbers in panels are monthly average values colour-coded according to the anomaly relative to the 1991–2014 timeseries. Three months of anomaly data, between May and October, are required to show an average anomaly for any given year, except for deep water temperature at Rimouski station. Temperatures at 290 m and 75 m at Rimouski station and Shediac Valley station are considered to represent near-bottom temperatures.

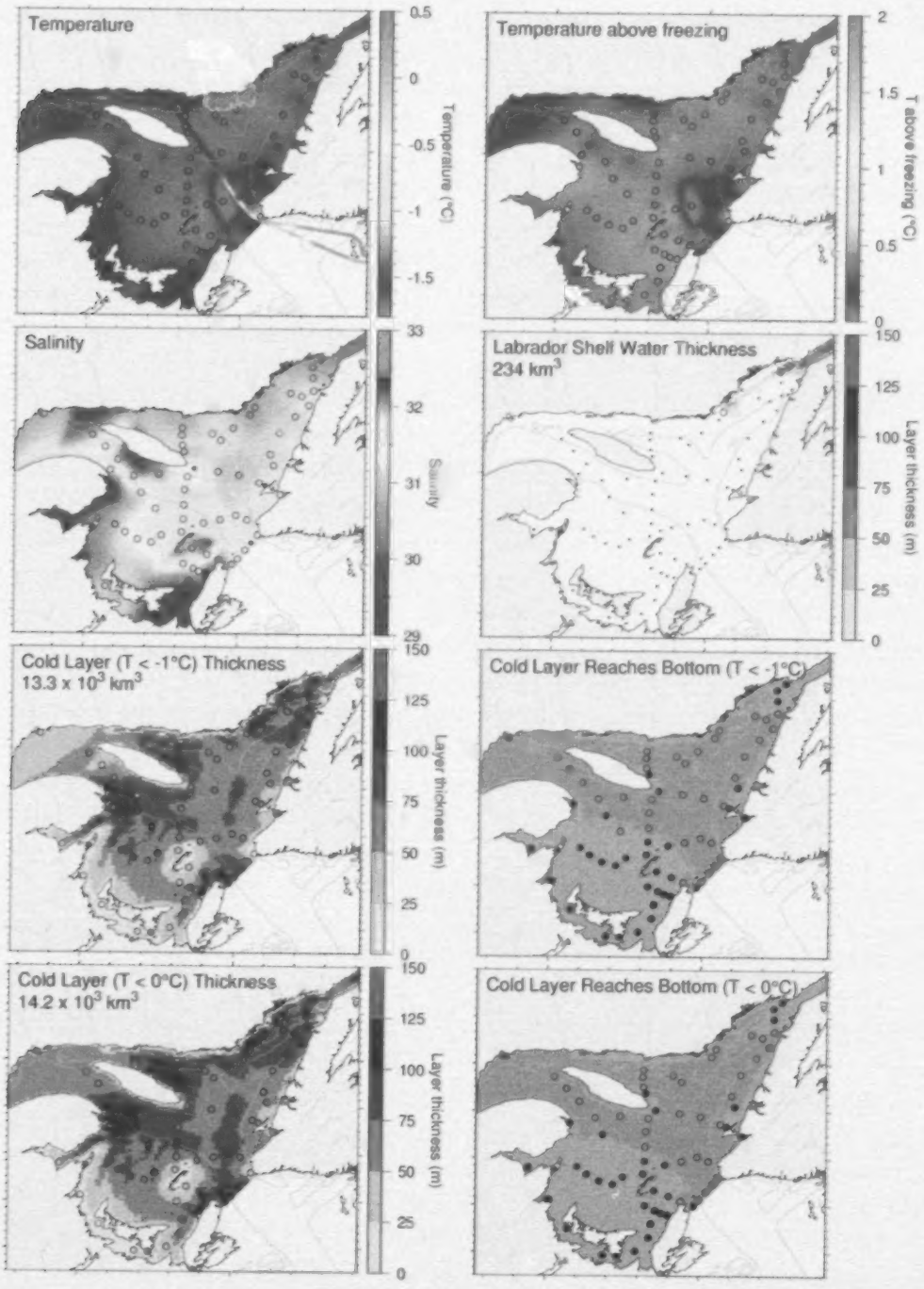

Fig. 68. March 2015 surface cold layer characteristics: surface water temperature (upper left), temperature difference with the freezing point (upper right), salinity (second row left), estimate of the thickness of the Labrador Shelf water intrusion (second row right), and cold layer (T<-1°C and <0°C) thicknesses and where they reach bottom. The symbols are coloured according to the value observed at the station, using the same colour palette as the interpolated image. A good match is seen between the interpolation and the station observations where the station colours blend into the background.

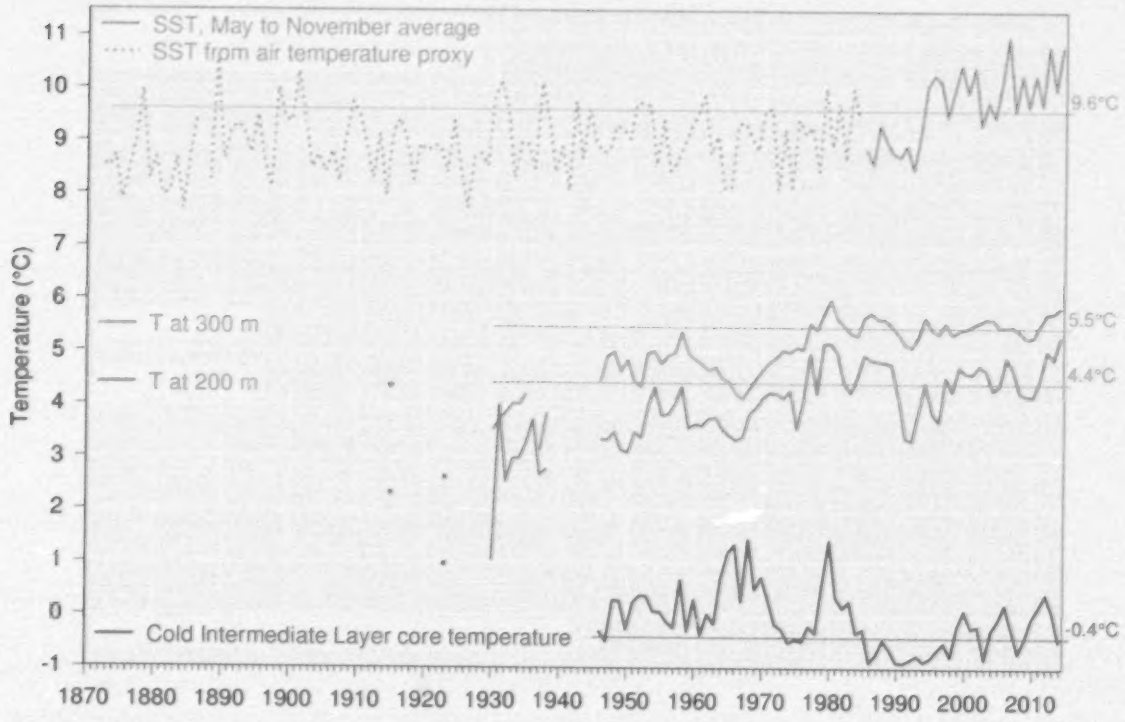

Fig. 69. Water temperatures in the Gulf of St. Lawrence. May–November SST averaged over the Gulf excluding the Estuary (1985–2014, red line), completed by a proxy based on April–November air temperature (1873–1984, red dashed line; average of all AHCCD stations in Fig. 4 but excluding Estuary stations at Baie Comeau and Mont-Joli). Layer-averaged temperature for the Gulf of St. Lawrence at 200 and 300 m (green lines). Cold intermediate layer minimum temperature index in the Gulf of St. Lawrence (blueline). SST air temperature proxy is similar to that of Galbraith et al. (2012). Climatological averages based on the 1981-2010 period are indicated by thin lines labeled on the right side. Figure adapted from (Benoît et al. 2012).

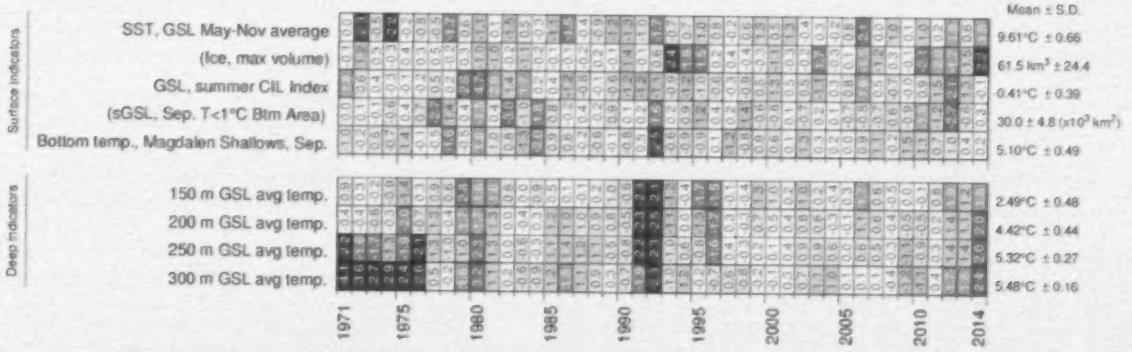
Surface indicators
Deep indicators
SST, GSL May-Nov average
(Ice, max volume)
GSL, summer CIL Index
(sGSL, Sep. T<1°C Btm Area)
Bottom temp., Magdalen Shallows, Sep.
150 m GSL avg temp.
200 m GSL avg temp.
250 m GSL avg temp.
300 m GSL avg temp.
Mean ± S.D.
9.61°C ± 0.66
61.5 km³ ± 24.4
0.41°C ± 0.39
30.0 ± 4.8 (x10³ km²)
5.10°C ± 0.49
2.49°C ± 0.48
4.42°C ± 0.44
5.32°C ± 0.27
5.48°C ± 0.16
1971 1975 1980 1985 1990 1995 2000 2005 2010 2014

Fig. 70. Surface and deep indicators used in the composite climate index (Fig. 71).

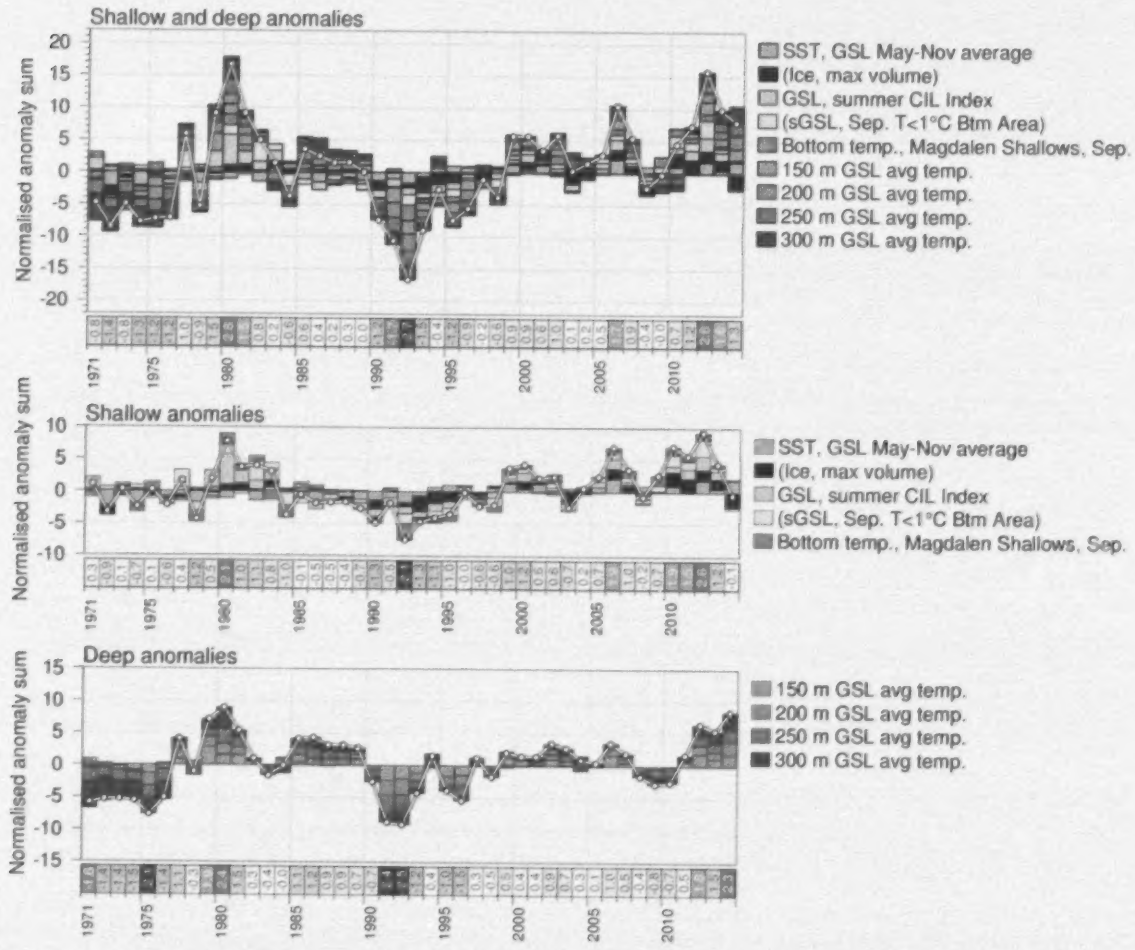
Shallow and deep anomalies
Normalised anomaly sum
SST, GSL May-Nov average
(Ice, max volume)
GSL, summer CIL Index
(sGSL, Sep. T<1°C Btm Area)
Bottom temp., Magdalen Shallows, Sep.
150 m GSL avg temp.
200 m GSL avg temp.
250 m GSL avg temp.
300 m GSL avg temp.
Shallow anomalies
Deep anomalies

Fig. 71. Composite climate indices (white lines and dots) derived by summing various normalized anomalies from different parts of the environment (colored boxes stacked above the abscissa are positive anomalies, and below are negative). Top panel sums anomalies representing the entire water column, middle panel sums shallow anomalies and bottom panel sums deep anomalies.